NATIONAL ADVISORY COMMITTEE FOR AERONAUTICS

SPECIAL REPORT No. 94

FULL-SCALE WIND-TUNNEL INVESTIGATION OF WING COOLING DUCTS

By F. R. Nickle and Arthur B. Freeman
Langley Memorial Aeronautical Laboratory

October 1938

FULL-SCALE WIND-TUNNEL INVESTIGATION OF WING COOLING DUCTS

By F. R. Nickle and Arthur B. Freeman

SUMMARY

The systematic investigation of wing cooling ducts at the N.A.C.A. laboratory has been continued with tests in the full-scale wind tunnel on ducts of finite span. These results extend the previous investigation on section characteristics of ducts to higher Reynolds Numbers and indicate the losses due to the duct ends. The data include comparisons between ducts completely within the wing and the conventional underslung ducts. Methods of flow regulation were studied and data were obtained for a wide range of internal duct resistance.

The results show satisfactory correlation between the finite span and the previously measured section characteristics obtained with full-span ducts. The effects of the various design parameters on the duct characteristics are discussed. The cooling power required for the internal duct installation is shown to be only a small percentage of the engine power.

INTRODUCTION

The aerodynamic advantages resulting from the relatively small frontal areas of liquid-cooled engines have been largely offset by the excessive high-speed drag of conventional radiator installations. Meredith (reference 1) and Worth (reference 2) have shown that the internal or cooling drag is materially reduced by placing the radiator at the low velocity section of an expanding duct. External drag, attributed mainly to interference and exposed frontal area, can be reduced by locating such a radiator duct assembly wholly within an essential part of the airplane such as the wing. The net gain realized from this cooling installation depends on the extent to which the following losses may be reduced:

1. Interference losses caused by breaks in the wing surface at the inlet and outlet of the duct.

2. Energy losses in the air passing through the duct, due to the expansion and to the friction along the duct walls.

3. Induced drag loss due to the increased weight of the radiators required for the low velocity cooling.

Systematic investigations of wing-duct cooling are now in progress at this laboratory. Recent tests made in the N.A.C.A. full-scale wind tunnel (reference 3) and in the 7- by 10-foot closed-throat wind tunnel (reference 4) indicate that duct-radiator combinations may be mounted in a wing so that interference and duct losses are small. The total loss in such a cooling system, neglecting weight, is only slightly greater than the power required to force the air through the radiator core. The tests referred to in reference 4 were made with a full-span duct and simulated radiator, under two-dimensional-flow conditions, and the results are presented as section characteristics.

The purpose of the present full-scale investigation is to correlate the duct section characteristics found in reference 4 with the performance of installations of finite span and to extend the test data to higher Reynolds Numbers. The results of the full-scale-tunnel tests include data on the characteristics of several of the through duct arrangements described in reference 4, underslung radiator ducts, and cross-wing radiator-duct combinations with inlet on the lower and outlet on the upper wing surface. The effects of variations in radiator pressure drop and methods for efficiently controlling the air flow through the ducts were also investigated.

Design parameters, such as size, shape, and location of duct inlets and outlets, were varied systematically. Estimates of the power absorbed by various duct-radiator combinations, neglecting the effect of weight and heat, are given. The effects of propeller slipstream, recovery of heat energy, and ground cooling characteristics of duct radiators are included in a further investigation.

APPARATUS AND TESTS

Wing

The fabric-covered 2:1 tapered airfoil described in reference 5 and modified as outlined in the following paragraph was used for this investigation. The span was

45.75 feet, center-section chord 9.37 feet, area 337.5 square feet, and aspect ratio 6.20. Ailerons were locked in the neutral position and all gaps were sealed.

The constant-chord center section, extending over 10.7 percent of the wing span, was altered to an N.A.C.A. 23017 section which is representative of modern design and affords a direct comparison with the results of reference 4. The transition from the U.S.A. 45 to the N.A.C.A. 23017 section was extended over approximately one-half the semispan. For convenience in changing duct inlets, the portion of the center section extending from the leading edge to the 20-percent-chord point was made readily detachable. The duct span extended over 8.38 percent of wing span. The wing, including a typical duct installation, is shown in figure 1. The center section was covered with sheet aluminum and the internal structure was arranged so that there were no obstructions except the radiator to the air flow through the duct passages. A 20-percent chord, split trailing-edge flap, with a span equal to the standard duct width, was installed at the center section.

Radiator

A perforated flat plate was used in these tests to simulate a radiator. This plate, hereafter referred to as the "radiator", had 3/4-inch holes spaced on 1-inch centers, and measured 15 by 46 by 1 inches. Since large expansion ratios were desired, the radiator height used was determined by the maximum which could be installed in the given thickness of the wing. Calibration tests showed that this radiator gave a static-pressure drop of approximately four times the face dynamic pressure, which is in close agreement with the pressure drop across a standard Army Air Corps 0.230- by 0.360- by 9-inch radiator core.

Although the basic radiator was used for all the tests, other cooling installations, including a baffled air-cooled engine, were simulated by increasing the radiator pressure drop. This was accomplished by placing wire screens of 16 and 40 meshes per inch behind the radiator and plugging a number of the radiator holes. Relative pressure drops for each arrangement, as determined by preliminary tests of the radiator installed in a duct, are plotted in figure 2 as functions of the velocity at the radiator face. Some scale effect is evident, especially for the higher pressure-drop arrangements.

Twenty-five pairs of static-pressure and total-head tubes were built into the radiator for the purpose of determining the quantity of air passing through the ducts. The method of installation was similar to that described in reference 4. Calibrations showed that the dynamic pressure measured by the tubes was directly proportional to the dynamic pressure immediately ahead of the radiator and that the arrangement was not sensitive to changes in air direction. To simplify the measuring equipment, the tubes were confined to one-half the radiator width, symmetrical flow being assumed about the vertical center line of the radiator. A photographically recording, multiple-tube manometer was employed to record the tube pressures.

Ducts

The various radiator-duct combinations tested are classified under three general headings:

1. Through duct.

2. Underslung duct.

3. Cross-wing duct.

The radiator was located at the maximum section of each duct. All ducts were mounted at the center section of the wing and were rectangular in cross section. A standard duct width of 46 inches (8.38 percent of the wing span) was maintained for all combinations except those termed "narrow duct." With the exception of the restricted inlet combinations, expansion occurred only in the vertical plane. Duct dimensions are given in percentages of the N.A.C.A. 23017 center-section chord, unless otherwise noted. Inlet and outlet sizes are specified as minimum distances between upper and lower duct surfaces.

Through duct.- The through duct was mounted entirely within the wing, the radiator being located 0.5c behind the leading edge. The ratio of the area at the inlet to the radiator area varied with inlet size from 1/1.7 to 1/3.9. Adjustable upper and lower duct surfaces provided uniform expansion for each installation.

Inlet openings were formed by replacing the plain wing nosepiece with combinations of upper and lower noses. These noses had a leading-edge radius of 0.005c as recom-

mended in reference 4. The six upper noses used are shown in combination with a typical lower nose in figure 3. The position of the first break in the wing surface caused by each upper nose is noted and becomes the designation for that nose. Figure 4 shows the five lower noses used. Combination of these upper and lower noses gave a range of inlet sizes from 0.033c to 0.08c. A typical through duct inlet is shown in figure 5.

As previous tests (reference 4) indicated that variations in outlet position on the upper surface of wing from 0.60c to 0.75c had negligible effects on duct characteristics, the outlet position was held within these limits in providing outlet openings varying in size from 0.02c to 0.08c (fig. 6a). Figure 7 shows an 0.08c outlet installation. An alternate type of outlet (fig. 6c) was provided by the deflection of the 0.20c trailing-edge split flap, which is shown deflected 15° in figure 8.

Devices for regulating the air flow by varying the duct openings in flight were installed on several through duct combinations. The inlet flap shown in figures 6b and 9 resembled an airfoil in cross section and was hinged at its leading edge. Deflection of this flap had an effect equivalent to moving the inlet position rearward and gave a variation of inlet size from 0.033c to 0.074c. Two types of outlet flaps were tested. Type A, shown in figure 6b, was used with a normal 0.06c outlet and varied the outlet size from 0.02c to 0.06c. Type B (fig. 6f) resembled a symmetrical airfoil in cross section and was hinged about its trailing edge. In the closed position this flap conformed to the contour of the upper wing surface and restricted the outlet size to 0.04c; with the flap deflected the outlet size was 0.08c.

Narrow ducts were formed by blocking off approximately one-half the standard duct width as shown in figure 10. The spanwise width of the narrow duct was 24 inches.

Restricted inlets were formed by blocking off one-third or two-thirds of the width of inlet of the standard duct. The side walls behind the inlet expanded to the standard duct width at the radiator. This modification was applied to one of the arrangements having a 0.06c inlet size; the resulting expansion ratios were 1/3.2 and 1/6.5.

Underslung duct.- Details of the underslung duct arrangement appear in figure 6d. The radiator was located 0.46c behind the leading edge and extended below the wing. The lower cowling and the straight duct side walls were attached to the radiator and the entire assembly was retractable. The upper duct surface was formed within the wing and was slotted to allow vertical movement of the radiator. Inlet size, outlet size, and exposed radiator area varied with the amount of radiator extension. The expansion ratio for a given inlet size was varied by altering the upper duct surface. Figure 11 shows a typical underslung duct installation.

Cross-wing duct.- The cross-wing duct (fig. 6e) had an underslung-duct inlet and a normal through-duct outlet. The radiator was inclined to the chord line, its center being located approximately 0.50c behind the leading edge. Movements of the hinged inlet lip varied the inlet size from 0.04c to 0.08c. Outlet variations were identical to those shown for the through duct in figure 6a.

Duct designation.- This report employs the same system of duct designation described in reference 4. Each duct arrangement is represented by four terms, grouped as follows:

Inlet size.

Inlet position.

Outlet size.

Outlet position.

Inlet and outlet sizes were previously defined; the method for specifying inlet and outlet positions is indicated in figure 6. For the through duct, the inlet position is specified by giving the upper nose designation. (See fig. 3.) The meaning of symbols, consisting of letters and numbers, that comprise the four terms of the various duct designations are tabulated below. The interpretations of five sample duct designations follow the table.

TERM AND SIGNIFICANCE	TYPICAL SYMBOLS	MEANING OF SYMBOLS
First: Minimum size of inlet opening	3.5, 6.0	Linear dimension of inlet size (fig. 6)
	F1, F4	One of five inlet flap positions (fig. 6b)
Second: Inlet position	1,5	Distance of inlet position behind leading edge of wing (figs. 3 and 6)
	2a, 4a	Distance of inlet position above chord line (fig. 3)
	L31	Inlet opening located below wing (figs. 6d and 6e)
Third: Minimum size of outlet opening	2, 4	Linear dimension of outlet size (fig. 6)
	A2	One of two type-A outlet flap positions (fig. 6b)
	B3	One of three type-B outlet flap positions (fig. 6f)
	F5, F10	Trailing-edge outlet flap deflected 5°, 10°, etc. (fig. 6c)
Fourth: Outlet position	61, 75	Distance of outlet position behind leading edge of wing (fig. 6)
	TE	Trailing-edge split flap used as outlet
	L57	Outlet opening located below wing (fig. 6d)

4.6 - 2a - 2 - 75 represents a through duct (no letter "L" appears), minimum inlet opening 4.6 percent of center-section chord (first term), inlet position 2 percent above chord line (second term), minimum outlet opening 2 percent of chord (third term), outlet position 75 percent of chord behind leading edge (fourth term).

6.0 - 0 - F15 - TE indicates a through duct, 6 percent inlet, inlet position at intersection of chord line and wing surface, trailing-edge outlet flap deflected 15°, outlet at trailing edge of wing.

F1 - 2a - B3 - 61 indicates a through duct, inlet flap in position 1, inlet position 2 percent above chord line, outlet flap B in position 3, 61 percent outlet position.

4.0 - L31 - 6 - 65 indicates a cross-wing duct ("L" in second term but not in fourth), 4 percent inlet, 31 percent inlet position with opening below wing, 6 percent outlet, 65 percent outlet position.

3.5 - L31 - 3.5 - L57 indicates an underslung duct ("L" in second and fourth terms), 3.5 percent inlet, 31 percent inlet position with opening below wing, 3.5 percent outlet, 57 percent outlet position with opening below wing.

Tests

The tests were made in the N.A.C.A. full-scale wind tunnel (reference 6). Figure 12 shows the plain wing (without duct) mounted in the wind tunnel. Lift and drag of the plain wing were measured over the complete angle-of-attack range from below zero lift to maximum lift. Similar tests were made with each duct arrangement installed in the wing. Measurements of the air velocity in the duct at the radiator face were taken at lift coefficients of approximately 0, 0.2, 0.6, and 1.0.

All combinations were tested at a tunnel velocity of approximately 60 miles per hour. A number of combinations were tested at various air speeds from 25 to 100 miles per hour to determine possible scale effects.

SYMBOLS

C_L, wing lift coefficient.

c_l, center-section lift coefficient.

c, wing chord at center section.

S, area of wing.

A_I, minimum area of duct inlet opening.

A_R, radiator frontal area.

Q, quantity of air passing through radiator $(A_R V_R)$.

V, air velocity in free stream, or flight speed.

V_R, air velocity in duct at radiator face.

q, free stream dynamic pressure $(\frac{1}{2} \rho V^2)$.

q_R, radiator face dynamic pressure $(\frac{1}{2} \rho V_R^2)$.

ΔP, pressure drop across the radiator.

K, relative pressure drop $(\Delta P/q_R)$.

ΔD, drag increment of radiator-duct combinations.

$V_{R/V}$, flow ratio.

η, duct efficiency.

P_T, power required for cooling.

C_P, cooling power coefficient $C_P = \frac{(V_{R/V})^2}{\eta}$

RESULTS AND DISCUSSION

The important radiator-duct characteristics are given by means of three parameters, $V_{R/V}$, η, and C_P. The air-flow ratio, $V_{R/V}$, is the ratio of the air velocity

at the face of the radiator to the free stream air velocity and is a measure of the quantity of air that will flow through the duct.

The duct efficiency, η, is the ratio of the useful power expended in forcing air through the radiator core to the total power required to overcome the added drag due to the radiator-duct installation. (Power due to changes in radiator weight is omitted throughout the discussion.)

$$\eta = \frac{\text{useful work}}{\text{total work}} = \frac{Q\Delta P}{\Delta DV} .$$

$$Q = A_R V_R$$

$$\Delta P = Kq_R$$

$$\Delta D = \Delta C_D q S$$

$$\eta = \frac{KA_R V_R q_R}{\Delta C_D q S V}$$

$$\eta = \frac{KA_R}{\Delta C_D S} \left(V_{R/V}\right)^3 .$$

It is important to note that η is a measure of the "duct efficiency" and does not indicate the optimum "radiator-duct" combination.

The power coefficient C_P is given as a figure of merit for comparing the various radiator-duct combinations, the optimum radiator-duct arrangement having the lowest value of C_P.

The total power required for cooling is:

$$P_T = \Delta DV = \Delta C_D q S V$$

Substituting

$$\Delta C_D = \frac{KA_R}{\eta S} \left(V_{R/V}\right)^3$$

and

$$A_R = \frac{Q}{V_R}$$

Then

$$P_T = C_P K Q q$$

in which

$$C_P = \frac{(V_{R/V})^2}{\eta}$$

The total power required for a given radiator-duct combination depends therefore on the power coefficient, air quantity, relative pressure drop through radiators, and the free-stream dynamic pressure.

The duct parameters $V_{R/V}$, and η are plotted against C_L in figures 13 to 28 for all the test arrangements, and a summary of the important duct characteristics for the representative high speed and climb C_L values of 0.2 and 0.7 is given in table I. No important scale effect on $V_{R/V}$ or η was found (fig. 29), so that the data for test speeds other than 60 miles per hour are not shown.

In general, the maximum lift was not affected appreciably by the better duct arrangements. Serious adverse effects were noted for only one arrangement, the through duct with the 4a inlet position. Slight increases occurred in several cases. Typical lift curves for various duct arrangements are shown in figure 30. The angle-of-zero lift was affected but slightly by the presence of the duct.

Through-Duct Characteristics

Inlet size.- The variations in $V_{R/V}$ and η with inlet size for the high-speed attitude ($C_L = 0.2$) are shown in figure 31. For each curve, the inlet position, outlet size, and outlet position are constant. Results for the 2a nose with 6- and 8-percent outlets indicate that best duct efficiency is obtained with an inlet somewhat smaller than the outlet. The flow ratio, $V_{R/V}$, is not affected by changes in inlet size, except for inlet

sizes considerably smaller than those for best efficiency. The power coefficient, C_P, is therefore lowest for the ducts of highest efficiencies. These trends are similar for the 0 nose except that inlet size variations have little effect on efficiency.

At the climb condition ($C_L = 0.7$, table I), efficiency tends to increase as the inlet size increases. Results for the 2a and 0 noses are somewhat erratic, especially for the 2- and 4-percent outlets. The effects of inlet size on $V_{R/V}$ and C_P are similar to those noted for the high-speed condition.

It was noted from the velocity distribution measurements at the radiator that when the inlet size became so small that the included expansion angle in the duct exceeded about 9° to 10°, flow separation occurred at the duct walls, and the flow measurements became erratic. The results obtained with duct inlet sizes smaller than 4 percent are therefore somewhat less consistent than those for the larger inlets.

Inlet position.- The curves of figure 32a, plotted for the high-speed condition, indicate that inlet position is the most critical factor in duct design. As the inlet position moves forward and above the chord line both the flow ratio and efficiency increase. As the inlet position is moved below the chord and toward the trailing edge, the flow decreases until a point is reached where there is no flow. At the climb condition (fig. 32b), due to the changed pressure distribution over the wing, the 0 or 1 nose gives the greatest flow ratio and efficiency; and in contrast to the high-speed condition, $V_{R/V}$ varies but slightly with inlet position.

These results indicate for an optimum duct arrangement that the inlet position should vary with the lift coefficient and the inlet flap arrangement is suggested for this purpose in a later chapter.

Outlet size.- Figure 33 shows the effect of outlet size on η and $V_{R/V}$ for the high-speed condition. These curves are shown for a 6-percent inlet with three different nose positions, 2a, 0, and 3. In each case the flow ratio increases almost directly with the outlet size. Results for the climb condition are similar. This trend is

consistent with previous tests (reference 4), indicating that the air flow can be readily controlled at the outlet.

For the 2a nose, an outlet size equal to or slightly greater than the inlet size gives best efficiency at high speed. The power coefficient is approximately constant for outlet sizes of 6 percent or smaller but increases for the 8-percent outlet. For the 0 nose with 6-percent inlet ($C_L = 0.2$) the efficiency does not peak within the limits of the test, increasing directly with outlet size. The outlet size for maximum efficiency will probably be only slightly larger than 8 percent. The power coefficient tends to be minimum for the 6-percent outlet, but variations with outlet size are small.

For the climb condition, all inlet sizes and positions tested show best duct efficiencies with the 6-percent outlet. The power coefficient, however, increases with outlet size with the rate of increase becoming markedly greater for outlet sizes greater than 6 percent.

Outlet position.- The effect of varying the outlet position has not been studied in this investigation. To aid in the design of the various ducts, the outlet position was allowed to vary from the 61- to 75-percent-chord position; however, the results of reference 4 have shown that these variations do not appreciably change the duct characteristics.

Narrow duct.- The results of reference 4 indicate that best section efficiencies are obtained with maximum radiator heights, which might imply the use of the narrowest possible duct for any given cooling installation. The duct efficiencies for finite span ducts, however, decrease as the duct spans become smaller owing to the end losses. To study the effects of the duct ends on the efficiency, tests of a duct having approximately one-half the standard duct width were made using a 6.0-0 inlet with four different outlets. The results are plotted in figure 25 and compared to characteristics for similar ducts of standard width in figure 34.

The narrow-duct characteristics show the same trend as those for the standard duct for lift coefficients below 0.7. At the higher lift coefficients, efficiencies for the narrow duct decrease, whereas this is true for the standard duct only when the 8-percent outlet is used. It

should be noted that the duct end effects are particularly large when the duct is throttled by the small outlets, whereas when the duct outlet is opened and a large flow occurs the end effects become relatively unimportant. This may be due to the disturbed flow over the sharp edges of the duct at the leading edge, and indicates the desirability of rounding the side entries of the duct to obtain high efficiencies in the high-speed conditions.

Restricted-inlet duct.- Throttling the air flow by varying the span of the inlet has been suggested, and the results of several tests with an arrangement in which the inlet was restricted to two-thirds and one-third the full radiator span, are shown in figure 24. The test data for the one-third opening were erratic and unreliable owing to the excessive rate of expansion of the air along the side walls of the duct. The flow ratios for the two-thirds opening and for an inlet with no restrictions are essentially the same. These results indicate that throttling by spanwise restriction of the inlet opening may be unsatisfactory since if the inlet is closed sufficiently to throttle the air flow, breakdown in flow occurs on the duct side walls with resultant loss in efficiency.

Change in pressure drop.- The data in table I are directly applicable to the design of radiator-duct installations only when the design radiator has approximately the same relative pressure drop as the test radiator. A limited number of tests were made to determine the effect of variations in radiator pressure drop on the duct characteristics. These tests were confined to the 6.0-2a inlet with four different outlets. The resistance in the duct was varied from the condition of full closed ($K = \infty$) to full open ($K = 0$), and the results are shown in figure 26. The highest efficiency was obtained for all arrangements with a relative pressure drop $K = 13.2$.

Variations of $V_{R/V}$, η, and ΔC_D with relative pressure drop are shown in figure 35 for $C_L = 0.2$. The function $\frac{1}{\sqrt{1 + K}}$ is used mainly for convenience in the plotting. Dotted portions of the efficiency curves have been extrapolated.

Figures 36 and 37 are presented as aids in converting the $V_{R/V}$ and C_P values given in table I to approxi-

mately comparable values for a given design pressure drop other than that for the standard radiator used for the tests.

Inlet flap.- Inasmuch as the data on inlet positions (fig. 32) indicated that the optimum position for the inlet occurred with nose 2a or 4a in the high-speed condition and with nose 0 or 1 in the climb condition, an inlet flap was designed (fig. 6b) by means of which it was possible to change from a small inlet in position 2a in the high-speed condition to a larger inlet extending well below the chord line for climb. Best efficiencies could then be obtained in both the high-speed and climb conditions. It was found that ducts having an inlet flap in these two positions show characteristics (fig. 17 and table I) very similar to those for plain through duct with inlet and outlets in similar positions.

The inlet opening for the closed flap position (F1) was 3.3 percent of the chord; and, as previously mentioned, the results tend to be inconsistent owing to the too rapid expansion in the inlet, and an opening of 4.6 percent would probably be preferable.

Outlet flaps.- The purpose of the outlet flaps is to control the amount of air flow through the duct by varying the outlet size so that the required $V_{R/V}$ value may be obtained for all flight conditions.

The type-A outlet flap, used in combination with the plain 6-percent outlet, effectively throttles the flow. The A4 position gives approximately the same flow ratio obtained previously with the plain 4-percent outlet; similarly, the A2 position may be compared to the plain 2-percent outlet (fig. 18 and table I). The efficiencies and power coefficients, although somewhat erratic, tend to be higher for these flapped outlets than for the straight outlets providing the same $V_{R/V}$ ratio.

Figures 19 to 21 show test results for the type-B outlet flap. The B1 position corresponds to a 4-percent plain outlet; the B3 position corresponds to an 8-percent plain outlet. Approximately the same flow ratios are shown for corresponding plain and flapped outlets (table I), and the power coefficients are essentially the same. The characteristics of the type-B flap may therefore be predicted with considerable accuracy from the data on the corresponding through ducts.

In comparing the relative merits of flaps A and B it will be noted (table I) that in many cases the flaps are of equal merit; however, in several cases flap B appears to be superior.

Combined inlet and outlet flaps.- The foregoing discussion indicates that a duct arrangement combining the advantages of inlet and outlet flaps will be superior to any other through-duct arrangement. A limited number of tests were made with a through-duct arrangement having a 2a nose, inlet flap, and type-B outlet flap. The results are shown in figure 22 and table I. In general, the flap combinations duplicated the performance of similar plain ducts.

These results are shown mainly to indicate the possibilities of flap combinations. At the time the tests were made, sufficient information was not available for selecting an optimum arrangement. For example, the inlet opening of 3.3 percent of the chord selected for high speed is not the best (see section on "Inlet Flap"), and further the plain-duct results show that a 2-percent outlet would give better efficiency at high speed than the 4-percent outlet tested (flap in position B1). A study of table I indicates that a flap which varies the inlet from 4.6-2a to 7.4-2a used in combination with an outlet flap having a range from 2 percent to 6 percent will provide an arrangement superior to the one tested.

The use of the outlet flap will be necessary in a practical design both to properly control the air quantity and to reduce the cooling power required in high-speed flight. The inlet flap may in many cases not be needed, and by reference to table I it may be noted that ducts with excellent efficiency may be designed without the inlet flap. For the best possible arrangement, however, both flaps are required.

Trailing-edge flap outlet.- Test results for the trailing-edge split-flap outlet are shown in figure 23 and table I. In general, this outlet is inferior to the normal through-duct outlet. The flow ratio increases with flap deflection for both high speed and climb, but power coefficients are excessively high for the larger deflections. At $C_L = 0.2$, the 5° flap position shows erratic results, indicating an irregular velocity distribution at the radiator. In one case (6.0 - 1 - F5 - TE), negative flows

were indicated and the results were therefore omitted from table I.

Underslung Duct

The results of the tests on the underslung ducts are shown in figure 27. Both the flow ratio and power coefficient for any given inlet size are higher than for the corresponding through-duct arrangement. The flow ratio $(V_{R/V})$ does not change appreciably with the lift coefficient; however, the efficiency and power coefficient are more favorable at climb.

The effect of the expansion between the inlet and the radiator on the power coefficient, C_P, is shown in figure 38. These data indicate that for the same air quantity the minimum power consumption is obtained with a large expansion ratio. Flow separation in the inlet will no doubt limit the gain possible from larger expansion ratios.

By retracting the radiator and cowling for the high-speed condition, a minimum value of $C_P = 0.18$ was obtained for the high-speed condition. Comparison with the best C_P values of about 0.10 obtained with the through ducts indicates the relative merits of the installations tested. More extensive tests with underslung cowlings are recommended, particularly with ducts having well-rounded entries on the side walls and greater lengths of expansion passages to reduce the expansion angle.

Cross-Wing Duct

Results on the cross-wing duct, which is essentially a hybrid arrangement between the underslung and through duct, are given in figure 28. The flow ratio is satisfactory for all cases with little variation between the high-speed and climb conditions (a characteristic of all scoop-type inlets). The duct efficiencies are consistently low, however, and the power coefficients correspondingly high. The poor performance of this arrangement is attributed to the rapid expansion in the inlet and to the exposed inlet scoop.

Comparison with Section Characteristics

A comparison of the results of this report with those

of reference 4 appears in table II. The "full"-span data (taken directly from reference 4) are compared with the finite-span results on a basis of equal section lift coefficients. The tests of reference 4, as noted elsewhere, were made so as to give section characteristics directly, while in the finite-span tests of this report the section lift was determined by calculation from pressure-distribution measurements at the center section.

In general, the finite arrangements give slightly lower flow ratios, lower efficiencies, and require more power. This inferior performance is caused by the end losses of the finite duct and the induced drag effects not included in the section characteristics.

Although in certain cases the power consumption of the finite-span duct is as much as 50 percent greater than that of the infinite-span duct, the total power will in most cases be sufficiently small so that this apparently large discrepancy may amount to only 1 or 2 percent of total engine horsepower.

APPLICATION TO DESIGN

A satisfactory duct-cooling installation should fulfill the following requirements:

1. Provide sufficient cooling air for all flight conditions.

2. Expend a minimum power, particularly in the high-speed condition.

In the latter requirement the total power should include both the cooling power and that required to overcome the induced drag due to the radiator weight.

The following procedure for designing radiator-duct combinations from the data given in this report is tentatively suggested. Knowing values of K and Q for any given design, a radiator area is assumed for a trial calculation, and the V_R necessary to provide the required air quantity is computed. Values of $V_{R/V}$ are then determined from the known or estimated high speed and climbing speed. Duct and flap arrangements giving the required

$V_{R/V}$ for high speed and climb are noted (table I and figures). A comparison of the high-speed and climb C_P values will then indicate the best arrangements for the area chosen and the cooling horsepower required may be computed from the power equation.

A typical example of radiator-duct computation for an airplane operating at sea level will be used to illustrate the suggested design procedure. The same type radiator core, flight conditions, and cooling requirements assumed in presenting a similar example in reference 4 are used here:

Rated horsepower at high speed and climb = 1,000 horsepower.

Maximum speed ($C_L = 0.25$) = 284 feet per second (194 miles per hour)

Best speed for climb ($C_L = 0.7$) = 170 feet per second (116 miles per hour)

Radiator - Army Air Corps 0.230- by 0.260- by 9-inch core, K = 3.7.

Cooling air quantity required, engine radiator and oil cooler, Q = 283 cubic feet per second.

For an assumed radiator area of 6.25 square feet, the required V_R is 45.3 feet per second.

Therefore

$$V_{R/V_{(C_L = 0.25)}} = \frac{45.3}{284} = 0.16$$

$$V_{R/V_{(C_L = 0.7)}} = \frac{45.3}{170} = 0.27$$

The difference in pressure drop between the design radiator (K = 3.7) and the test radiator (K = 4.1) is small; however, for illustrative purpose allowance will be made for the difference.

From figure 36

$$(V_{R/V})_{test} = 0.98\ (V_{R/V})_{design}$$

Therefore

$$(V_{R/V})_{(C_L=0.25)} = 0.16 \times 0.98 = 0.157$$

$$(V_{R/V})_{(C_L=0.7)} = 0.27 \times 0.98 = 0.265$$

From figure 13 (table I is applicable only for C_L = 0.2) at $C_L = 0.25$.

Designation	$V_{R/V}$	η	P_C (computed)
4.6 - 2a - 2 - 75	0.16	26	0.10
6.0 - 2a - 2 - 75	.16	21	.12

It is evident from table I that either of these arrangements can be converted to a 7.4 - 2a - 8 - 61 arrangement for climb by the use of inlet and outlet flaps. This duct combination has a $V_{R/V}$ of 0.28 and a C_P of 0.10 at $C_L = 0.7$. Since duct arrangement 4.6 - 2a - 2 - 75 has the lower value of C_P at $C_L = 0.25$, it is chosen for the high-speed condition.

The C_P values of table I are now converted to the equivalent design values by the use of figure 37.

$$C_{P\ high\ speed} = 0.10 \times 1.03 = 0.103$$

$$C_{P\ climb} = 0.10 \times 1.03 = 0.103$$

The high-speed and climb power requirements may now be obtained by substitution in the power equation

$$HP_T = \frac{C_P K Q q}{550}$$

(high speed) $HP_T = \frac{0.103 \times 3.7 \times 283 \times 96}{550} = 18.8$ horsepower

or 1.88-percent engine power

(climb) $HP_T = \frac{0.103 \times 3.7 \times 283 \times 34.4}{550} = 6.7$ horsepower

or 0.67-percent engine power

After similar computations have been made for several different assumed radiator areas and the weight horsepower for each arrangement determined, the best radiator duct arrangement can be selected.

In the event that the radiator duct is to be placed in a wing section other than the N.A.C.A. 23017 used for this investigation, ducts having the same characteristics as those reported herein could undoubtedly be designed by the aid of a comparison of the pressure distributions for the N.A.C.A. 23017 and the design section. It is particularly important that the inlet occupy the same relative position to the stagnation point on the design section as occurs on the N.A.C.A. 23017 section.

CONCLUDING REMARKS

The characteristics of finite-span cooling ducts are in substantial agreement with section characteristics previously obtained for full-span ducts in two-dimensional flow (reference 4). The quantity of air that will flow through the duct may be predicted with considerable accuracy from the section data; however, the power absorbed by the duct will be underestimated unless consideration is given to the loss at the duct ends. The results show that for the usual cases these duct-end losses will not exceed 1 percent to 2 percent of the engine power. Tests of ducts of several widths showed that the losses due to the duct ends are greatest when the flow through the duct is restricted. Rounding of the entry of the duct at the side walls is suggested.

For satisfactory air-flow control and low power consumption at high speed, a flap should be provided at the

duct outlet. For optimum duct performance at both the high-speed and climb conditions, both an inlet and outlet flap are required. The results showed that an outlet through the upper surface was superior to a flapped outlet through the trailing edge.

The underslung duct arrangements tested were less efficient than the ducts within the wing; however, they were efficient enough to merit design consideration for cases in which through ducts are structurally impossible.

The duct characteristics showed no important scale effects within the test Reynolds Number range of 4,000,000 to 10,000,000.

Langley Memorial Aeronautical Laboratory,
National Advisory Committee for Aeronautics,
Langley Field, Va., August 26, 1938.

REFERENCES

1. Meredith, F. W.: Note on the Cooling of Aircraft Engines with Special Reference to Ethylene Glycol Radiators Enclosed in Ducts. R. & M. No. 1683, British A.R.C., 1936.

2. Worth, Weldon: Bigger and Better Radiators. Aviation, vol. 34, no. 8, August 1935, pp. 19-21.

3. Silverstein, Abe, and Nickle, F. R.: Preliminary Full-Scale Wind-Tunnel Investigation of Wing Ducts for Radiators. N.A.C.A. Advanced Conf. Memo. Report, March 1938.

4. Harris, Thomas A., and Recant, Isidore G.: Investigation in the 7- by 10-Foot Wind Tunnel of Ducts for Cooling Radiators within an Airplane Wing. T.R. No. (to be published), N.A.C.A., 1938.

5. Parsons, John F.: Full-Scale Force and Pressure-Distribution Tests on a Tapered U.S.A. 45 Airfoil. T.N. No. 521, N.A.C.A., 1935.

6. DeFrance, Smith J.: The N.A.C.A. Full-Scale Wind Tunnel. T.R. No. 459, N.A.C.A., 1933.

Table I AERODYNAMIC CHARACTERISTICS OF DUCTS

Typical diagram	Arrangement	$C_L = 0.2$			$C_L = 0.7$			Figure No.
		V_R/V	η	C_p	V_R/V	η	C_p	
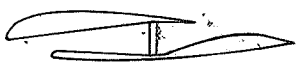	6.0-4a-8-61	.31	.64	.15	.29	.32	.26	16a
	7.2-4a-8-61	.31	.60	.16	.32	.48	.21	
	8.0-4a-8-61	.31	.57	.17	.32	.63	.16	
	4.6-2a-2-75	.15	.23	.10	.14	.31	.06	13a
	6.0-2a-2-75	.15	.18	.12	.14	.29	.07	
	4.6-2a-4-70	.22	.41	.12	.20	.45	.09	14a
	6.0-2a-4-70	.22	.39	.12	.21	.39	.11	
	4.6-2a-6-65	.27	.65	.11	.23	.50	.11	15a
	6.0-2a-6-65	.26	.58	.12	.27	.64	.11	
	7.4-2a-6-65	.26	.46	.15	.28	.81	.10	
	4.6-2a-8-61	.28	.42	.19	.26	.24	.28	16b
	6.0-2a-8-61	.31	.54	.18	.31	.47	.20	
	6.9-2a-8-61	.31	.58	.17	.32	.70	.15	
	7.4-2a-8-61	.31	.54	.18	.33	.65	.17	
	3.3-0-2-75	.12	.16	.09	.13	.70	.02	13b
	6.0-0-2-75	.12	.07	.21	.15	.55	.04	
	3.3-0-4-70	.16	.16	.16	.17	.31	.09	14b
	6.0-0-4-70	.17	.16	.18	.23	.91	.06	
	3.3-0-6-65	.18	.13	.25	.19	.19	.19	15b
	6.0-0-6-65	.21	.24	.18	.29	.89	.09	
	6.9-0-6-65	.21	.20	.22	.29	.94	.09	
	4.9-0-8-61	.27	.35	.21	.30	.41	.22	16c
	6.0-0-8-61	.27	.33	.22	.33	.51	.21	
	6.9-0-8-61	.27	.33	.22	.33	.60	.18	
	5.0-1-8-61	.27	.40	.18	.32	.46	.22	16d
	6.0-1-8-61	.27	.34	.21	.33	.64	.17	
	6.3-1-8-61	.28	.36	.22	.33	.66	.17	
	4.4-3-6-65	.03	0	–	.25	.49	.13	15c
	6.0-3-6-65	.03	0	–	.28	.53	.15	
	2.9-3-8-61	.05	0	–	.16	.07	.36	16e
	4.4-3-8-61	.07	0	–	.32	.54	.19	
	6.0-3-8-61	.07	0	–	.32	.49	.21	
	3.6-5-8-61	.02	0	–	.22	.17	.28	16f
	5.2-5-8-61	.02	0	–	.30	.38	.24	
	6.0-5-8-61	.05	0	–	.31	.43	.22	
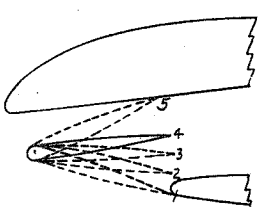	F1-2a-2-75	.17	.28	.10	.09	.06	.10	17a
	F1-2a-4-70	.16	.14	.18	.12	.05	.29	17b
	F1-2a-6-65	.17	.11	.26	.13	.06	.28	17c
	F1-2a-8-61	.20	.15	.27	.15	.06	.37	17d
	F2-2a-8-61	.25	.29	.22	.23	.19	.28	17d
	F3-2a-8-61	.30	.53	.17	.29	.37	.23	17d
	F4-2a-2-75	.14	.09	.22	.15	.69	.03	17a
	F4-2a-4-70	.20	.25	.16	.21	.61	.07	17b
	F4-2a-6-65	.25	.40	.16	.27	.74	.10	17c
	F4-2a-8-61	.30	.48	.19	.32	.51	.20	17d
	F5-2a-2-75	0	0	–	.14	.21	.09	17a
	F5-2a-4-70	0	0	–	.20	.31	.10	17b
	F5-2a-6-65	0	0	–	.27	.45	.16	17c
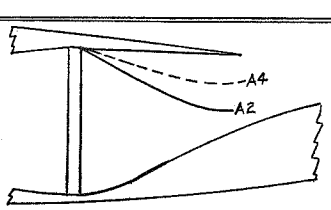	6.0-2a-A2-65	.14	.10	.20	.14	.08	.24	18b
	6.0-0-A2-65	.11	.05	.24	.14	.08	.24	18c
	4.6-2a-A4-65	.25	.50	.13	.21	.30	.15	18a
	6.0-2a-A4-65	.23	.30	.18	.23	.30	.18	18b
	6.0-0-A4-65	.17	.18	.16	.23	.49	.11	18c

Table I AERODYNAMIC CHARACTERISTICS OF DUCTS

Typical diagram		Arrangement	$C_L = 0.2$ V_R/V	η	C_p	$C_L = 0.7$ V_R/V	η	C_p	Figure No.
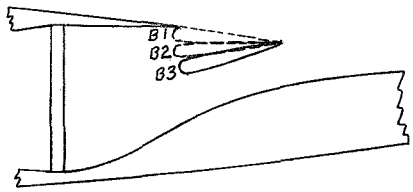		4.6-2a-B1-61	.21	.35	.13	.19	.38	.10	19a
		4.6-2a-B2-61	.28	.40	.20	.25	.32	.20	20a
		4.6-2a-B3-61	.30	.37	.24	.27	.24	.30	21a
		6.0-2a-B1-61	.21	.40	.11	.20	.46	.09	19a
		6.0-2a-B2-61	.29	.52	.16	.29	.65	.13	20a
		6.0-2a-B3-61	.32	.51	.20	.32	.46	.22	21a
		7.4-2a-B1-61	.20	.27	.15	.20	.55	.07	19a
		7.4-2a-B2-61	.29	.45	.19	.30	.69	.13	20a
		7.4-2a-B3-61	.33	.53	.21	.33	.58	.19	21a
		3.3-0-B1-61	.16	.14	.18	.16	.32	.08	19b
		3.3-0-B2-61	.20	.16	.25	.20	.14	.29	20b
		3.3-0-B3-61	.21	.13	.34	.21	.12	.37	21b
		6.0-0-B1-61	.17	.15	.19	.20	.60	.07	19b
		6.0-0-B2-61	.26	.30	.23	.30	.62	.15	20b
		6.0-0-B3-61	.29	.32	.26	.33	.51	.21	21b
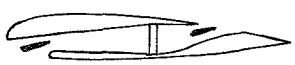		F1-2a-B1-61	.15	.15	.15	.12	.09	.16	22
		F4-2a-B2-61	.28	.49	.16	.30	.69	.13	
		F4-2a-B3-61	.32	.51	.20	.33	.56	.19	
		F5-2a-B3-61	0	0	—	.34	.43	.27	
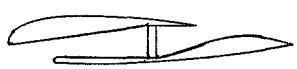	Restricted inlet $\frac{2}{3}$ open	6.0-0-8-61	.25	.29	.21	.30	.44	.20	24b
		6.0-0-6-65	.22	.25	.19	.28	.49	.16	
		6.0-0-A4-65	.19	.20	.18	.24	.32	.18	
	Restricted inlet $\frac{1}{3}$ open	6.0-0-8-61	0	0	—	.21	.14	.32	24a
		6.0-0-6-65	0	0	—	.19	.15	.24	
		6.0-0-A4-65	.16	.14	.18	.17	.12	.24	
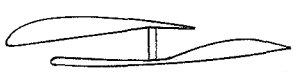	Narrow duct 2' wide	6.0-0-2-75	.09	.02	.40	.14	.31	.06	25
		6.0-0-4-70	.16	.09	.28	.21	.51	.09	
		6.0-0-6-65	.22	.19	.25	.27	.61	.12	
		6.0-0-8-61	.26	.26	.26	.30	.51	.18	
 Higher pressure drop thru radiator	K								
	5.1	6.0-2a-8-61	.29	.56	—	.30	.49	—	26d
	10	6.0-2a-8-61	.24	.60	—	.25	.56	—	26d
	13.2	6.0-2a-2-75	.13	.31	—	.13	.98	—	26a
	13.2	6.0-2a-4-70	.18	.52	—	.18	.76	—	26b
	13.2	6.0-2a-6-65	.21	.60	—	.21	.66	—	26c
	13.2	6.0-2a-8-61	.23	.63	—	.24	.65	—	26d
	100	6.0-2a-2-75	.07	.27	—	.08	.70	—	26a
	100	6.0-2a-4-70	.09	.40	—	.09	.56	—	26b
	100	6.0-2a-6-65	.09	.35	—	.09	.50	—	26c
	100	6.0-2a-8-61	.10	.35	—	.09	.31	—	26d
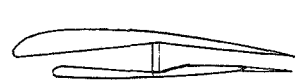		6.0-2a-F5-TE	.10	.07	.14	.11	.13	.09	23a
		6.0-2a-F10-TE	.19	.25	.14	.21	.39	.11	
		6.0-2a-F15-TE	.25	.36	.17	.26	.41	.17	
		6.0-0-F5-TE	0	0	—	.13	.13	.13	23b
		6.0-0-F10-TE	.12	.09	.16	.22	.37	.13	
		6.0-0-F15-TE	.20	.23	.17	.27	.40	.18	
		6.0-0-F25-TE	.31	.23	.42	.35	.43	.28	
		6.0-1-F5-TE	—	—	—	.13	.14	.12	23c
		6.0-1-F10-TE	.19	.12	.30	.21	.35	.13	
		6.0-1-F15-TE	.24	.19	.30	.27	.40	.18	

Table I AERODYNAMIC CHARACTERISTICS OF DUCTS

Typical diagram	Radiator Size - inches	Arrangement	$C_L = 0.2$ V_R/V	η	C_p	$C_L = 0.7$ V_R/V	η	C_p	Figure No.
		4.0-L31-6-65	.18	.12	.27	.22	.20	.24	
		6.0-L31-6-65	.23	.20	.26	.27	.38	.19	28a
		8.0-L31-6-65	.27	.12	.61	.29	.33	.25	
		4.0-L31-8-61	.22	.15	.32	.26	.19	.36	
		6.0-L31-8-61	.29	.33	.25	.32	.37	.28	28b
		8.0-L31-8-61	.31	.21	.46	.33	.35	.31	
									
	9	5.0-L31-5.0-L57	.37	.50	.27	.36	.65	.20	27d
	11	3.5-L31-3.5-L57	.22	.27	.18	.24	.43	.13	27c
	11	7.0-L31-7.0-L57	.37	.47	.29	.36	.51	.25	
	13	5.0-L31-5.0-L57	.29	.41	.20	.30	.61	.15	27b
	13	8.5-L31-8.5-L57	.38	.45	.32	.37	.51	.27	
	15	7.0-L31-7.0-L57	.33	.48	.23	.32	.67	.15	27a

TABLE II - COMPARISON OF INFINITE AND FINITE DUCTS

Arrangement	Spanwise Duct Width	High speed V_R/V	η	C_p	Climb V_R/V	η	C_p
6.0-2a-2-75	Full	.14	.20	.10	.15	.45	.05
	46 inches	.15	.18	.12	.14	.29	.07
6.0-2a-4-70	Full	.24	.74	.08	.26	1.17	.06
	46 inches	.22	.39	.12	.21	.39	.11
6.0-2a-6-65	Full	.30	.90	.10	.34	1.03	.11
	46 inches	.26	.58	.12	.27	.64	.11
6.0-2a-8-61	Full	.34	.96	.12	.36	.92	.14
	46 inches	.31	.54	.18	.31	.47	.20
6.0-0-4-70	Full	—	—	—	.26	1.00	.07
	46 inches	.17	.16	.18	.23	.91	.06
	24 inches	.16	.09	.28	.21	.51	.09
6.0-0-6-65	Full	.20	.24	.17	.33	1.10	.10
	46 inches	.21	.24	.18	.29	.89	.09
	24 inches	.22	.19	.25	.27	.61	.12
6.0-0-8-61	Full	.25	.27	.23	.37	1.04	.13
	46 inches	.27	.33	.22	.33	.51	.21
	24 inches	.26	.26	.26	.30	.51	.18

LEGENDS

(a) N.A.C.A. 23017 center section, no duct.

(b) N.A.C.A. 23017 center section showing typical duct installation.

Figure 1.- Cooling wing and duct arrangement.

Figure 2a.- Relative pressure drop of radiator assemblies.

Figure 2b.- Relative pressure drop of radiator assemblies

Figure 3.- Upper noses used to form duct inlets, showing inlet positions in percent of N.A.C.A. 23017 section chord (through duct).

Figure 4.- Lower noses used to form duct inlets (through duct).

Figure 5.- Typical through duct installation.

(a) Through duct installation, showing exit sizes and location.

(b) Through duct showing nose flap and exit flap 'A' for controlling air flow.

(c) Through duct showing exit through trailing edge split flap.

(d) Underslung radiator arrangement.

(e) Cross-wing duct arrangement.

(f) Through duct showing exit flap 'B' for controlling air flow.

Figure 6.-Radiator duct arrangements.

Figure 7.-Typical through duct outlet installation.

Figure 8.- Typical trailing edge split flap outlet installation.

Figure 9.- Inlet flap installation. Flap in position F3.

(a) Inlet. (b) Outlet.

Figure 10.- Narrow duct installation.

Figure 11.- Typical underslung duct installation.

Figure 12.- Plain wing mounted in full-scale wind tunnel

(a) Nose position 2a. (b) Nose position 0.

Figure 13.- Variation of duct efficiency and flow ratio with lift coefficient. Through duct, 2 percent outlet.

(a) Nose position 2a. (b) Nose position 0.

Figure 14.- Variation of duct efficiency and flow ratio with lift coefficient. Through duct, 4 percent outlet.

(a) Nose position 2a. (b) Nose position 0.

(c) Nose position 3.

Figure 15.- Variation of duct efficiency and flow ratio with lift coefficient. Through duct, 6 percent outlet.

(a) Nose position 4a. (d) Nose position 1.

(b) Nose position 2a. (e) Nose position 3.

(c) Nose position 0. (f) Nose position 5.

Figure 16.- Variation of duct efficiency and flow ratio with lift coefficient. Through duct, 8 percent outlet.

(a) 2 percent outlet. (c) 6 percent outlet.

(b) 4 percent outlet. (d) 8 percent outlet.

Figure 17.- Variation of duct efficiency and flow ratio with lift coefficient. Through duct with inlet flap.

(a) Nose position 2a, 4.6 percent inlet. (b) Nose position 2a, 6 percent inlet.

(c) Nose position 0, 6 percent inlet.

Figure 18.- Variation of duct efficiency and flow ratio with lift coefficient. Through duct with type A outlet flap.

(a) Nose position 2a. (b) Nose position 0.

Figure 19.- Variation of duct efficiency and flow ratio with lift coefficient. Through duct with type B outlet flap in B1 position.

(a) Nose position 2a. (b) Nose position 0.

Figure 20.- Variation of duct efficiency and flow ratio with lift coefficient. Through duct with type B outlet flap in B2 position.

(a) Nose position 2a. (b) Nose position 0.

Figure 21.- Variation of duct efficiency and flow ratio with lift coefficient. Through duct with type B outlet flap in B3 position.

Figure 22.- Variation of duct efficiency and flow ratio with lift coefficient. Through duct with both inlet and type B outlet flap.

(a) Nose position 2a. (b) Nose position 0.

(c) Nose position 1.

Figure 23.- Variation of duct efficiency and flow ratio with lift coefficient. Through duct with T.E. split flap outlet.

(a) Inlet 1/3 open. (b) Inlet 2/3 open.

Figure 24.- Variation in duct efficiency and flow ratio with lift coefficient. Through duct with restricted inlet.

Figure 25.- Variation in duct efficiency and flow ratio with lift coefficient. Narrow through-duct arrangement.

(a) Arrangement 6.0 - 2a - 2 - 75.

(b) Arrangement 6.0 - 2a - 4 - 70.

(c) Arrangement 6.0 - 2a - 6 - 65.

(d) Arrangement 6.0 - 2a - 8 - 61.

Figure 26.- Variation in duct efficiency and flow ratio with lift coefficient. Through duct with radiators of various pressure drops.

(a) Radiator height 15 inches (same as in through ducts).

(c) Radiator height 11 inches.

(b) Radiator height 13 inches.

(d) Radiator height 9 inches.

Figure 27.- Variation of duct efficiency and flow ratio with lift coefficient. Underslung duct.

(a) 6 percent outlet.

(b) 8 percent outlet.

Figure 28.- Variation of duct efficiency and flow ratio with lift coefficient. Cross-wing duct.

Figure 29.- Scale effect on flow ratio and power coefficient.

Figure 30.- Typical lift curves for the plain wing and various duct arrangements.

(a) 2-75 outlet.

(c) 6-65 outlet.

(b) 4-70 outlet.

(d) 8-61 outlet.

Figure 31.- Effect of inlet opening size on duct efficiency and flow ratio. $C_L = 0.2$.

(a) $C_L = 0.2$.

(b) $C_L = 0.7$.

Figure 32.- Effect of inlet position on duct efficiency and flow ratio. 6 percent inlet.

Figure 33.- Effect of outlet opening size on duct efficiency and flow ratio. 6 percent inlets, $C_L = 0.2$.

(a) Arrangement 6.0 - 0 - 2 - 75.

(c) Arrangement 6.0 - 0 - 6 - 65.

(b) Arrangement 6.0 - 0 - 4 - 70.

(d) Arrangement 6.0 - 0 - 8 - 61.

Figure 34.- Comparison of narrow and full width ducts of similar arrangement.

Figure 35.- Variation of drag, flow ratio, and duct efficiency with the conductivity factor, $1/\sqrt{1+K}$. $C_L = 0.2$.

Figure 36.- Flow ratio multiplying factors for radiators of various pressure drops.

Figure 37.- Power coefficient multiplying factors for radiators of various pressure drops.

Figure 38.- Effect of expansion ratio on radiator-duct power coefficient. Underslung duct.

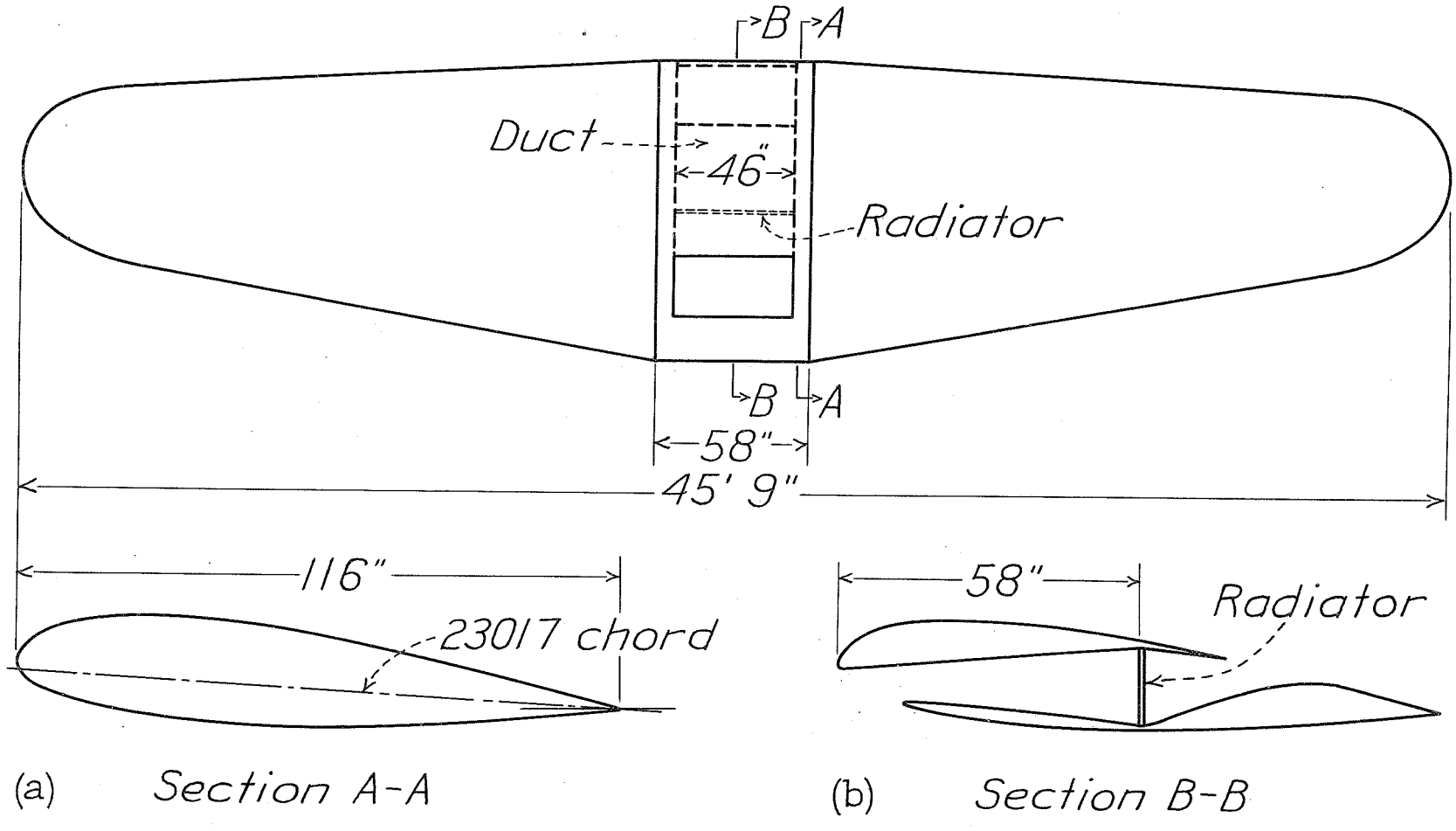
B
A
Duct
46"
Radiator
B
A
58"
45' 9"
116"
23017 chord
58"
Radiator
(a) Section A-A
(b) Section B-B

Figure 1

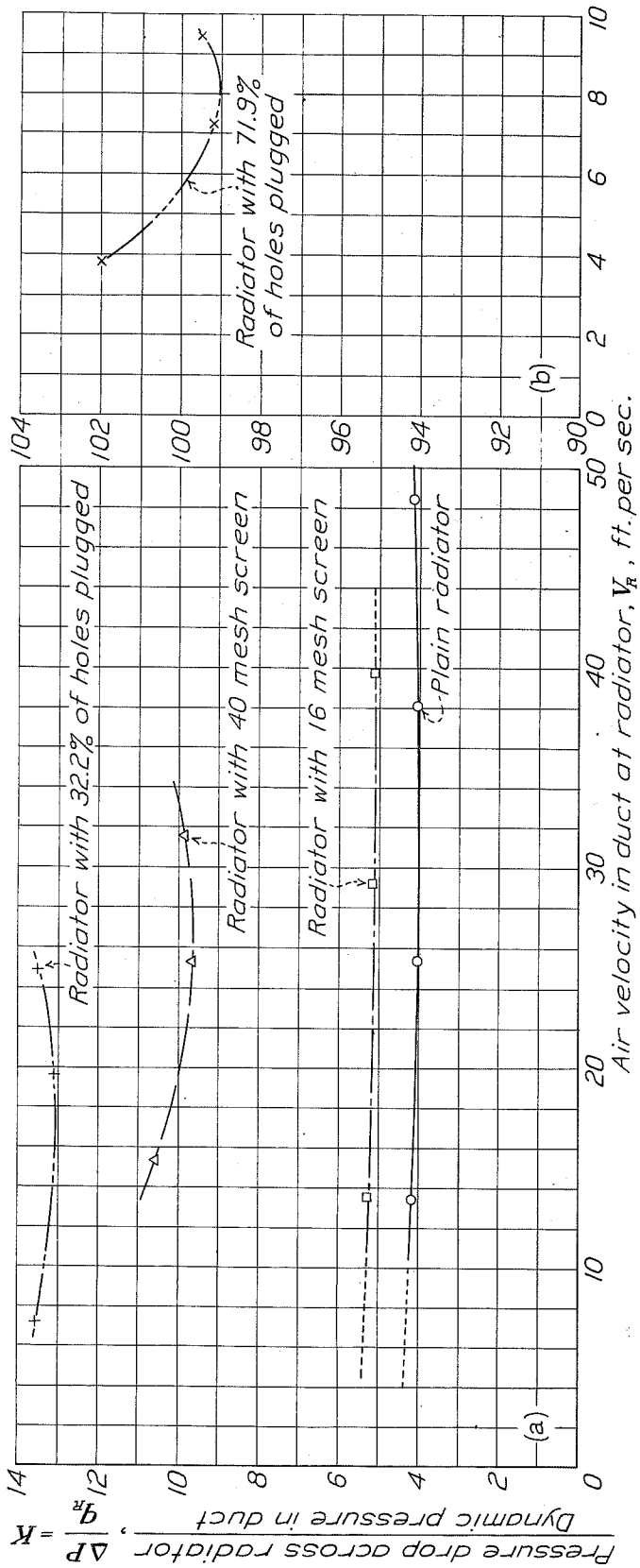
Pressure drop across radiator / Dynamic pressure in duct = ΔP/q_R = K
Air velocity in duct at radiator, V_R, ft. per sec.
Radiator with 32.2% of holes plugged
Radiator with 40 mesh screen
Radiator with 16 mesh screen
Plain radiator
Radiator with 71.9% of holes plugged
(a)
(b)

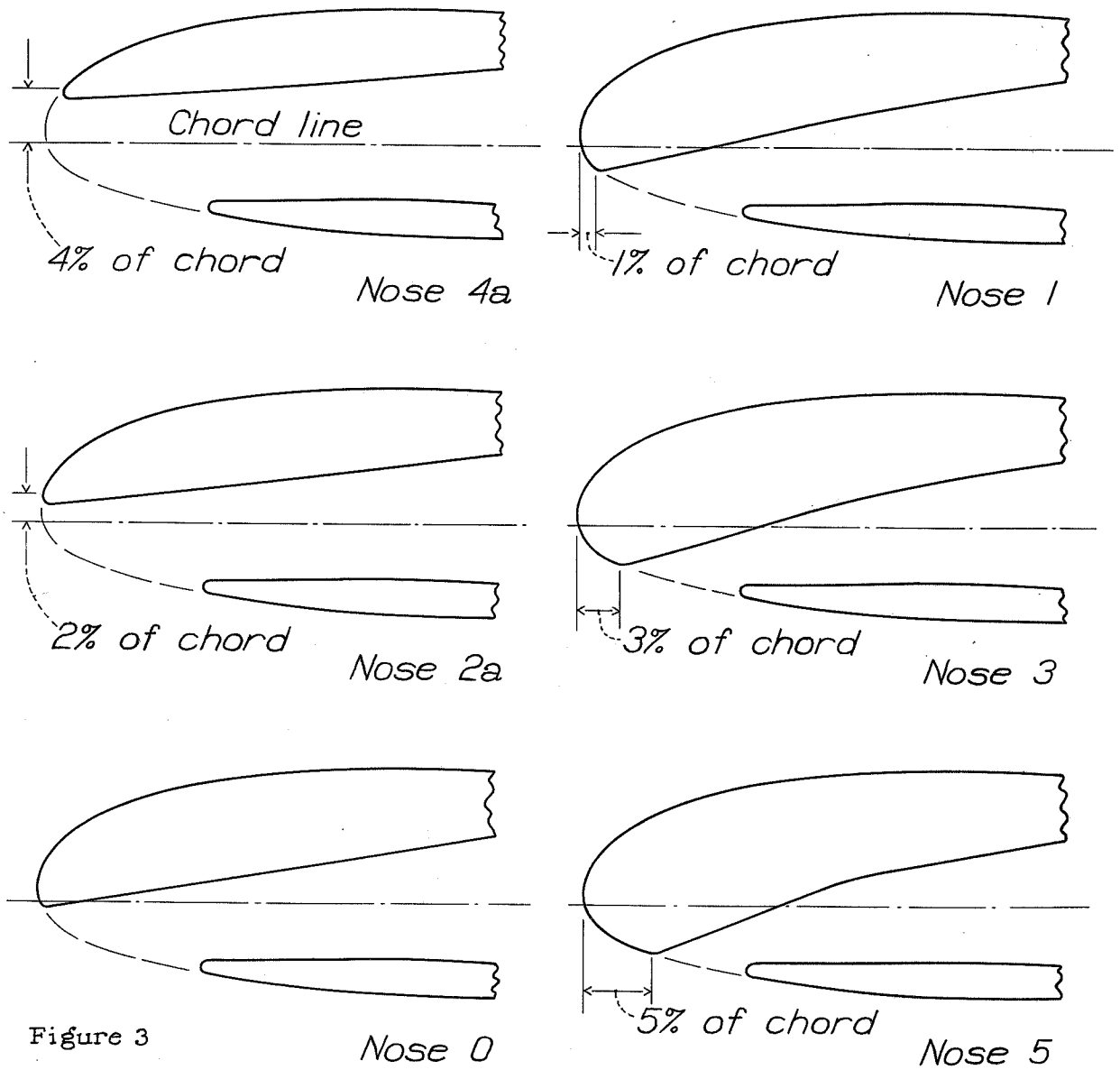

Figure 3

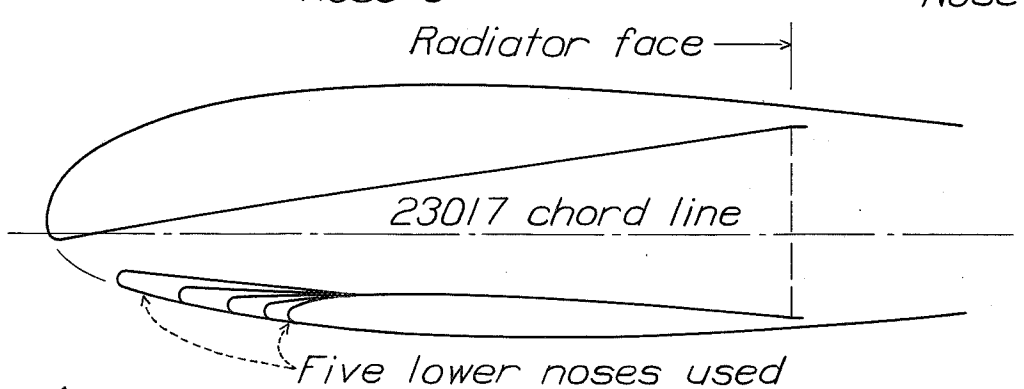

Figure 4

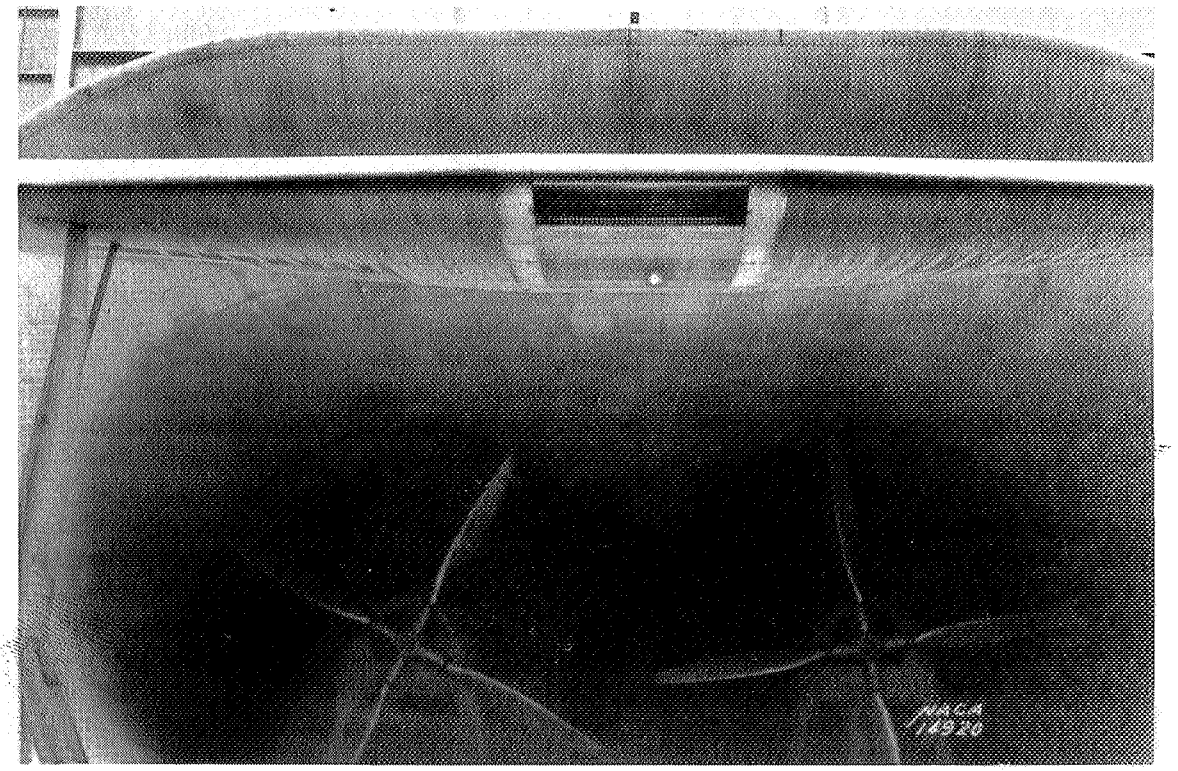

Figure 5.

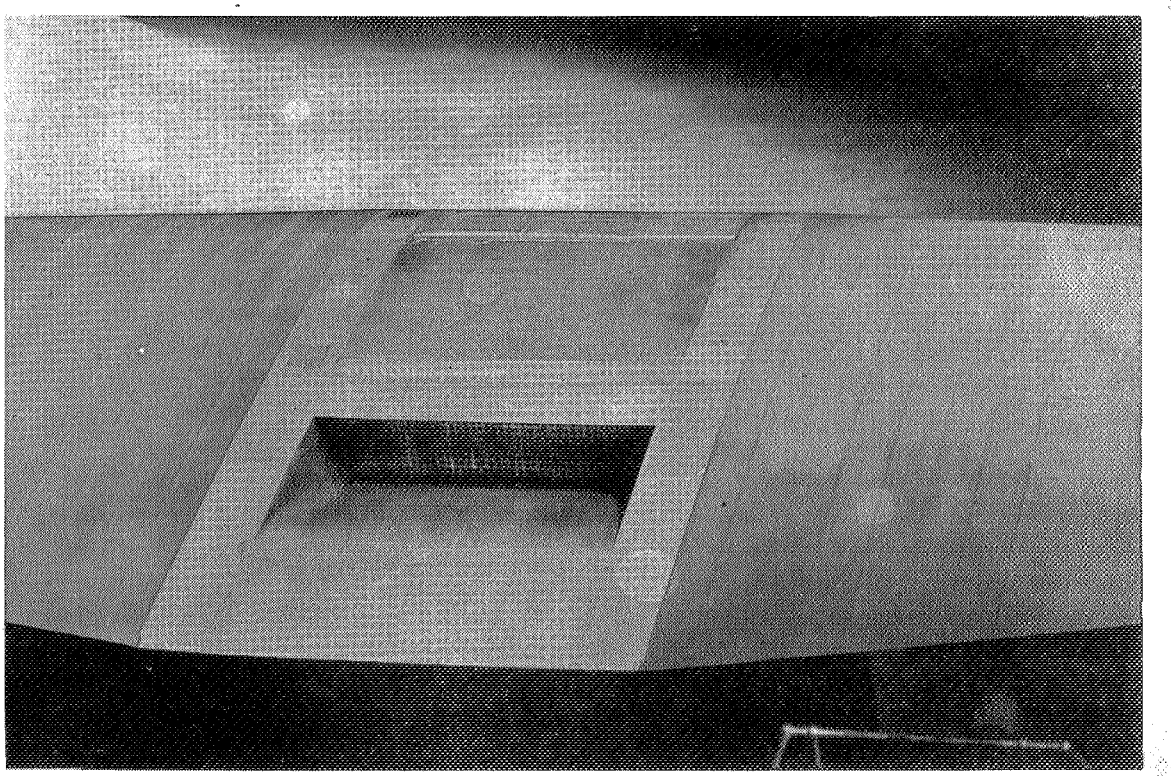

Figure 7.

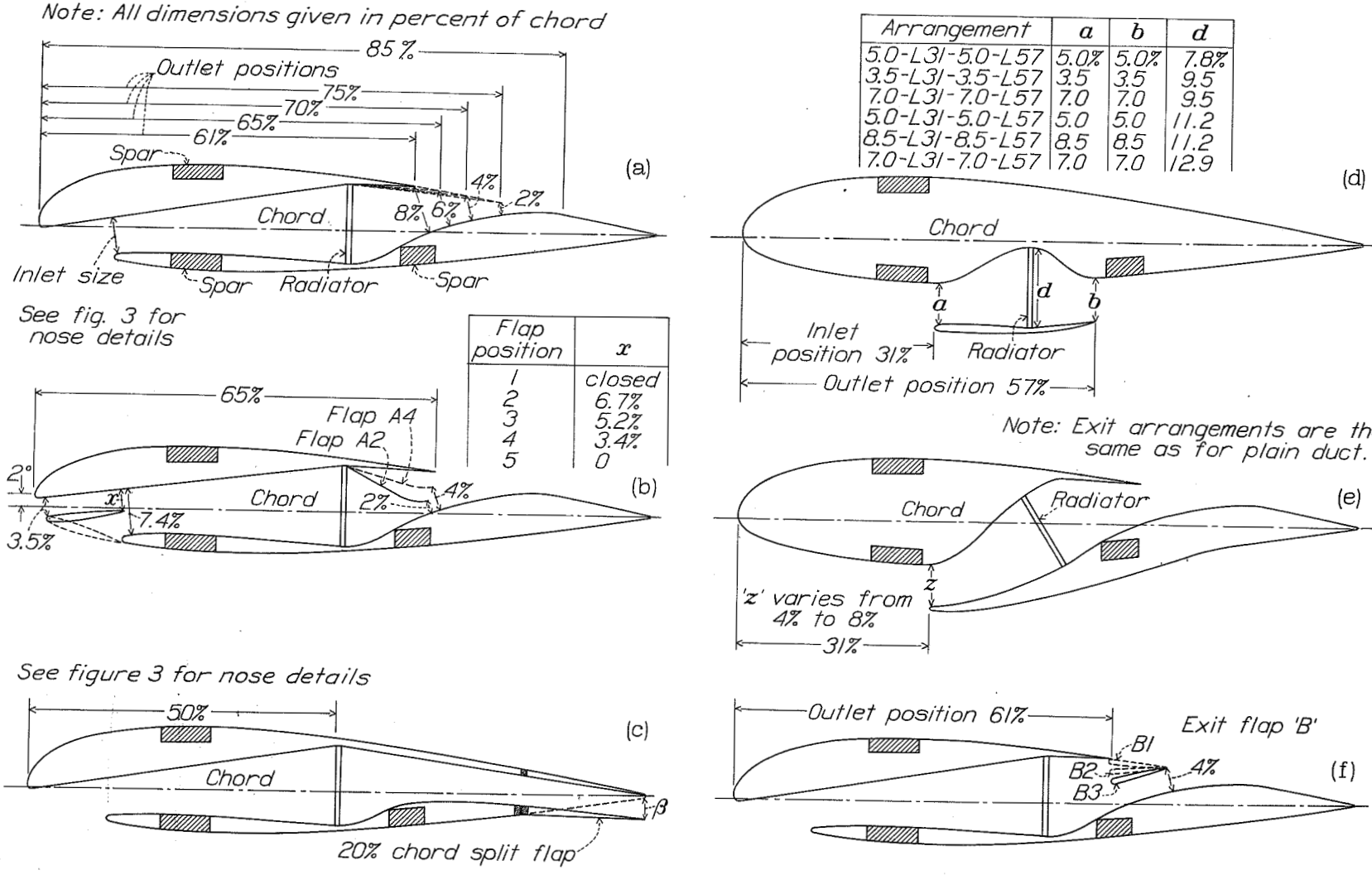
Note: All dimensions given in percent of chord
85%
Outlet positions
75%
70%
65%
61%
Spar
4%
2%
Chord
8%
6%
Inlet size
Spar
Radiator
Spar
(a)
See fig. 3 for nose details
Flap position
x
1 closed
2 6.7%
3 5.2%
4 3.4%
5 0
65%
Flap A4
Flap A2
2°
x
Chord
2%
4%
7.4%
3.5%
(b)
See figure 3 for nose details
50%
Chord
β
20% chord split flap
(c)
Arrangement
a
b
d
5.0-L31-5.0-L57 5.0% 5.0% 7.8%
3.5-L31-3.5-L57 3.5 3.5 9.5
7.0-L31-7.0-L57 7.0 7.0 9.5
5.0-L31-5.0-L57 5.0 5.0 11.2
8.5-L31-8.5-L57 8.5 8.5 11.2
7.0-L31-7.0-L57 7.0 7.0 12.9
(d)
Chord
a
d
b
Inlet position 31%
Radiator
Outlet position 57%
Note: Exit arrangements are the same as for plain duct.
Chord
Radiator
(e)
z
'z' varies from 4% to 8%
31%
Outlet position 61%
Exit flap 'B'
B1
B2
B3
4%
(f)

Figure 6.

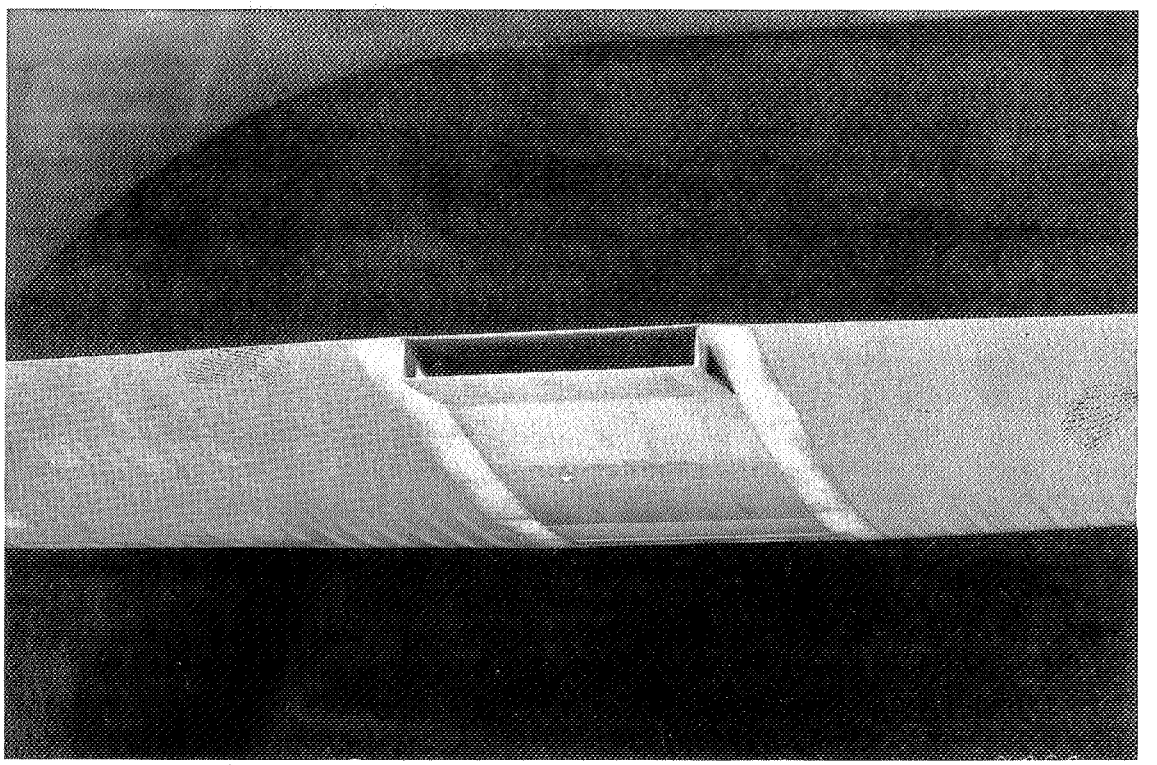

Figure 8.

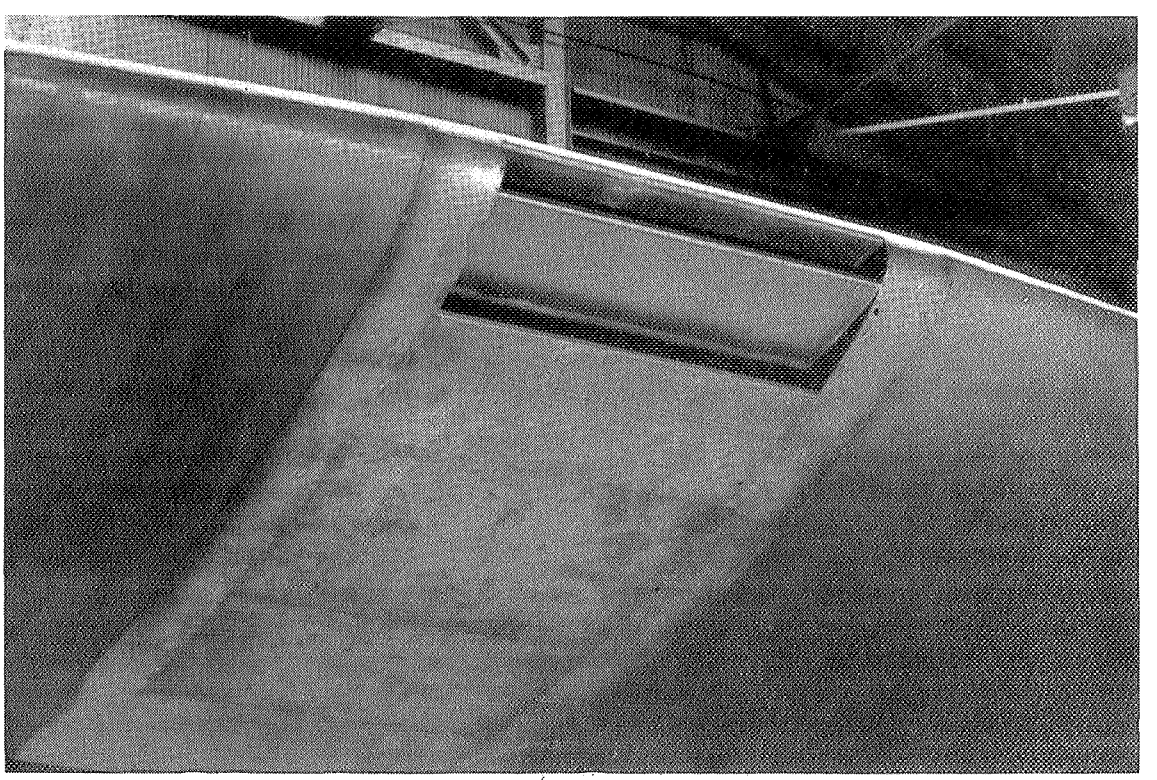

Figure 9.

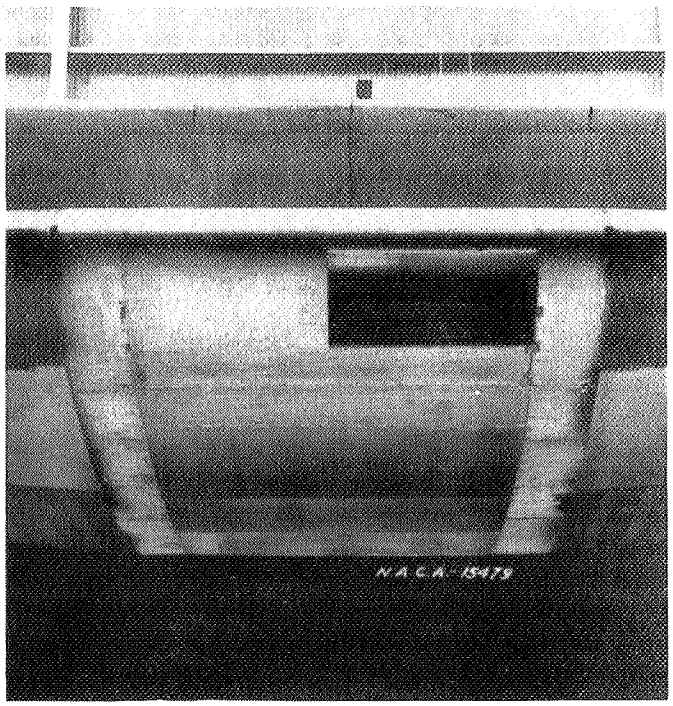

Figure 10a.

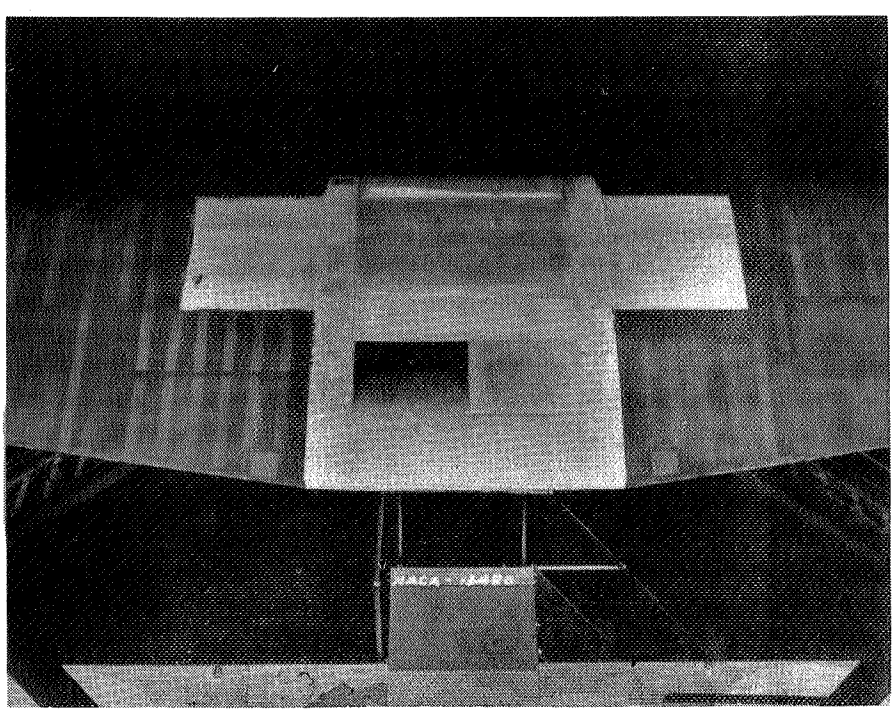

Figure 10b.

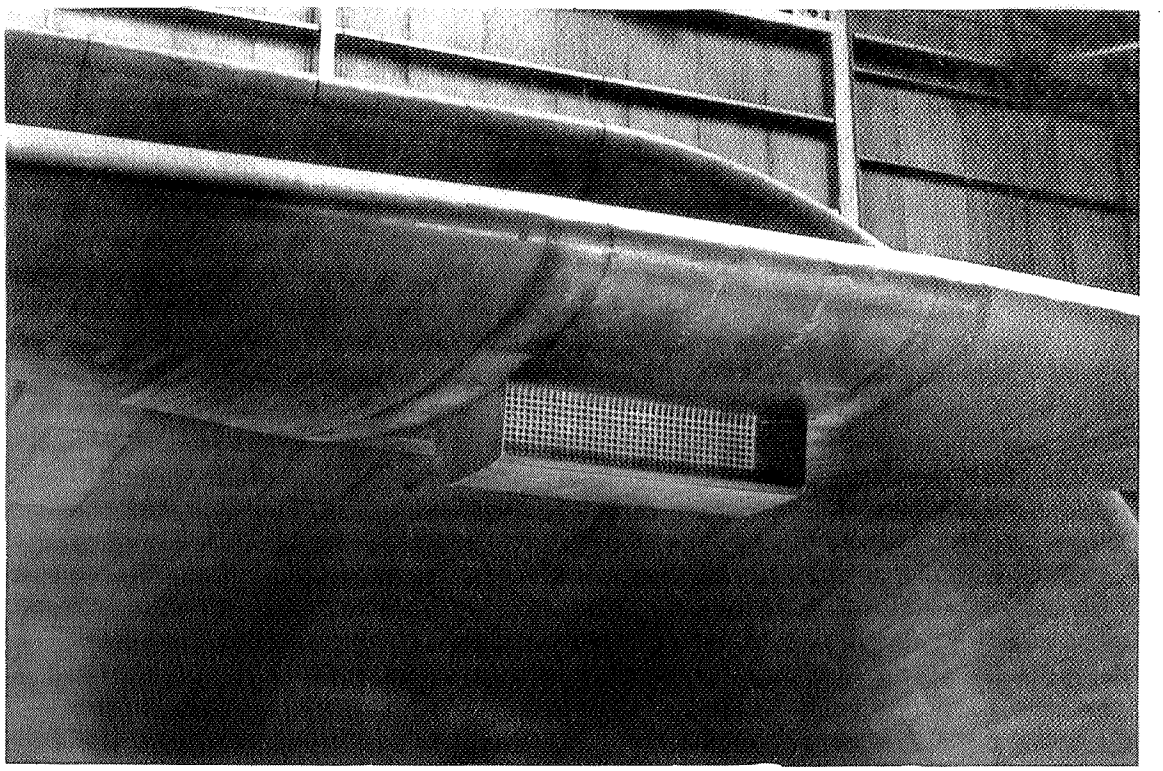

Figure 11.

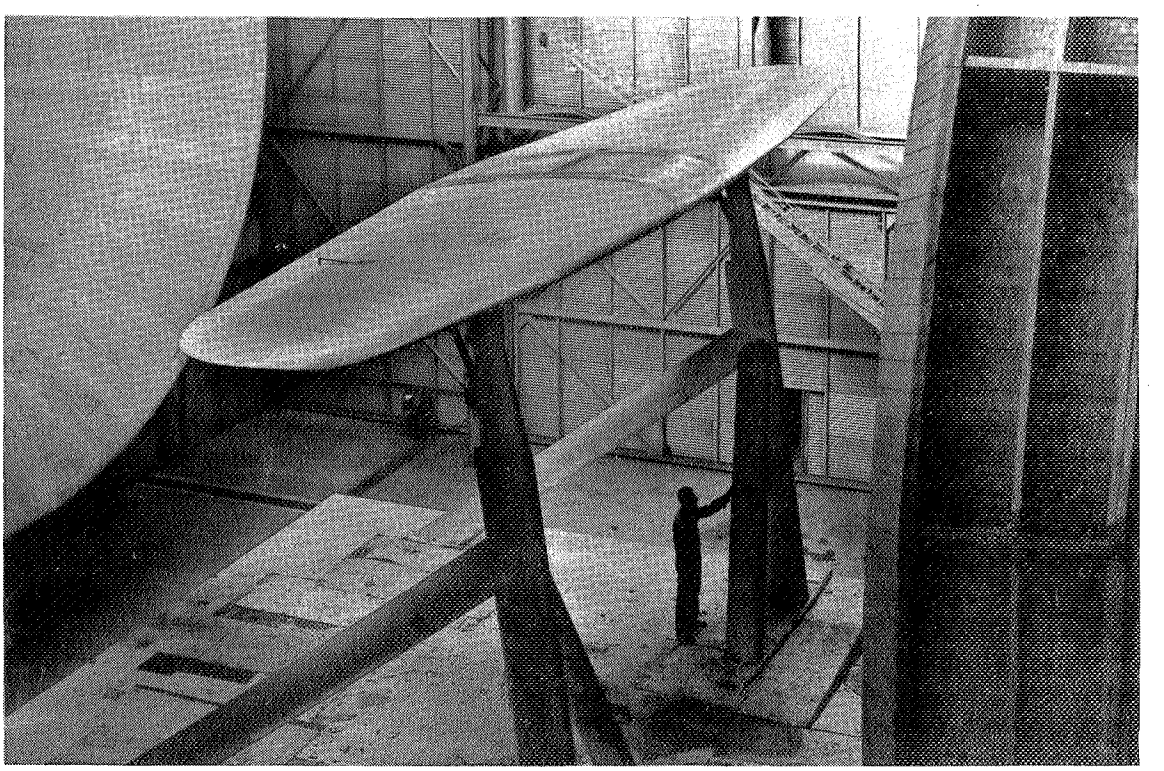

Figure 12.

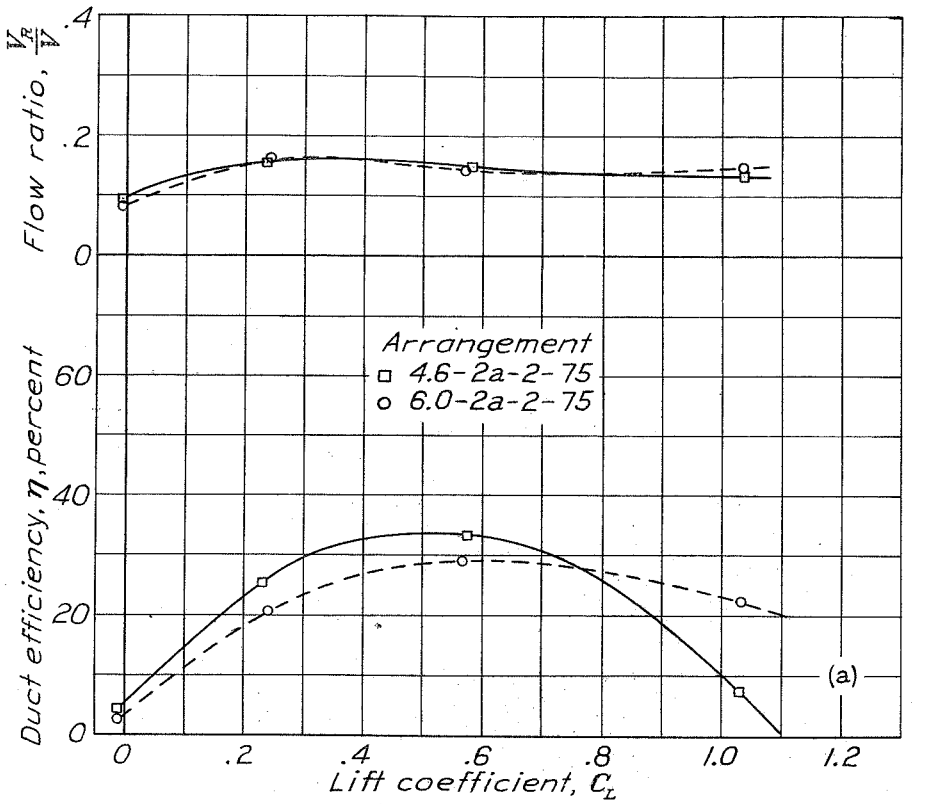

Figure 13a

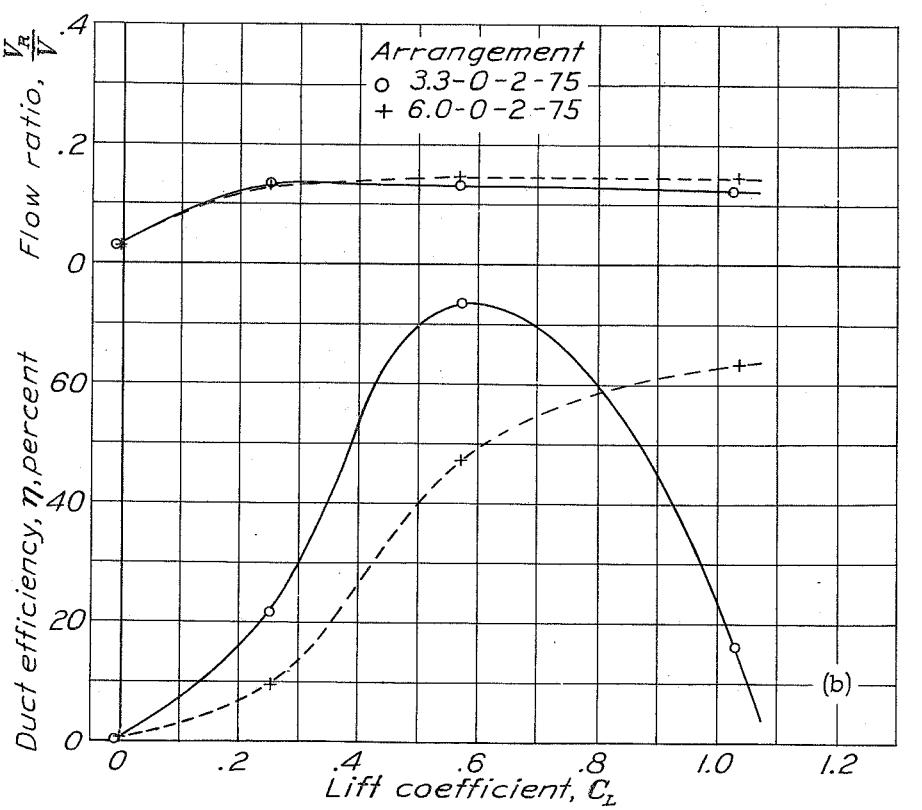

Figure 13b

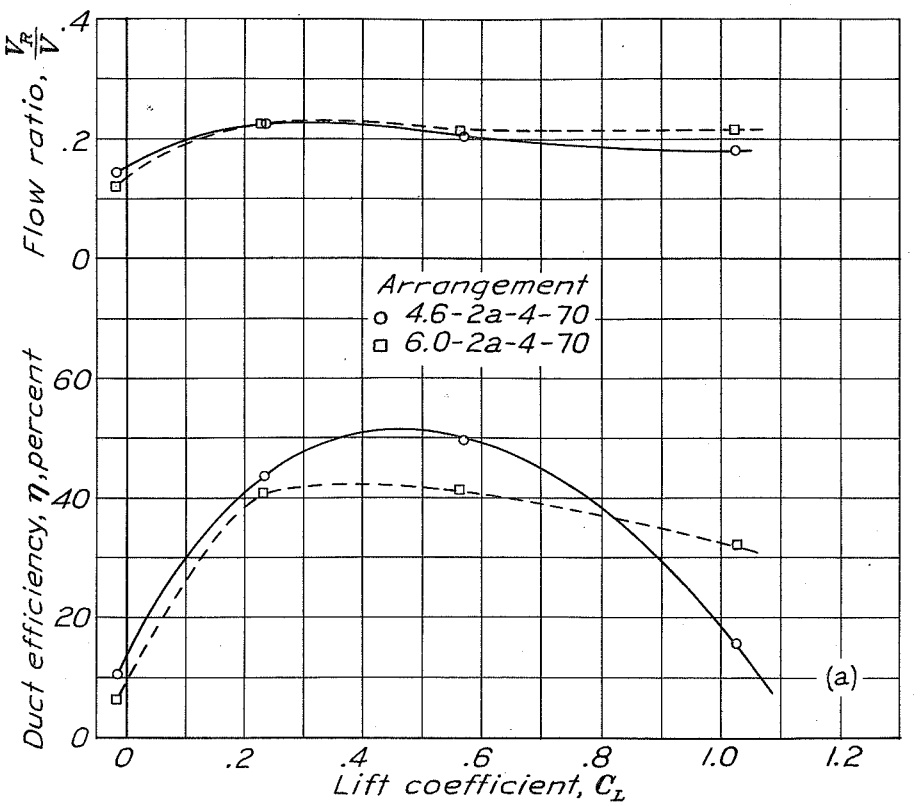

Figure 14a

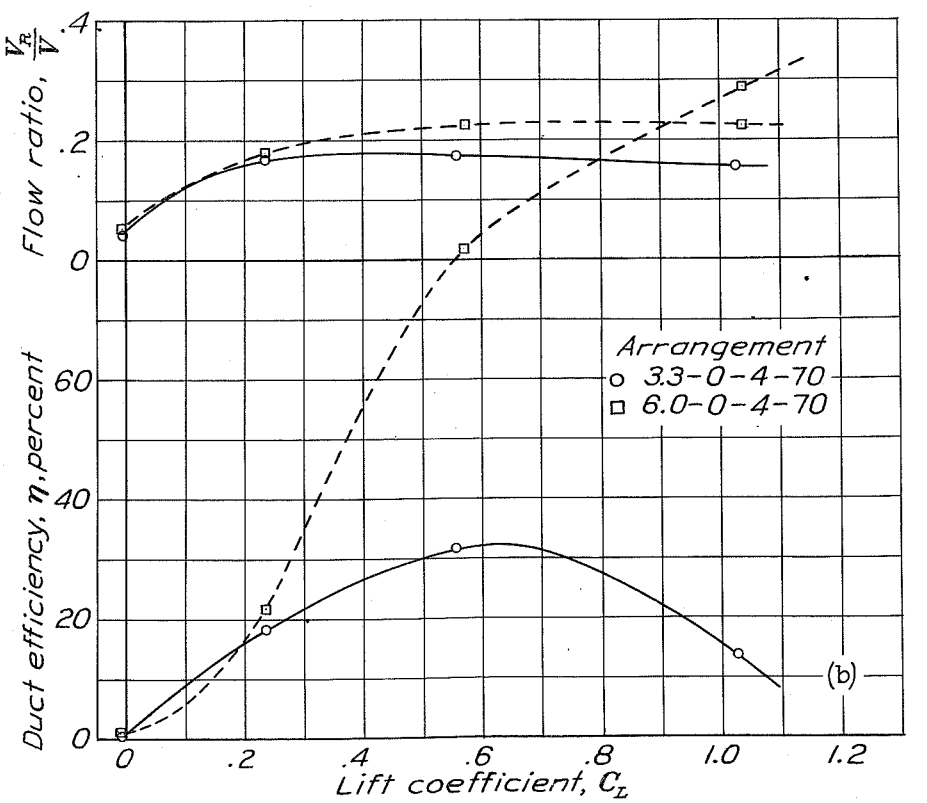

Figure 14b

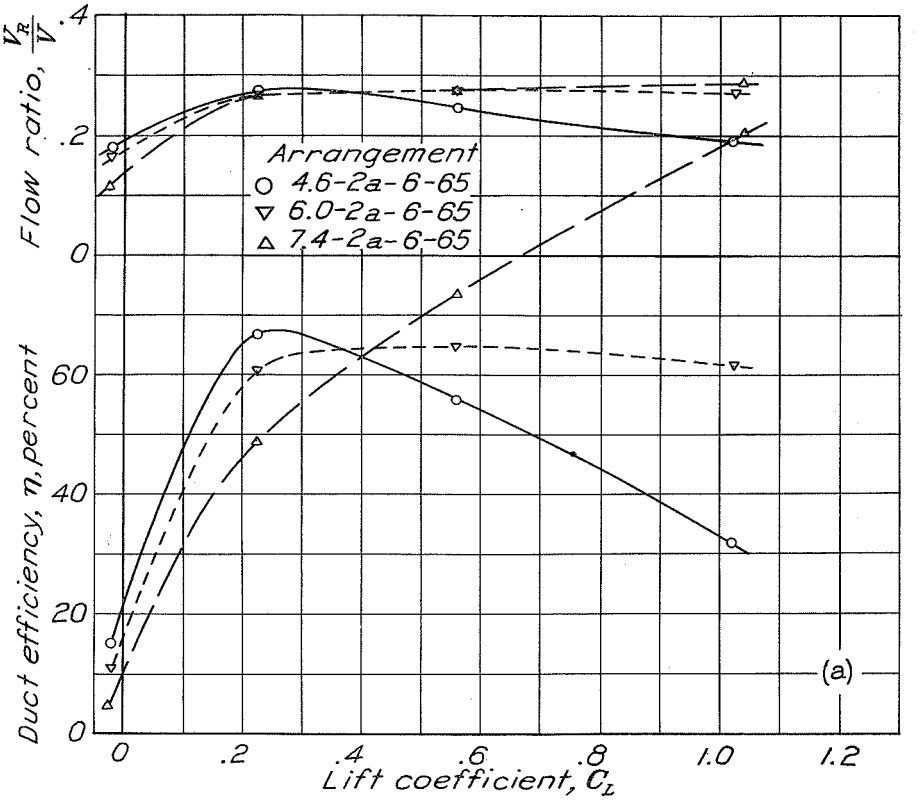

Figure 15a

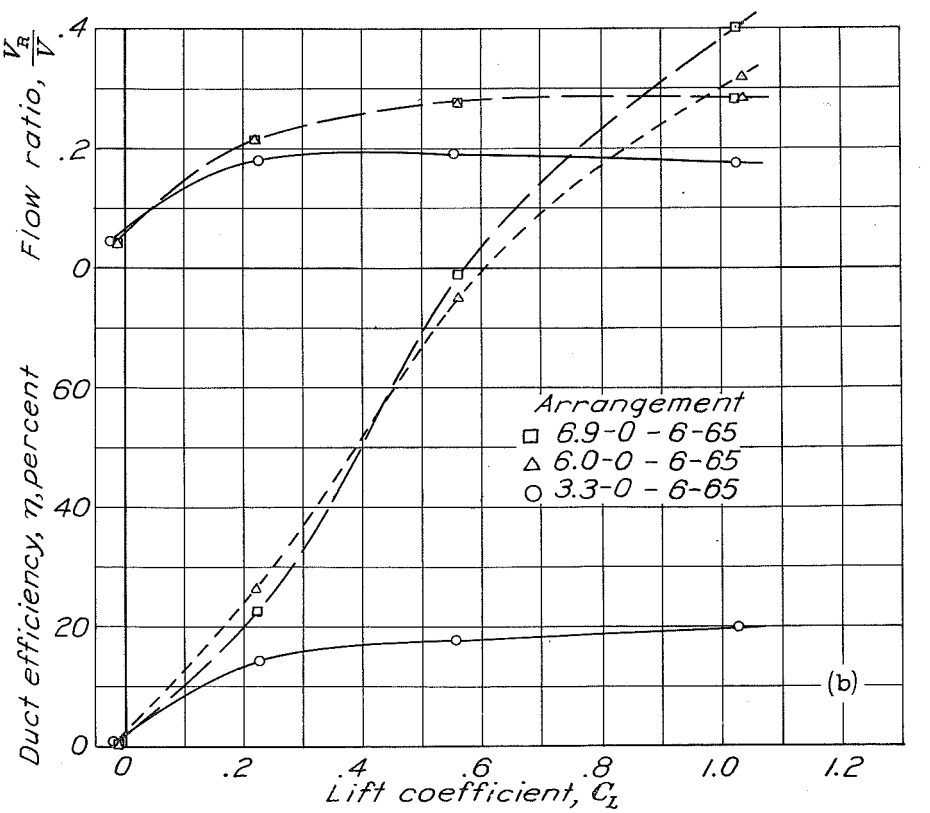

Figure 15b

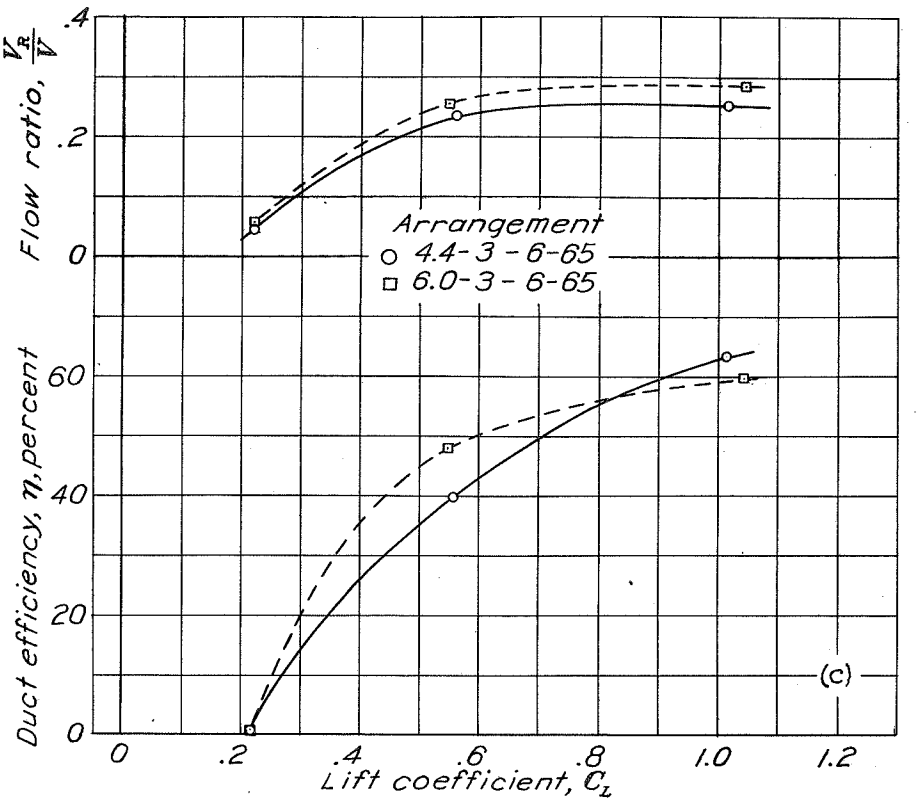

Figure 15c

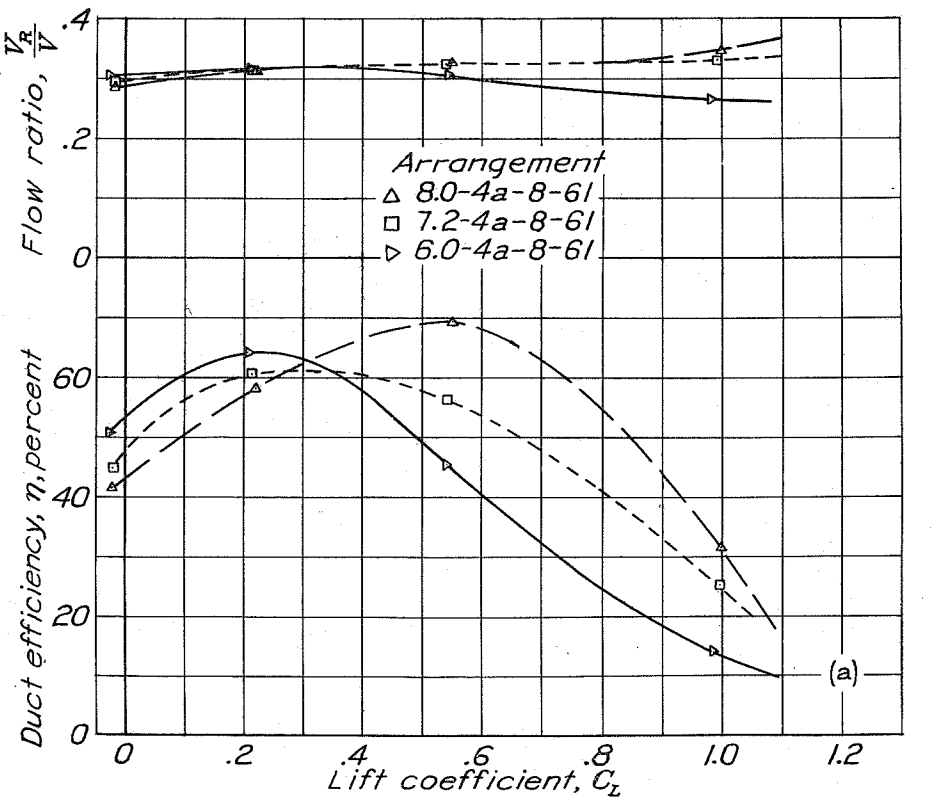

Figure 16a

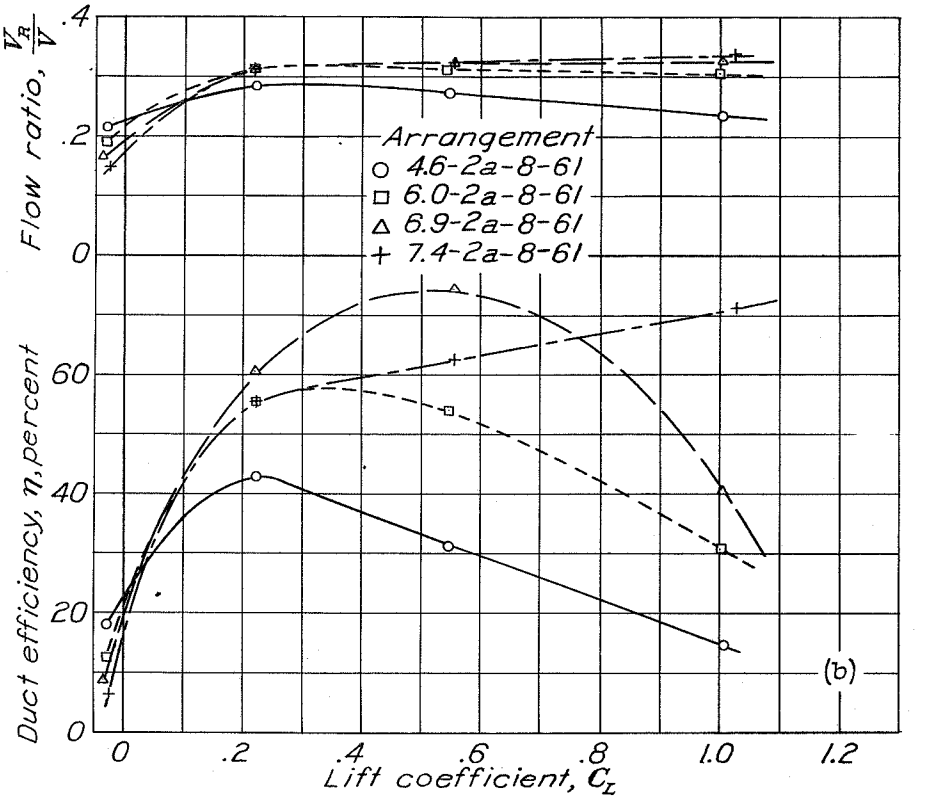

Figure 16b

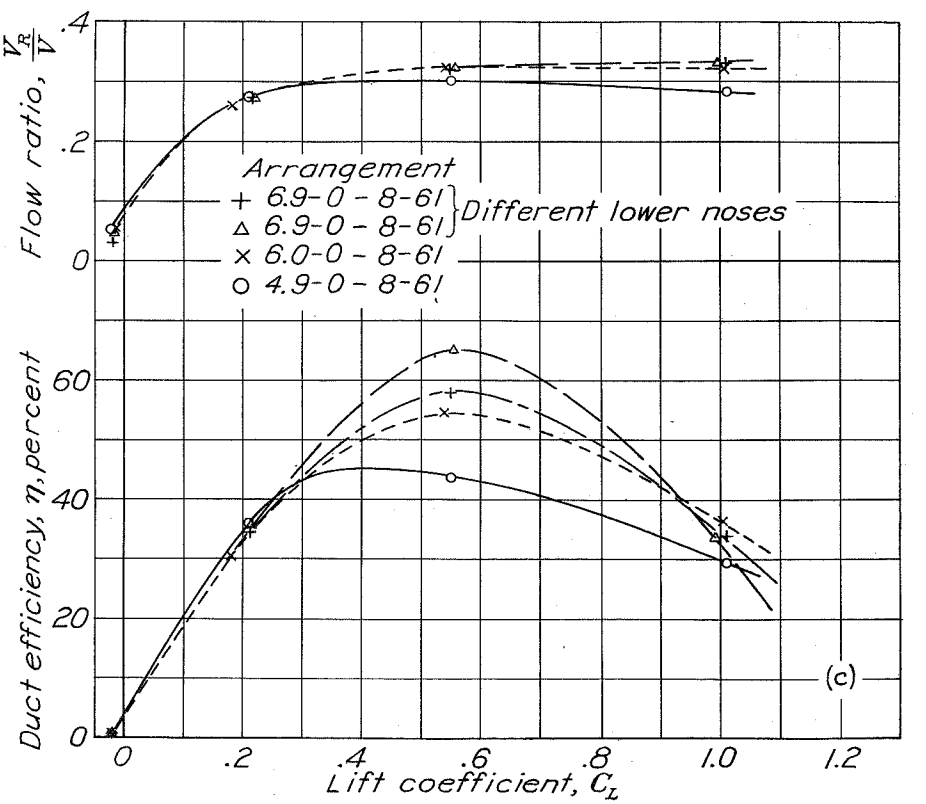

Figure 16c

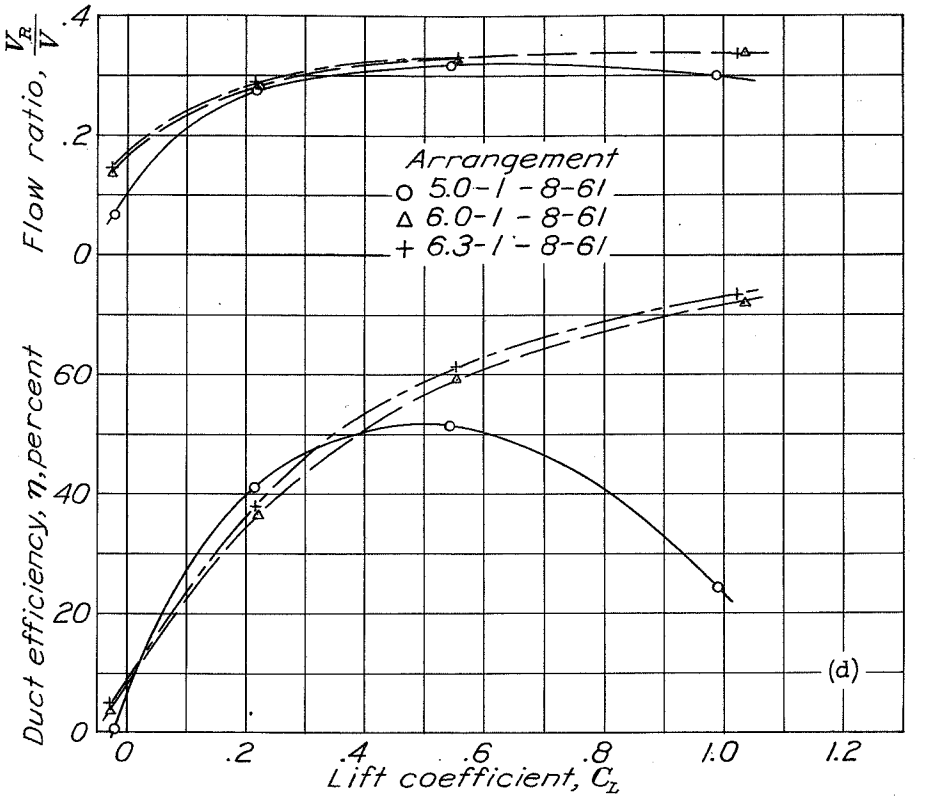

Figure 16 d

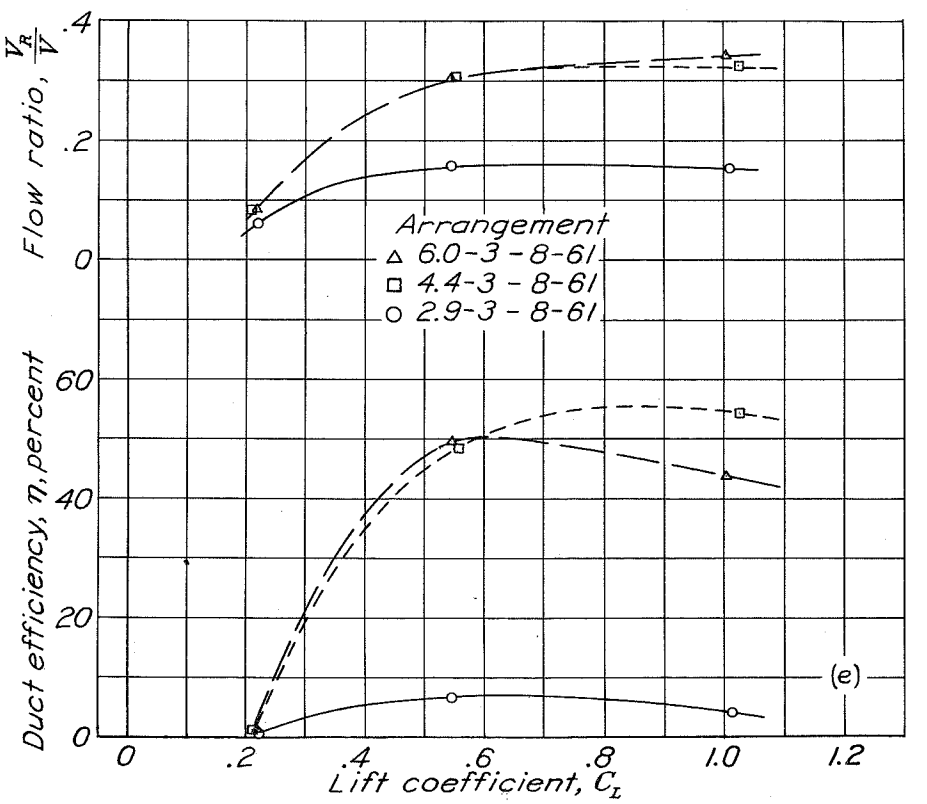

Figure 16 e

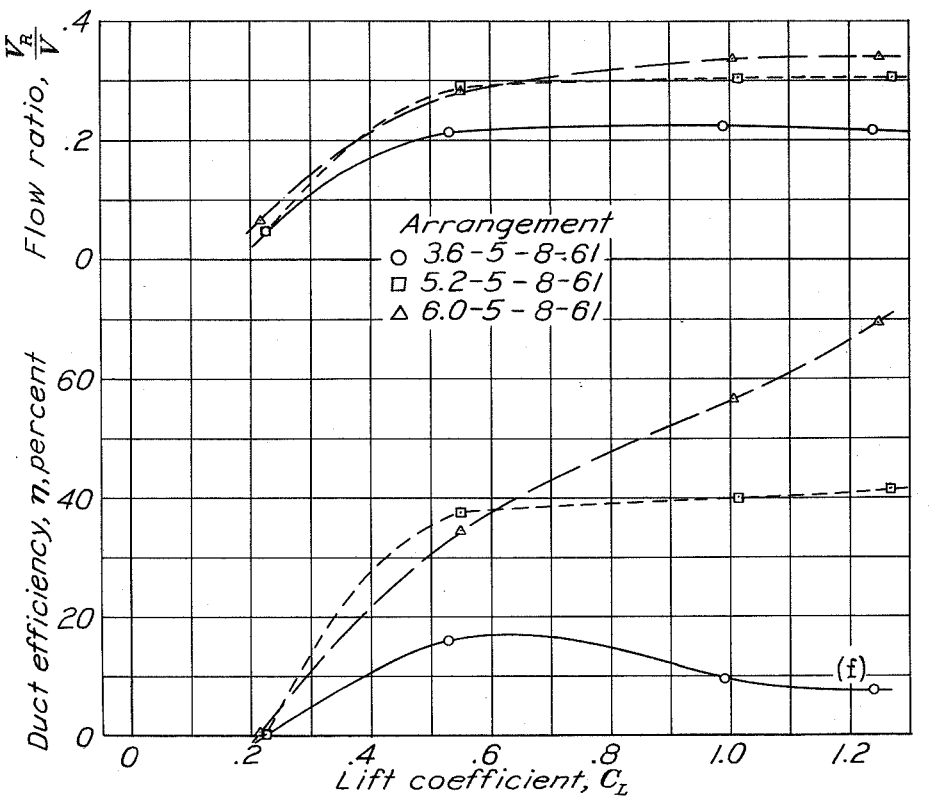

Figure 16f

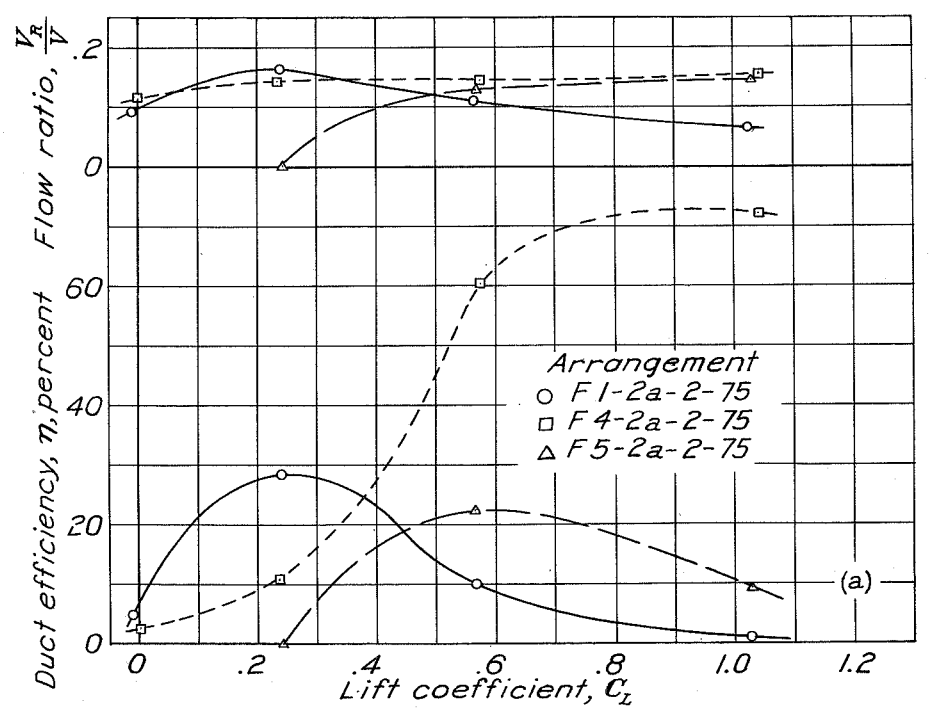

Figure 17a

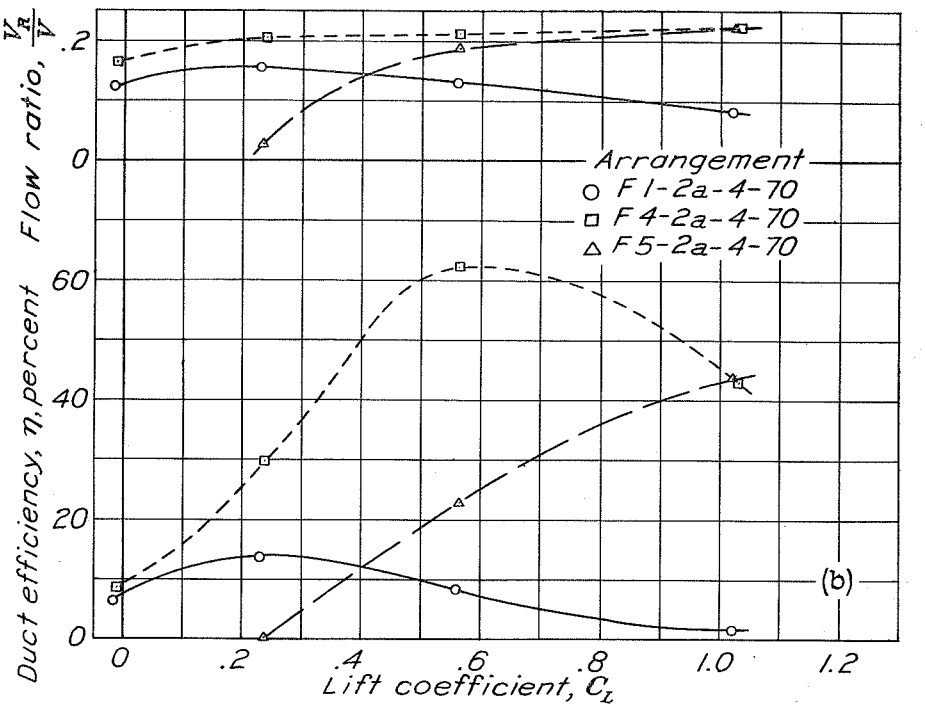

Figure 17b

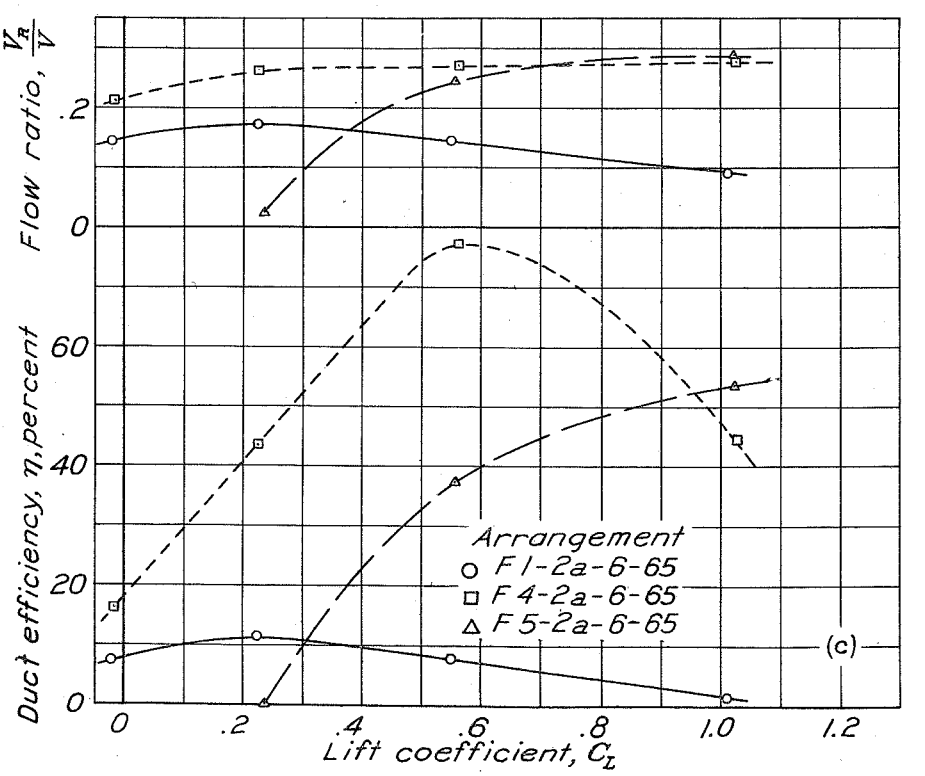

Figure 17c

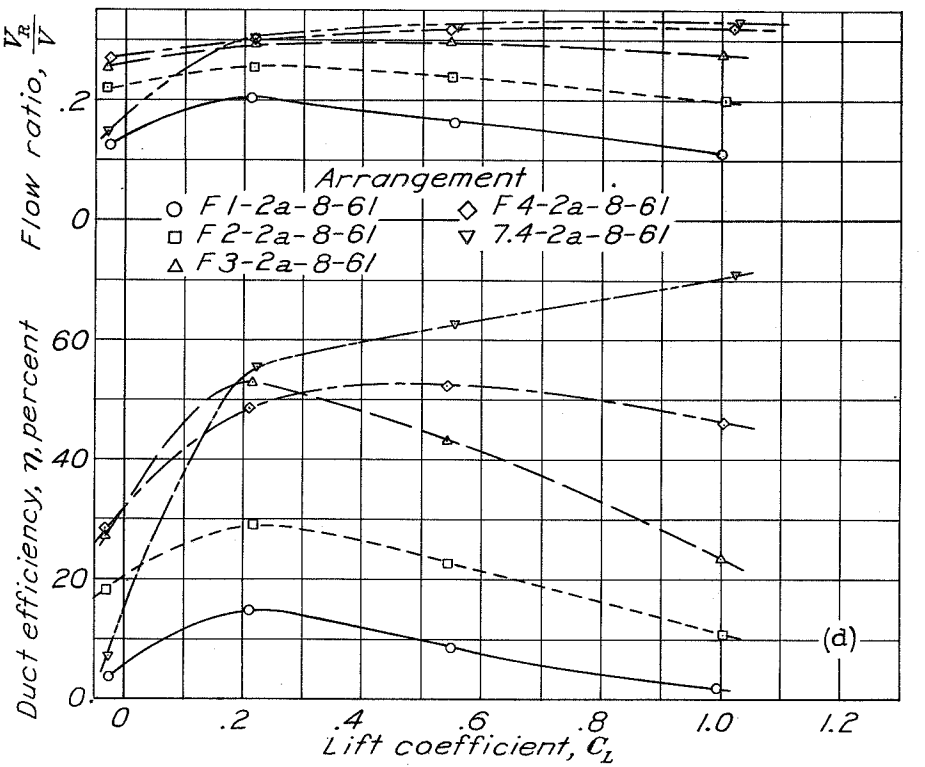

Figure 17d

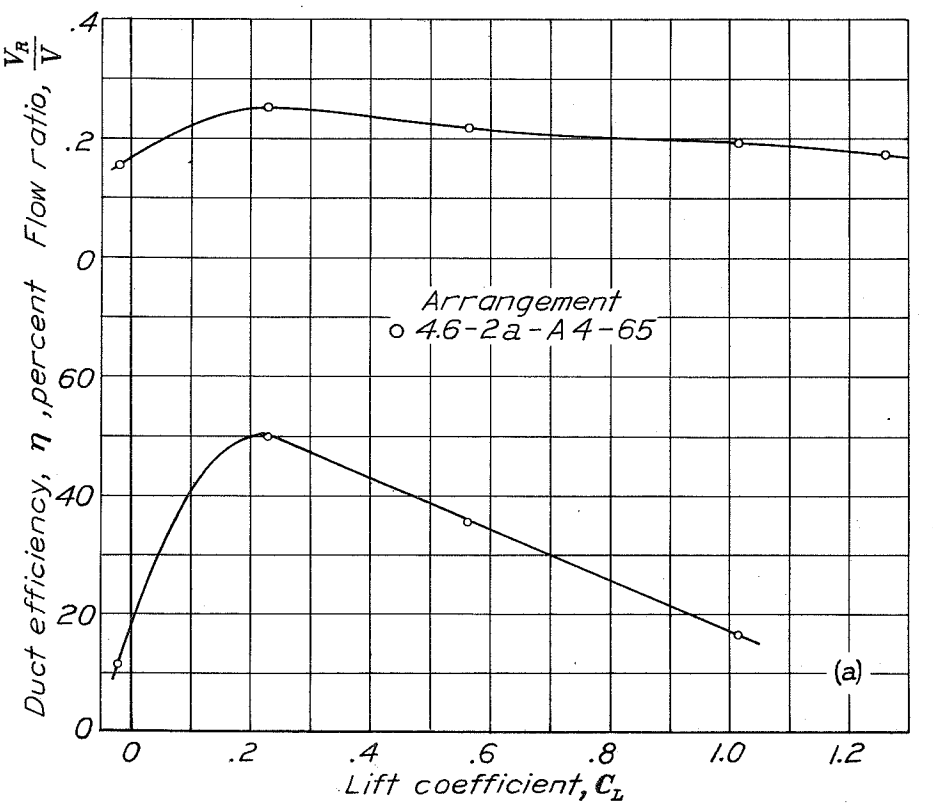

Figure 18a

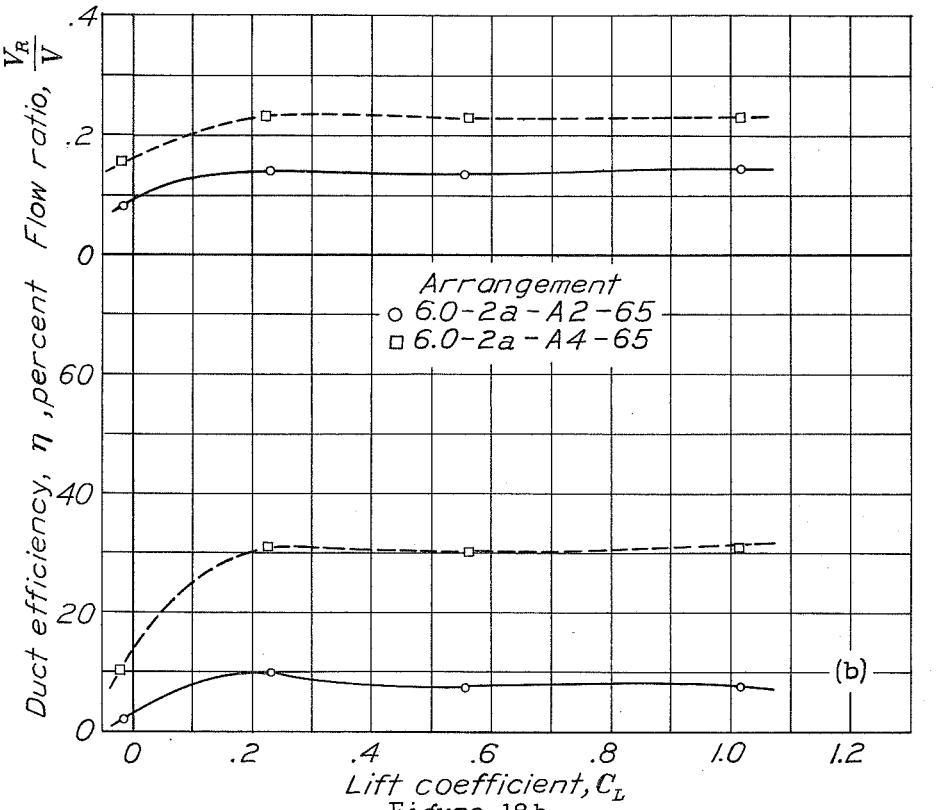

Figure 18b

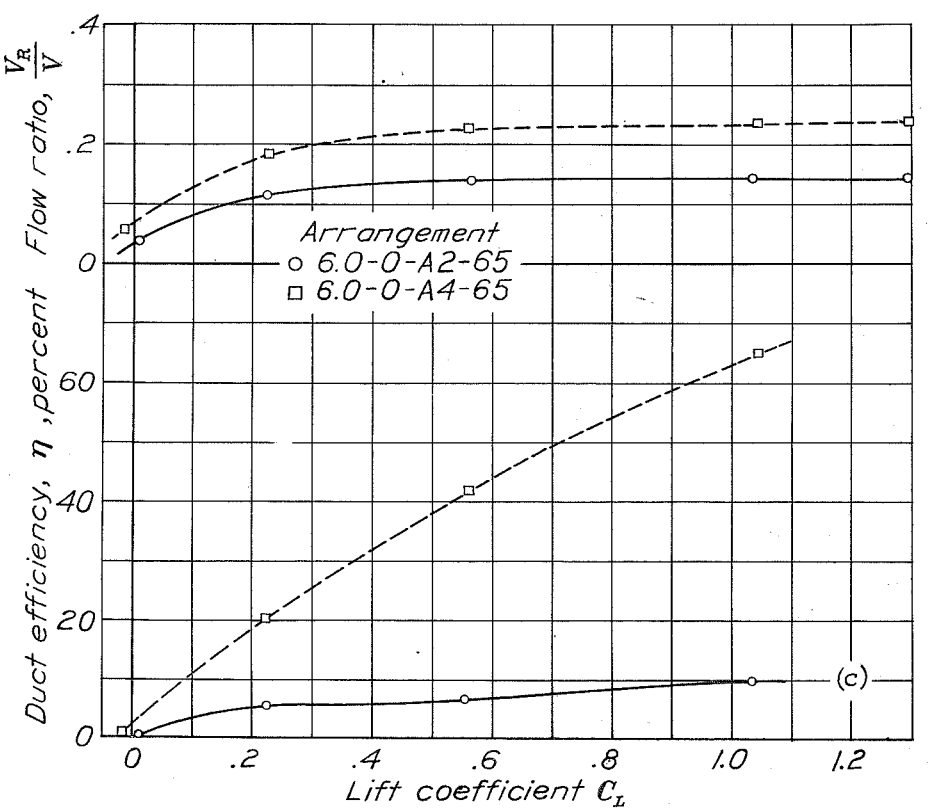

Figure 18c

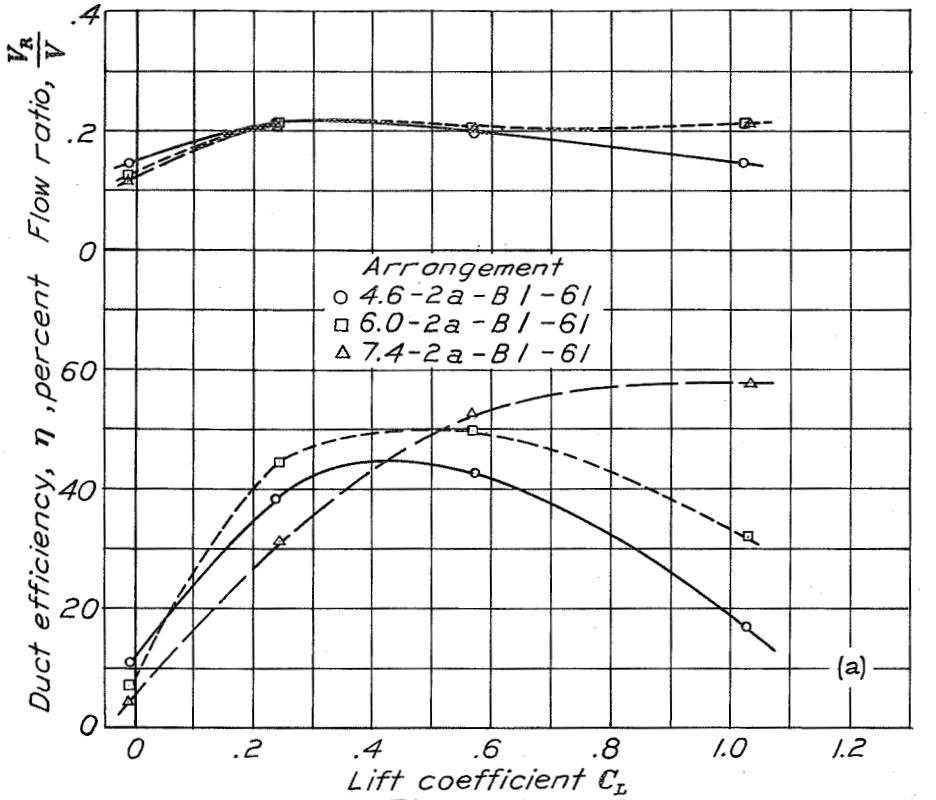

Figure 19a

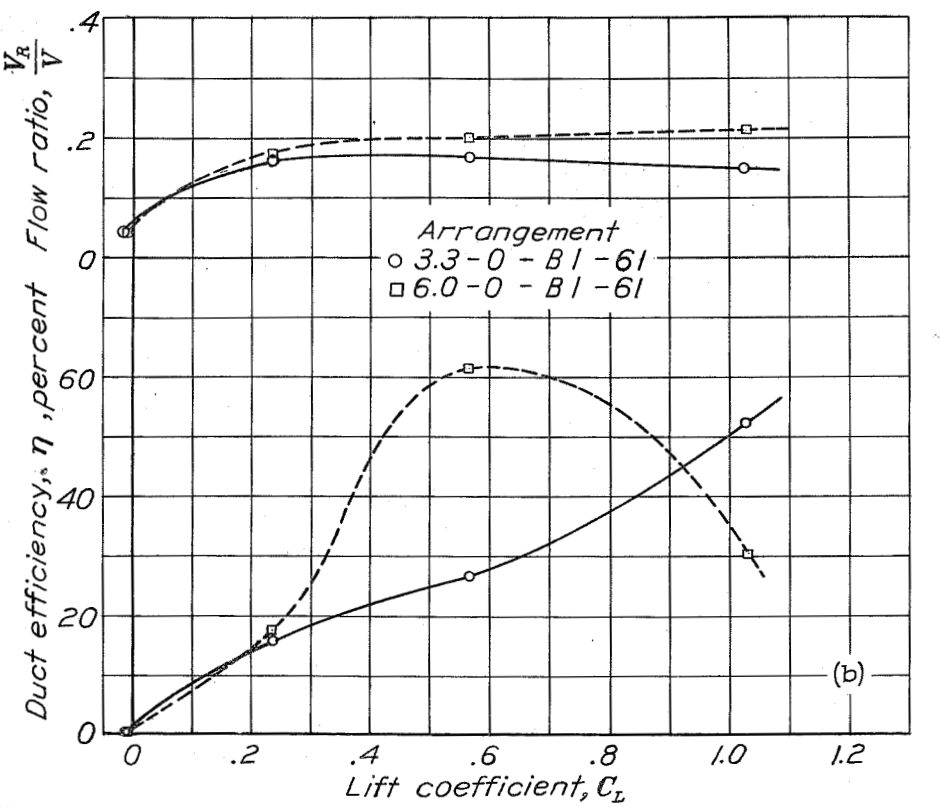

Figure 19b

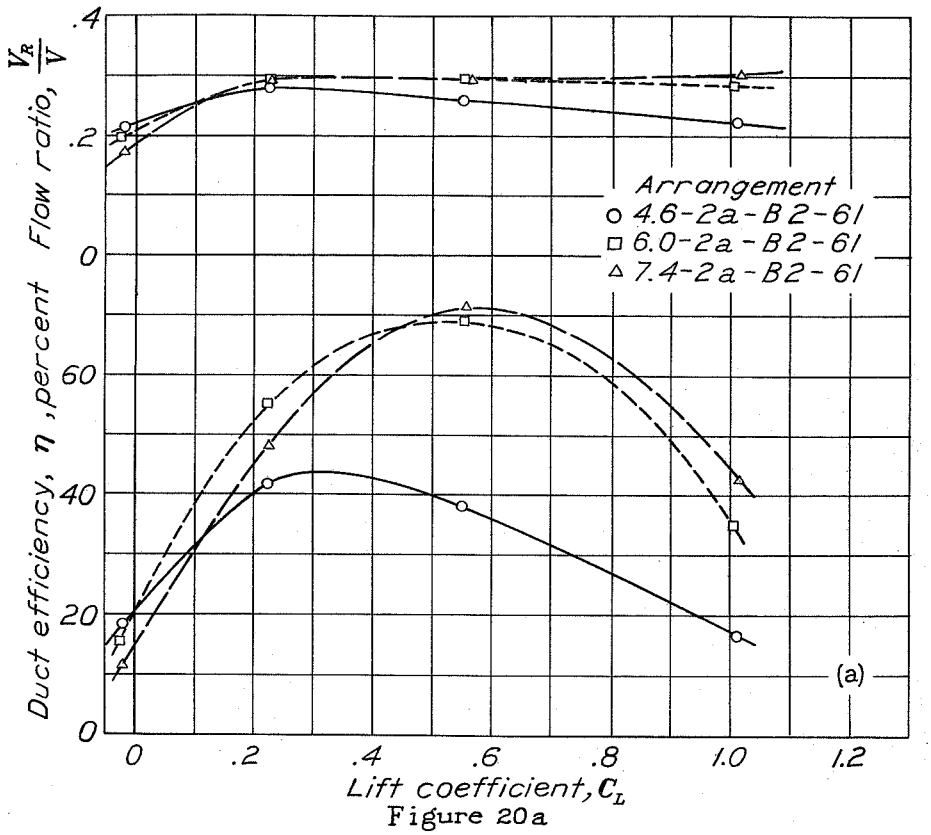

Figure 20a

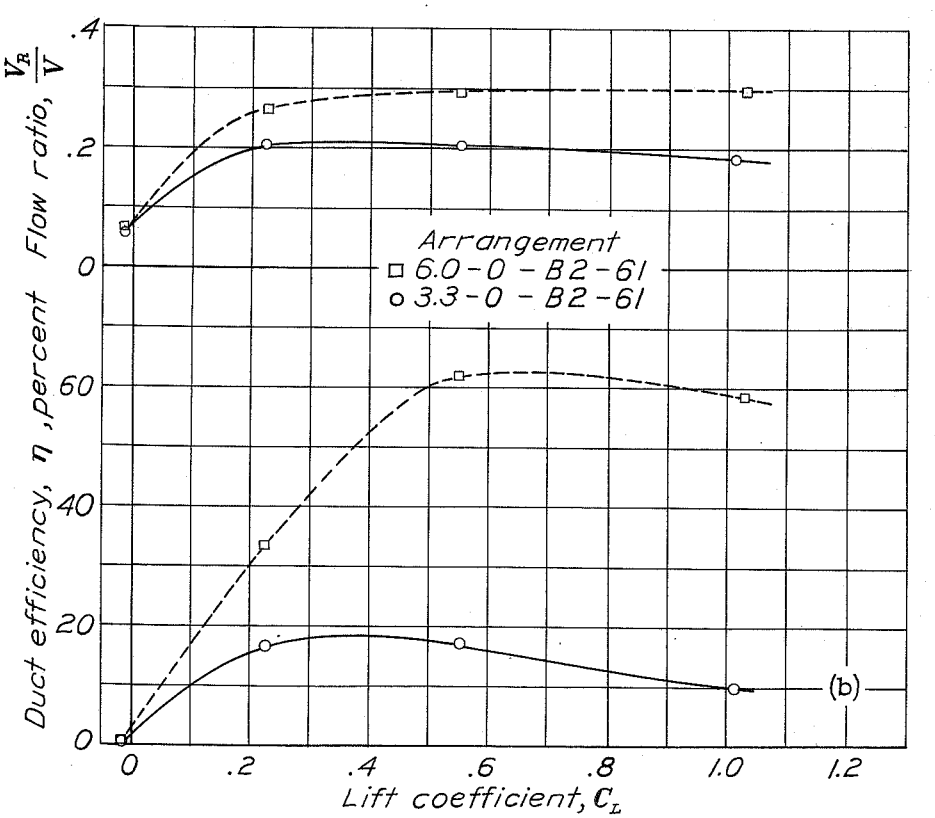

Figure 20b

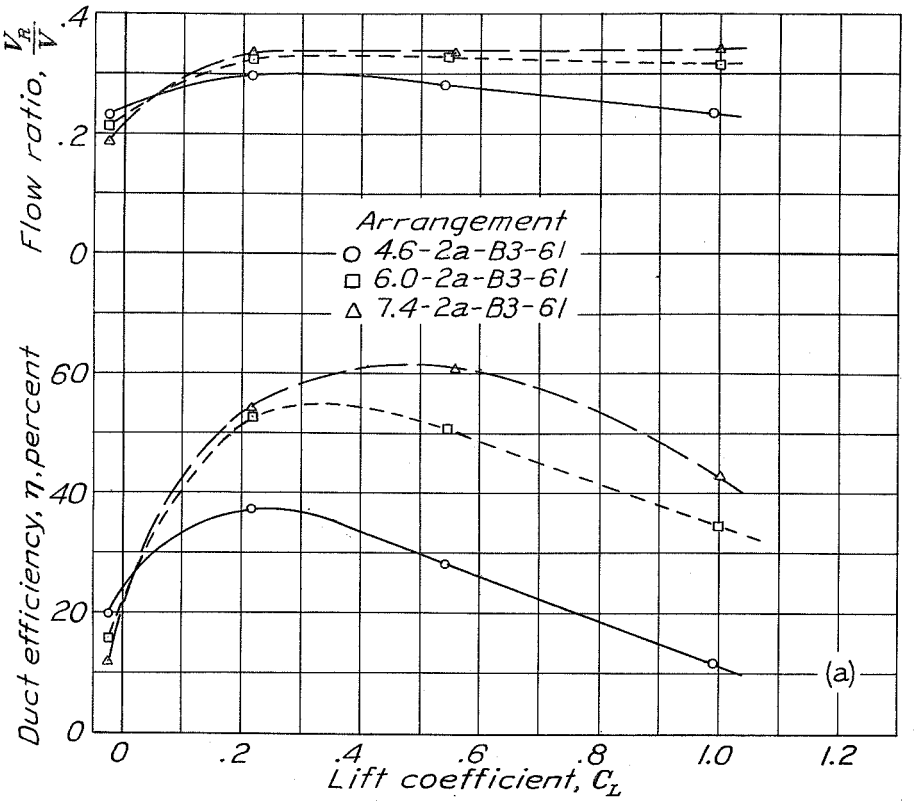

Figure 21a

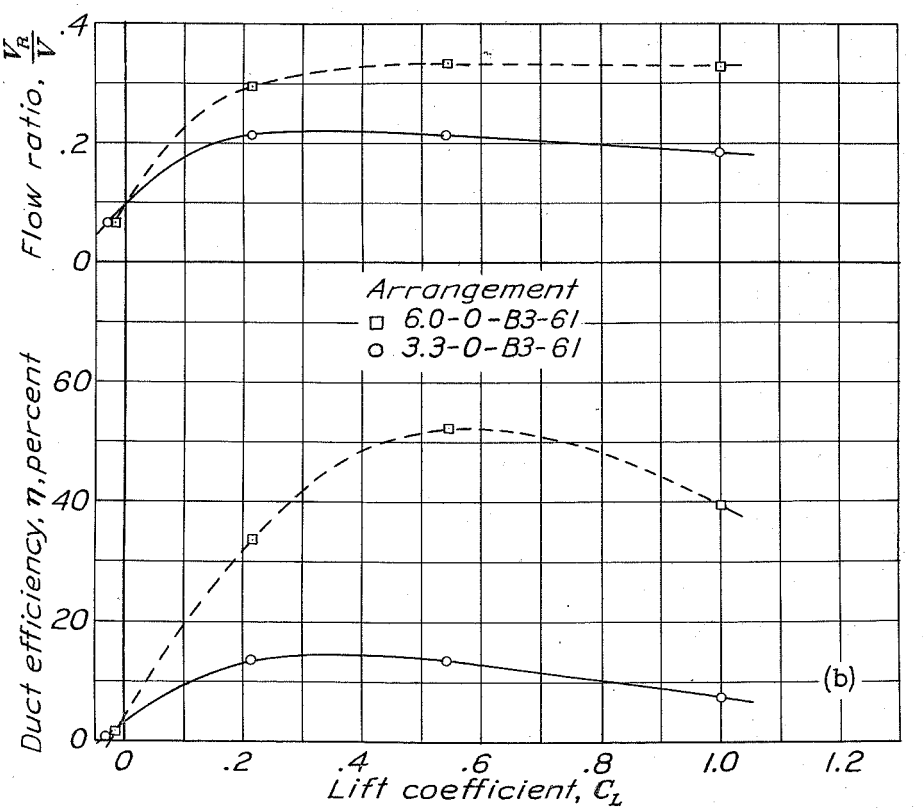

Figure 21b

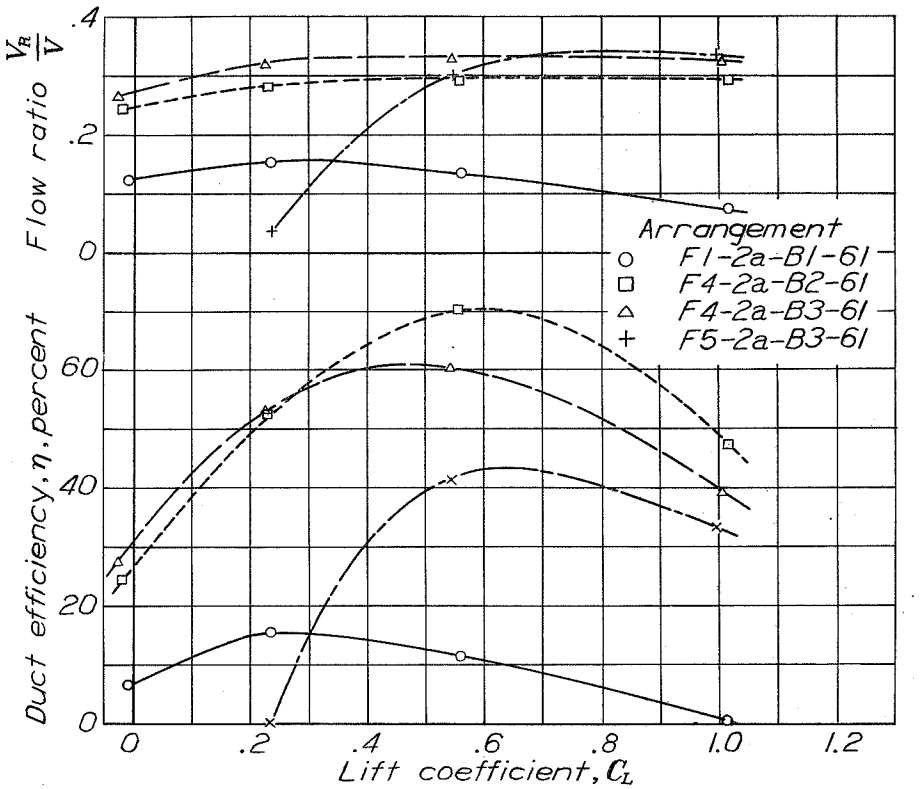

Figure 22

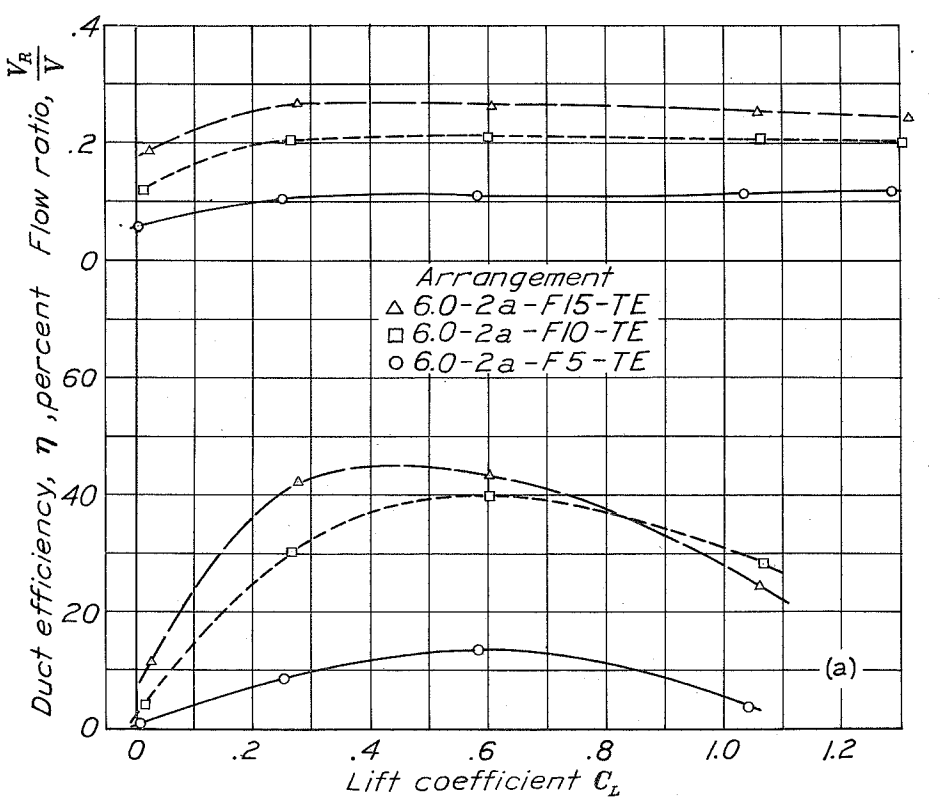

Figure 23a

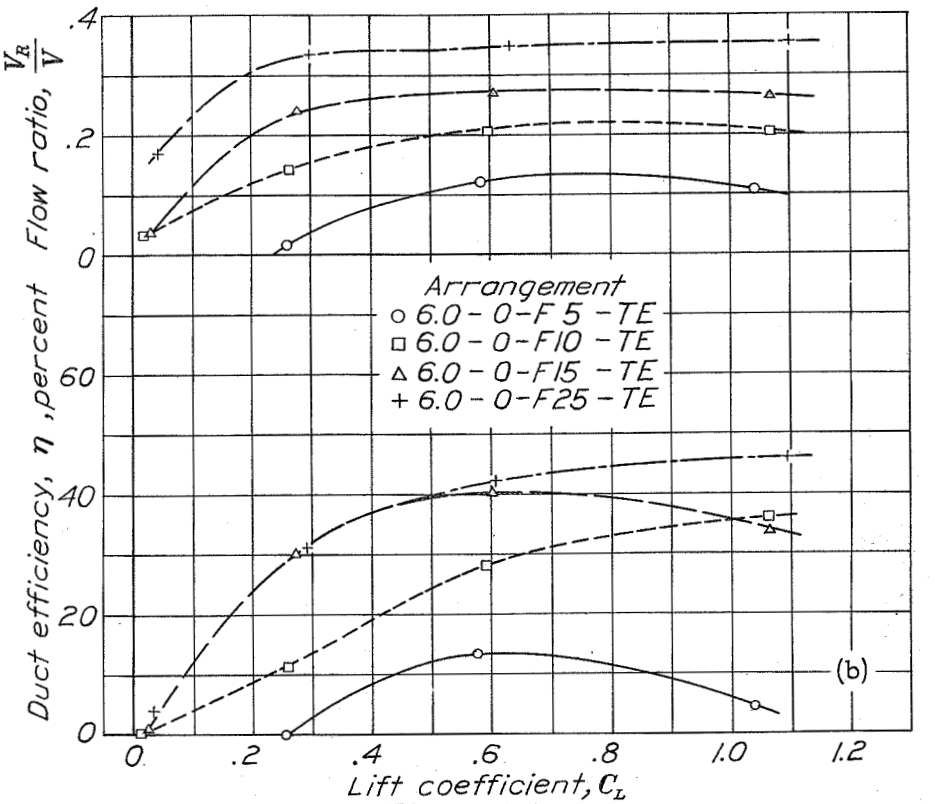

Figure 23b

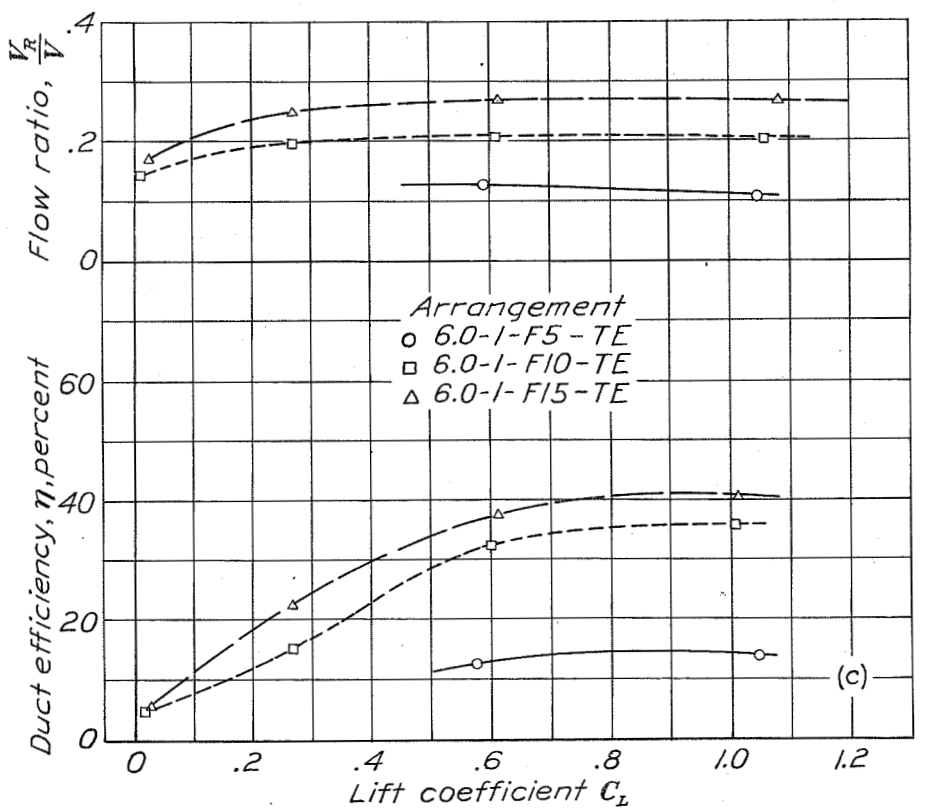

Figure 23c

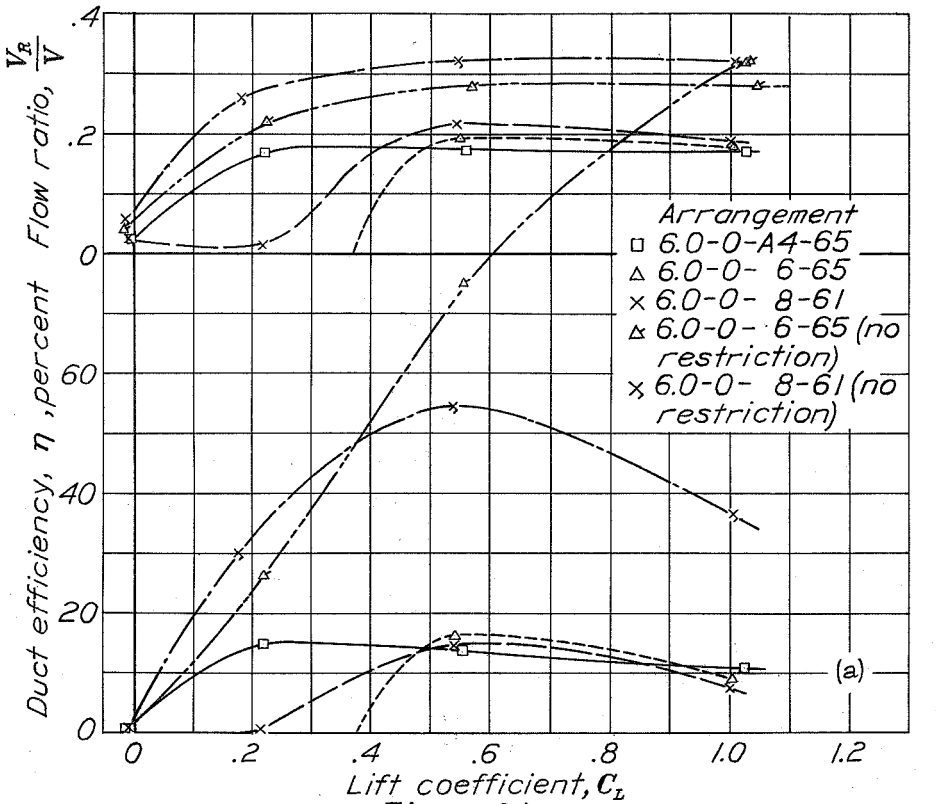

Figure 24a

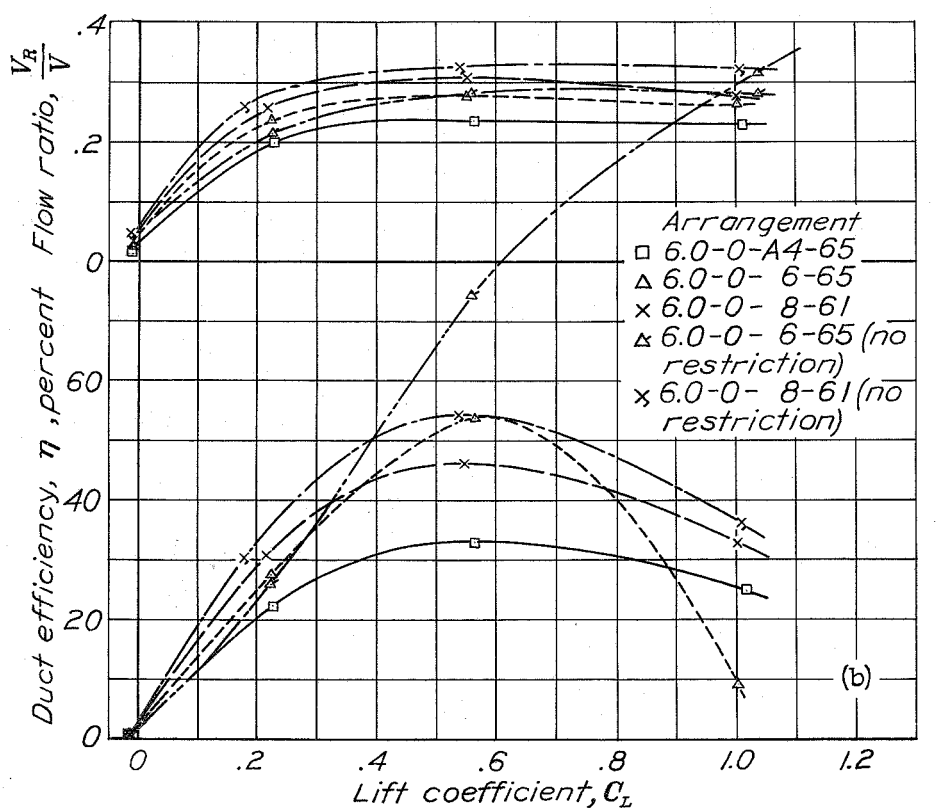

Figure 24b

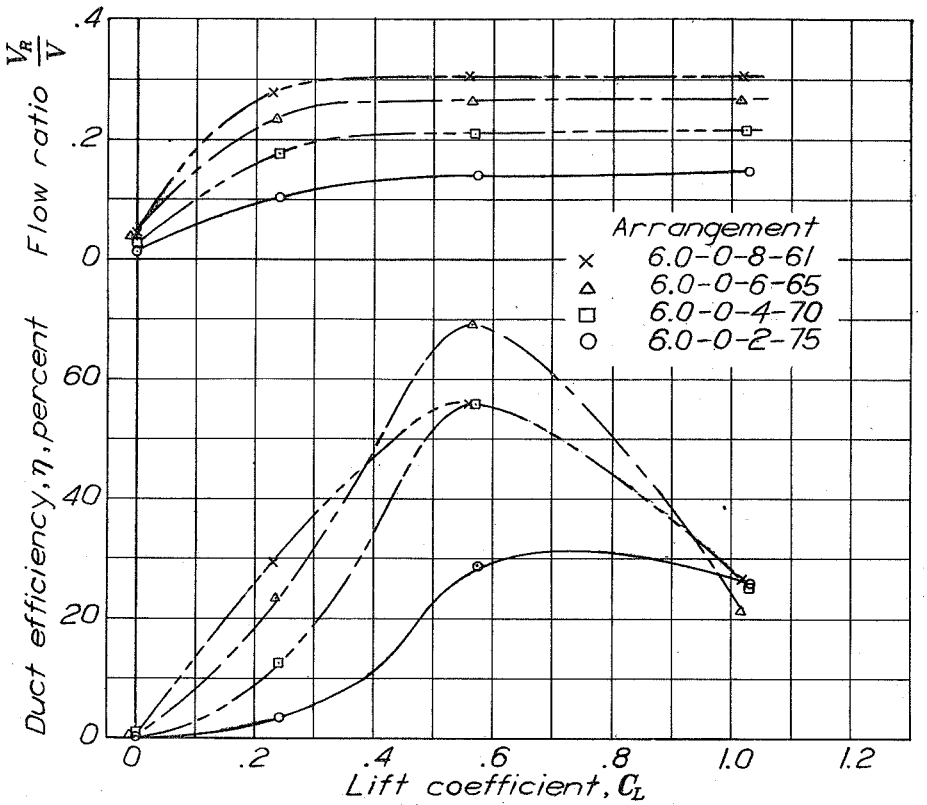

Figure 25

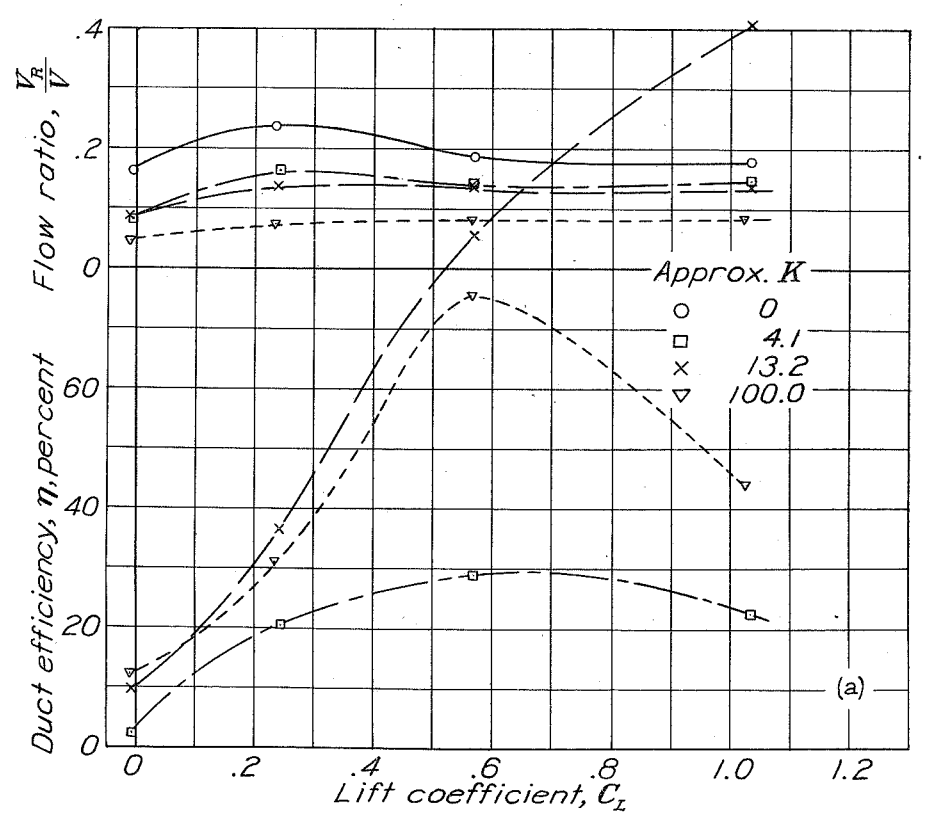

Figure 26a

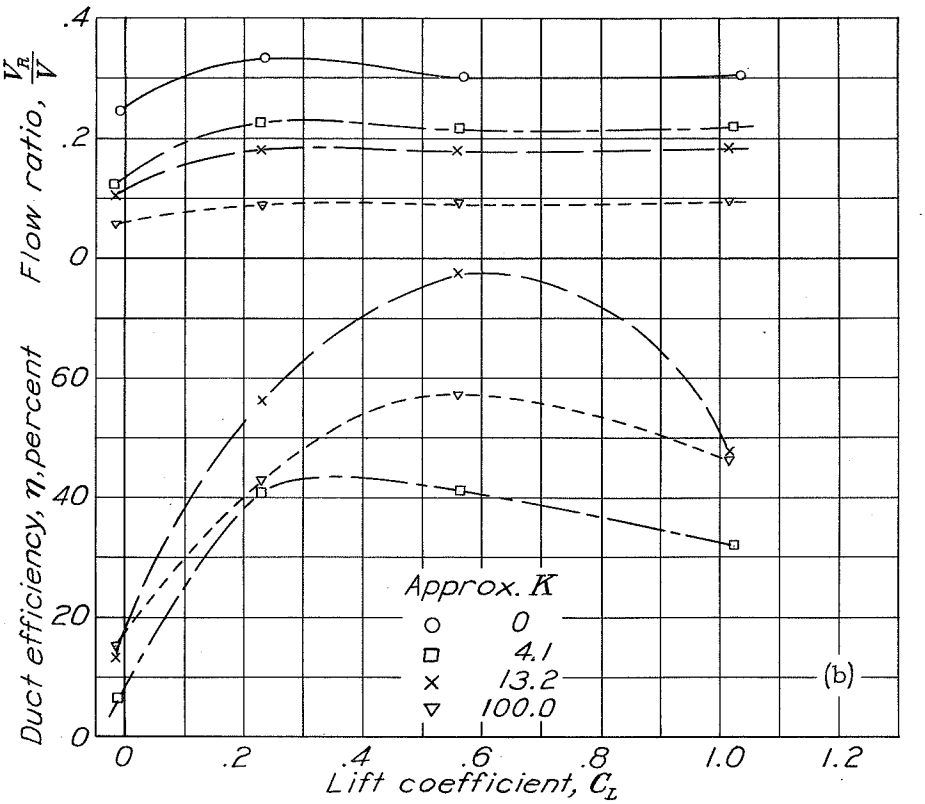

Figure 26b

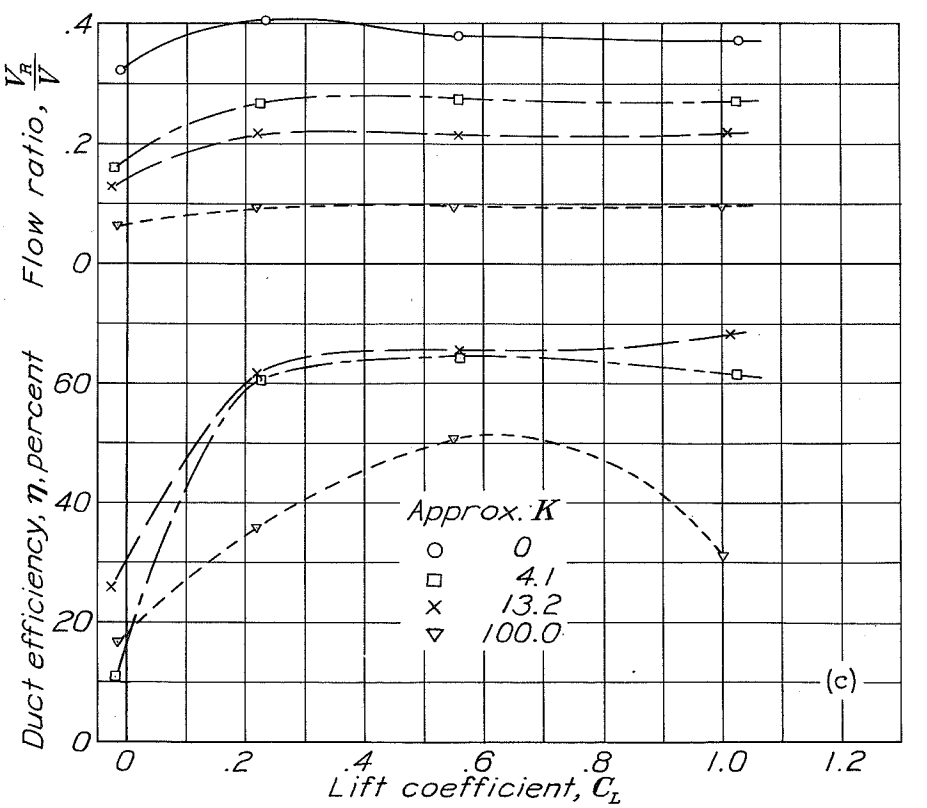

Figure 26c

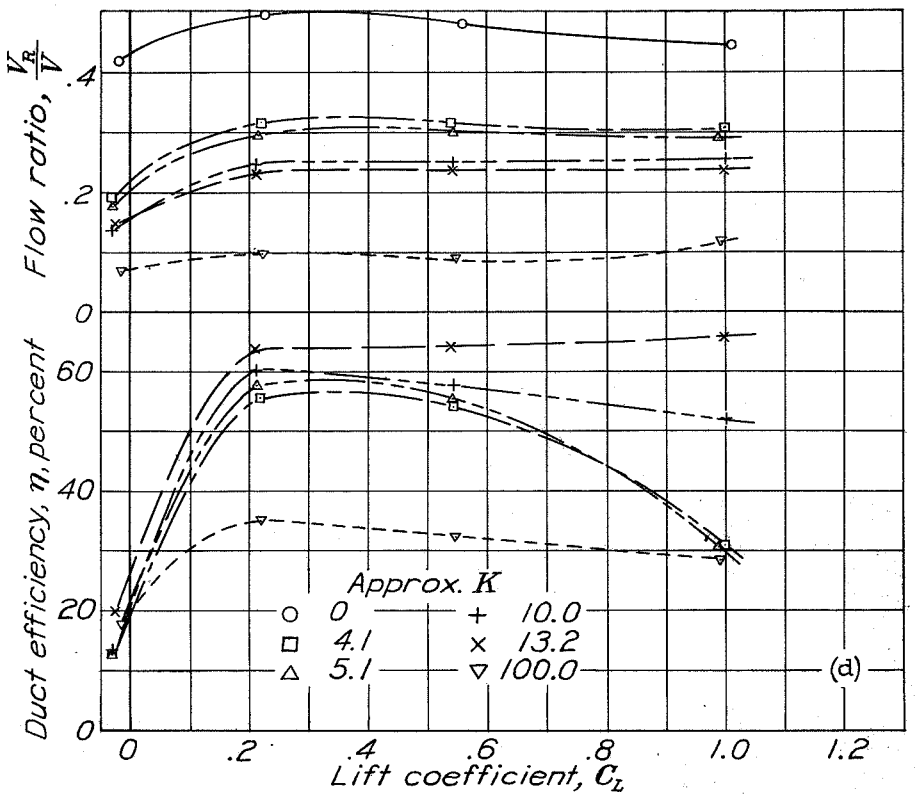

Figure 26d

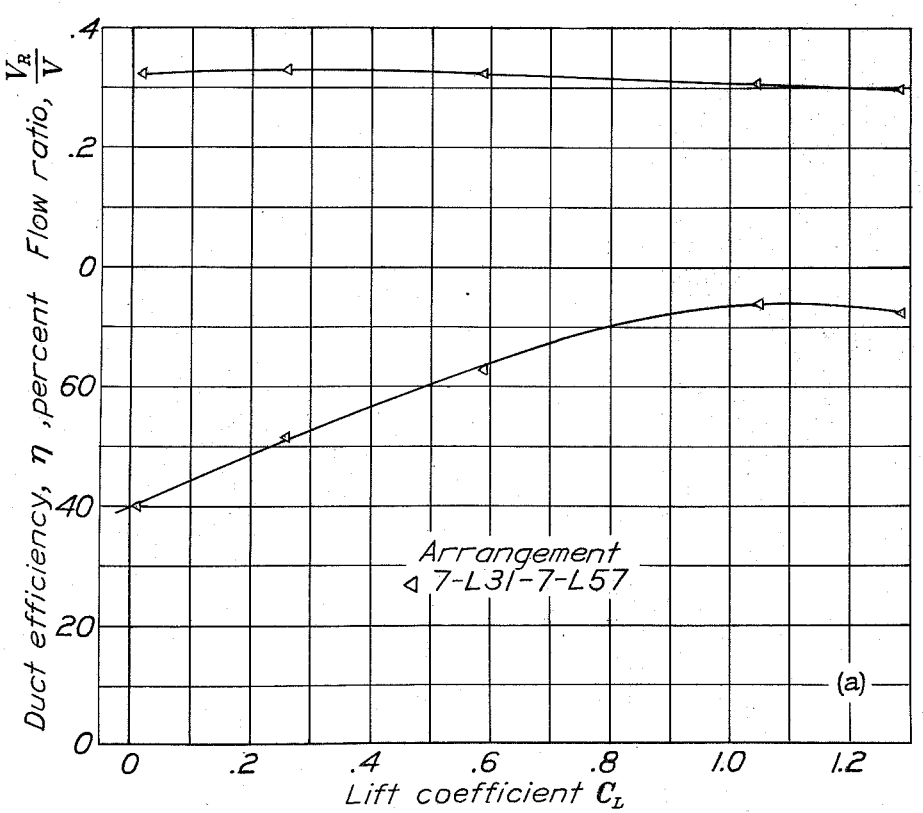

Figure 27a

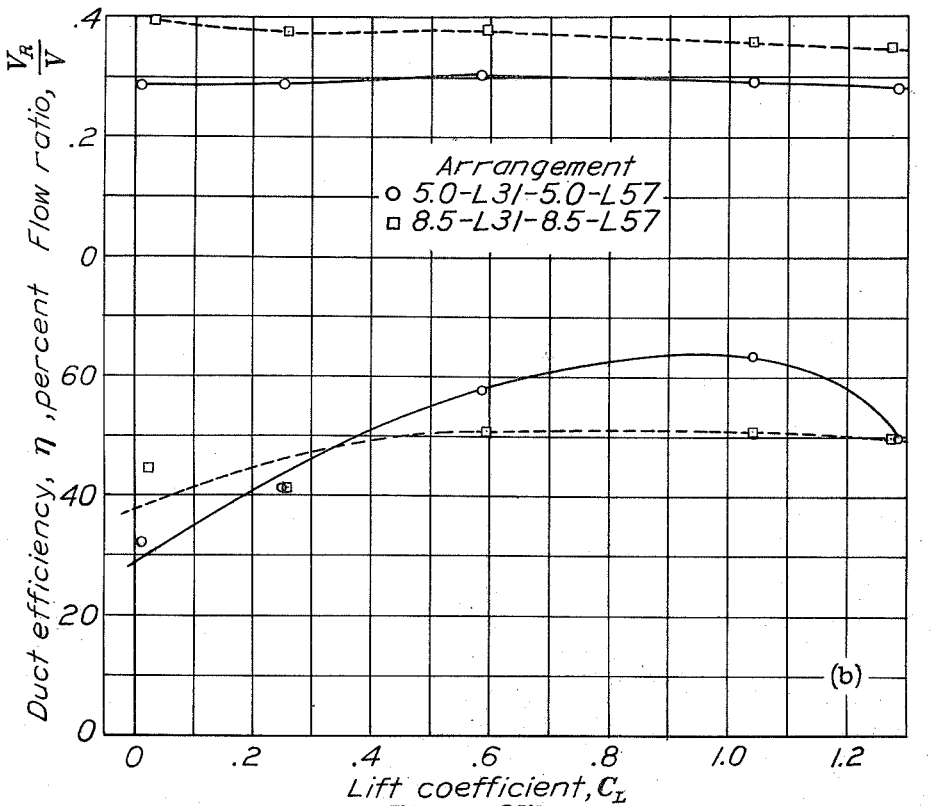

Figure 27b

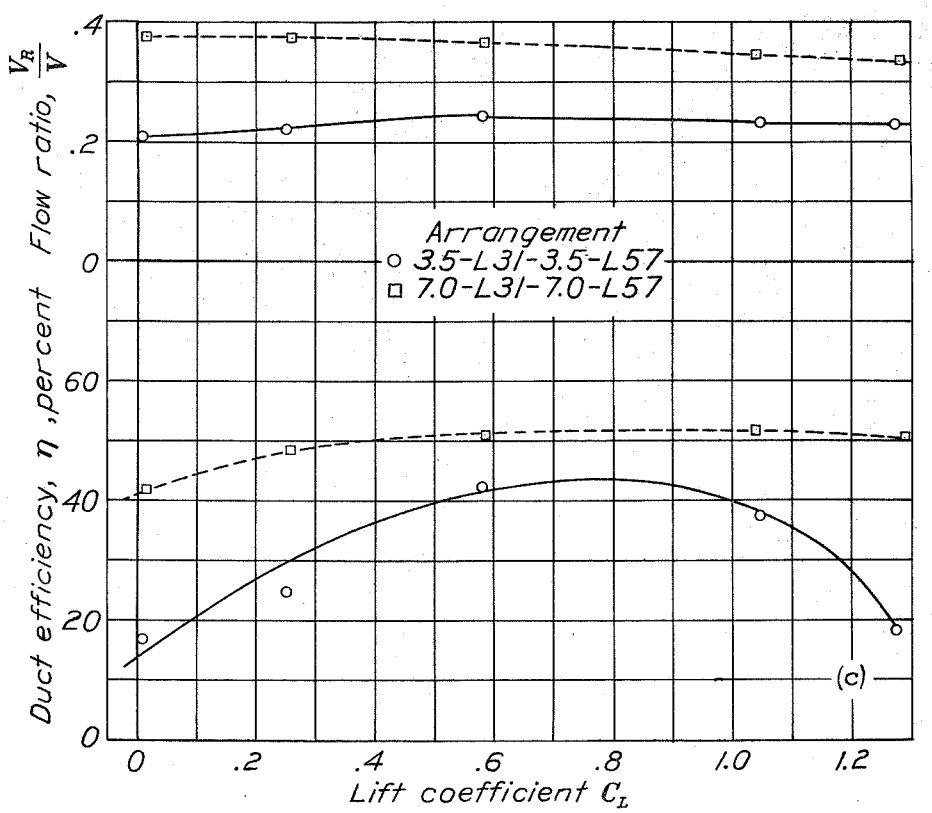

Figure 27c

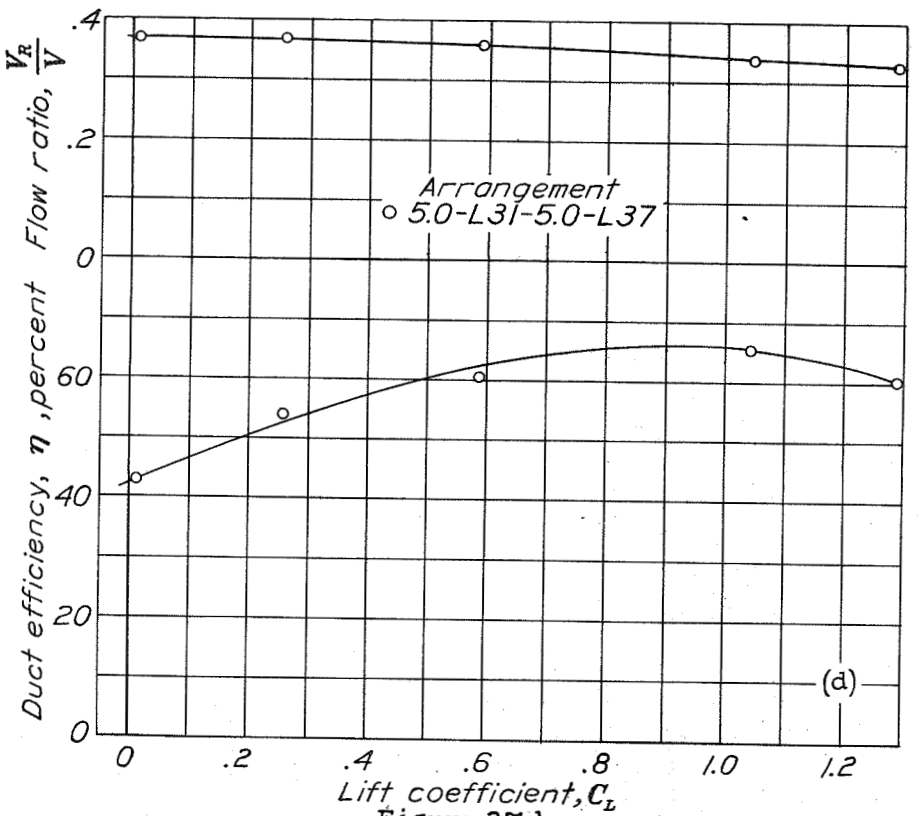

Figure 27d

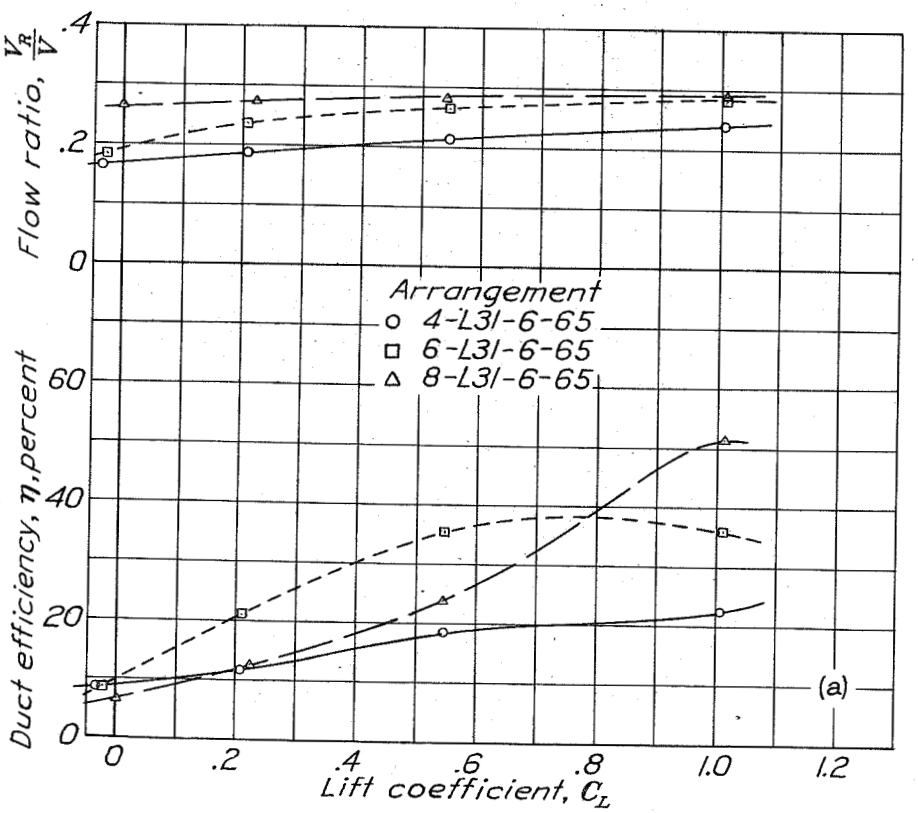

Figure 28a

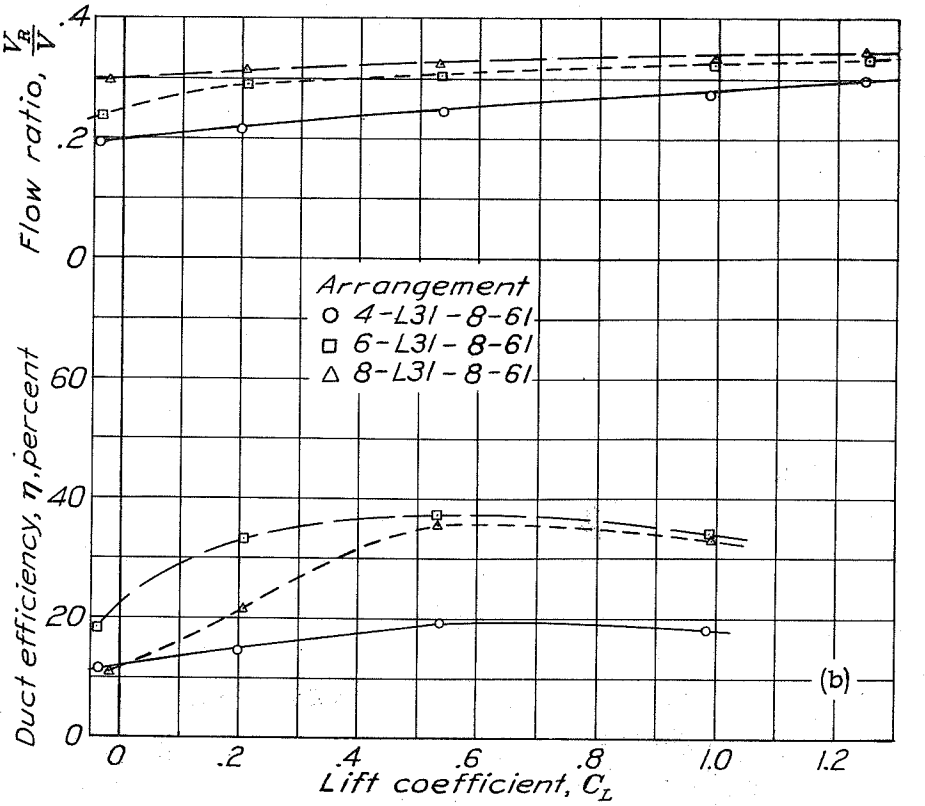

Figure 28b

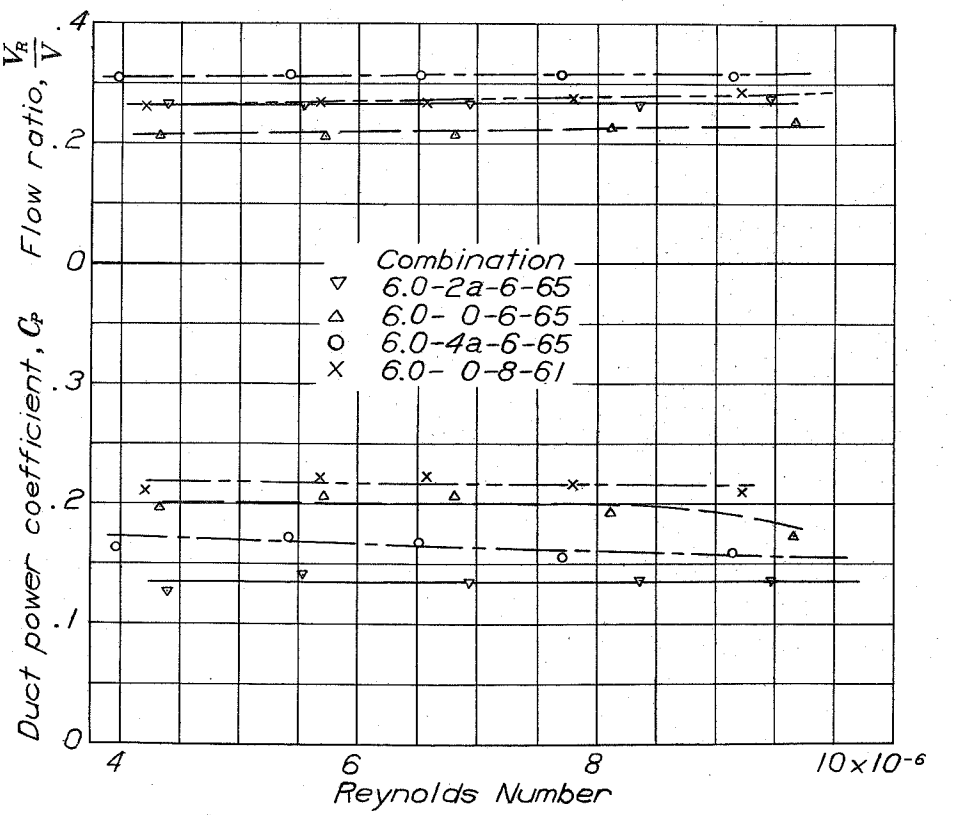

Figure 29

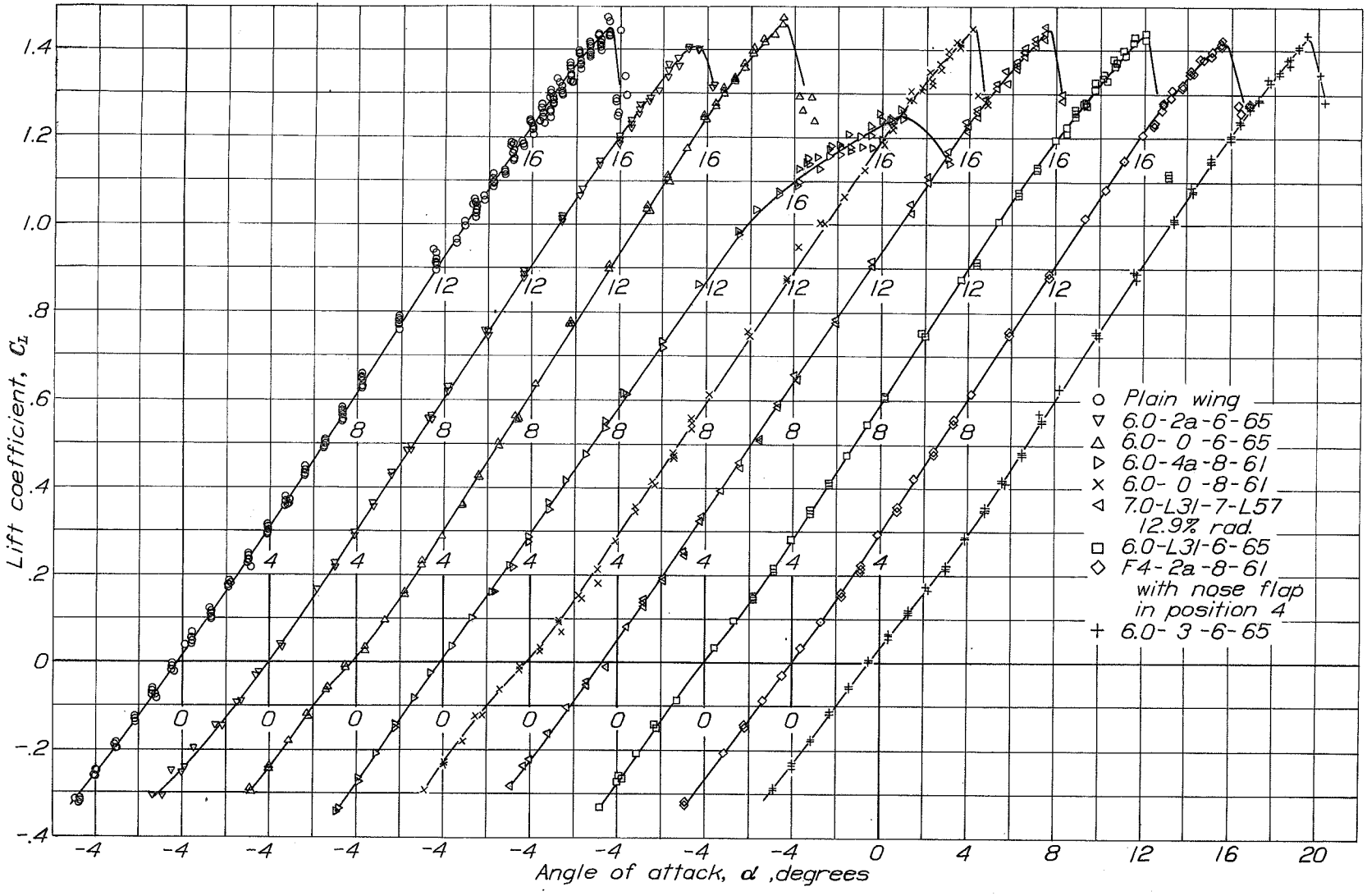
Lift coefficient, C_L
Angle of attack, α, degrees
1.4
1.2
1.0
.8
.6
.4
.2
0
-.2
-.4
-4
0
4
8
12
16
20
Plain wing
6.0-2a-6-65
6.0- 0 -6-65
6.0-4a-8-61
6.0- 0 -8-61
7.0-L31-7-L57
12.9% rad.
6.0-L31-6-65
F4-2a-8-61
with nose flap
in position 4
6.0- 3 -6-65

N.A.C.A.

Fig. 30

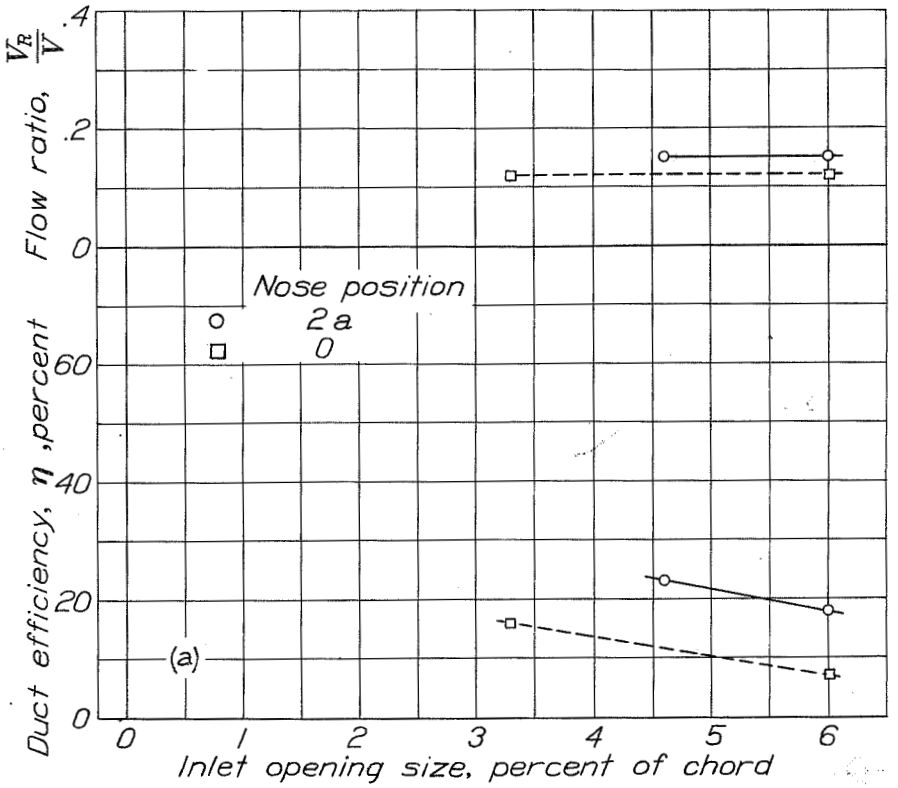

Fig.31a

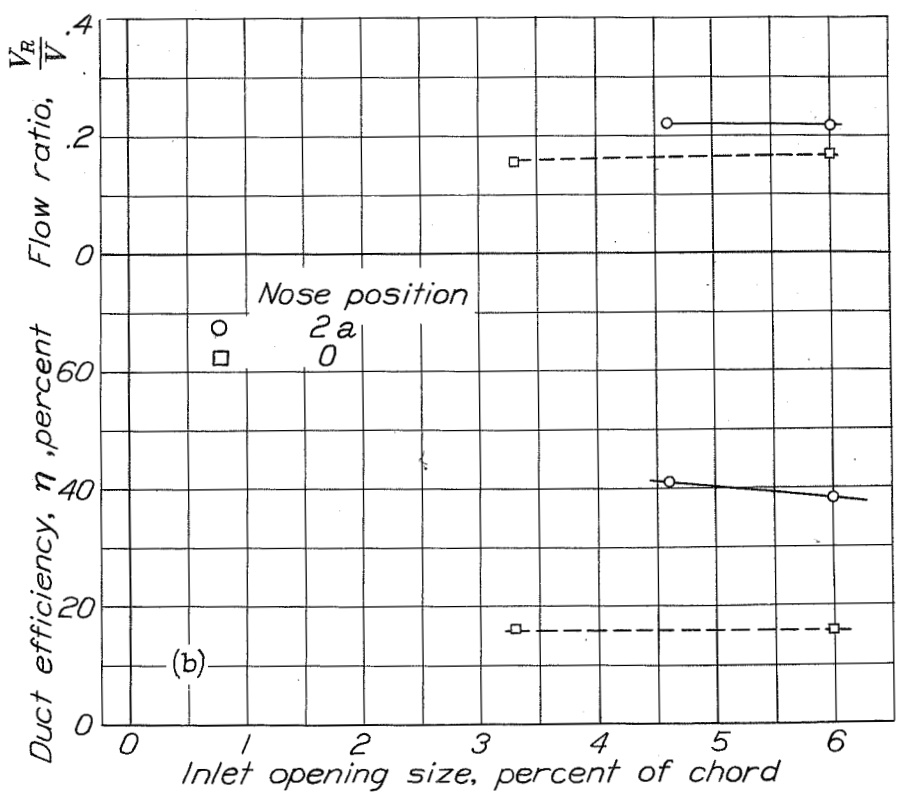

Fig.31b

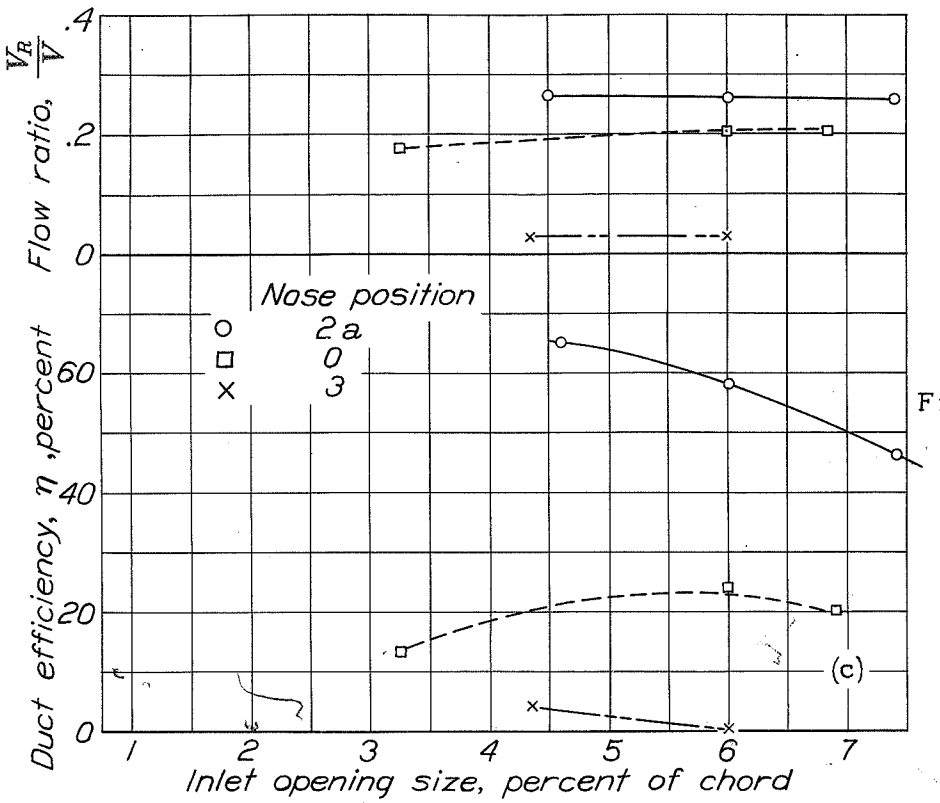

Fig. 31c

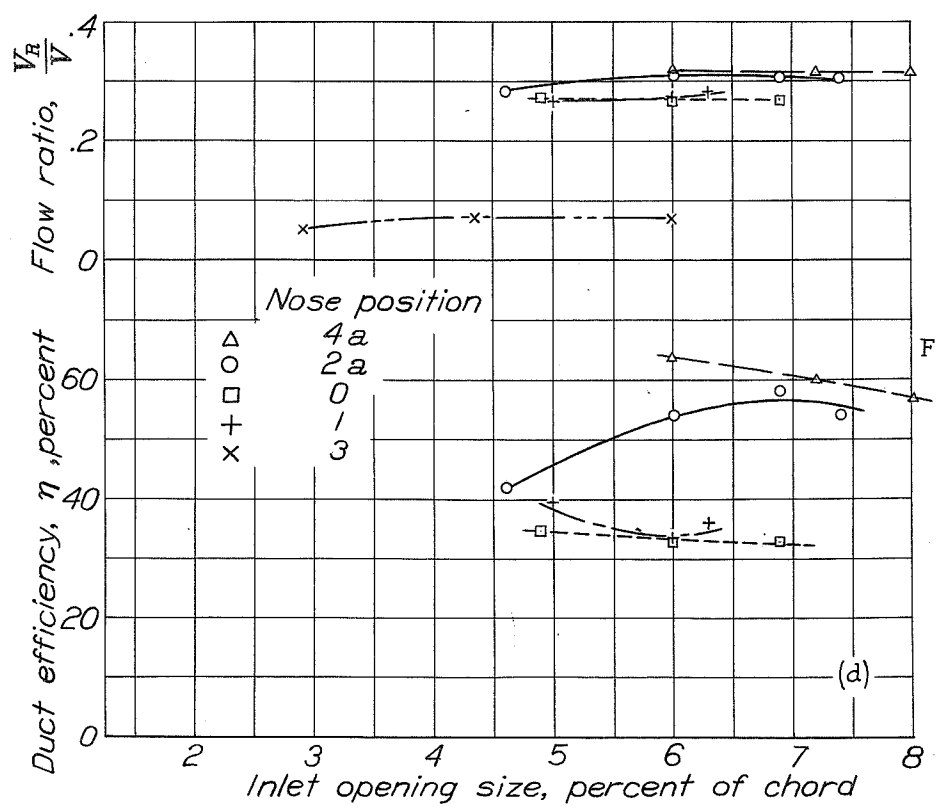

Fig. 31d

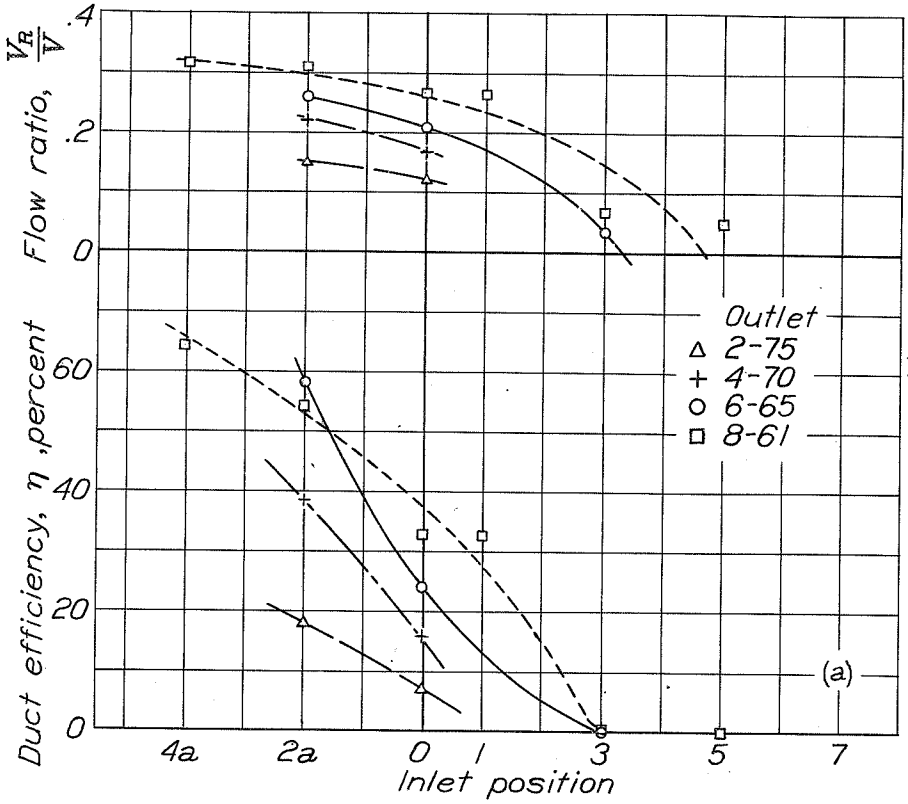

Figure 32a

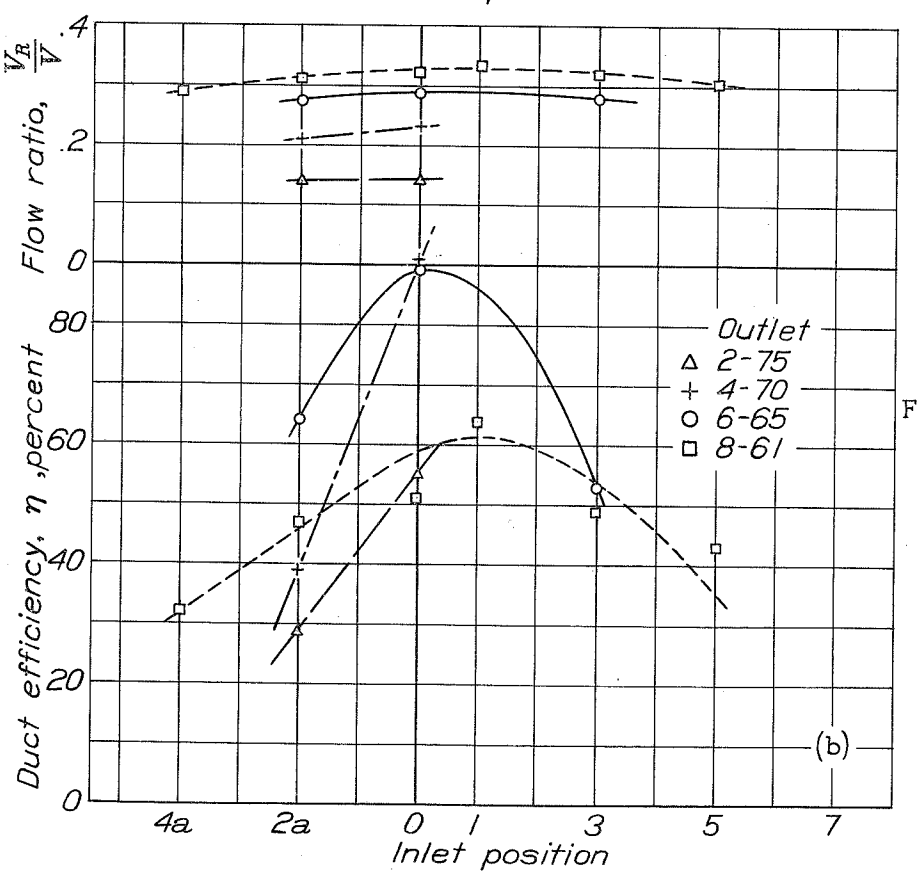

Figure 32b

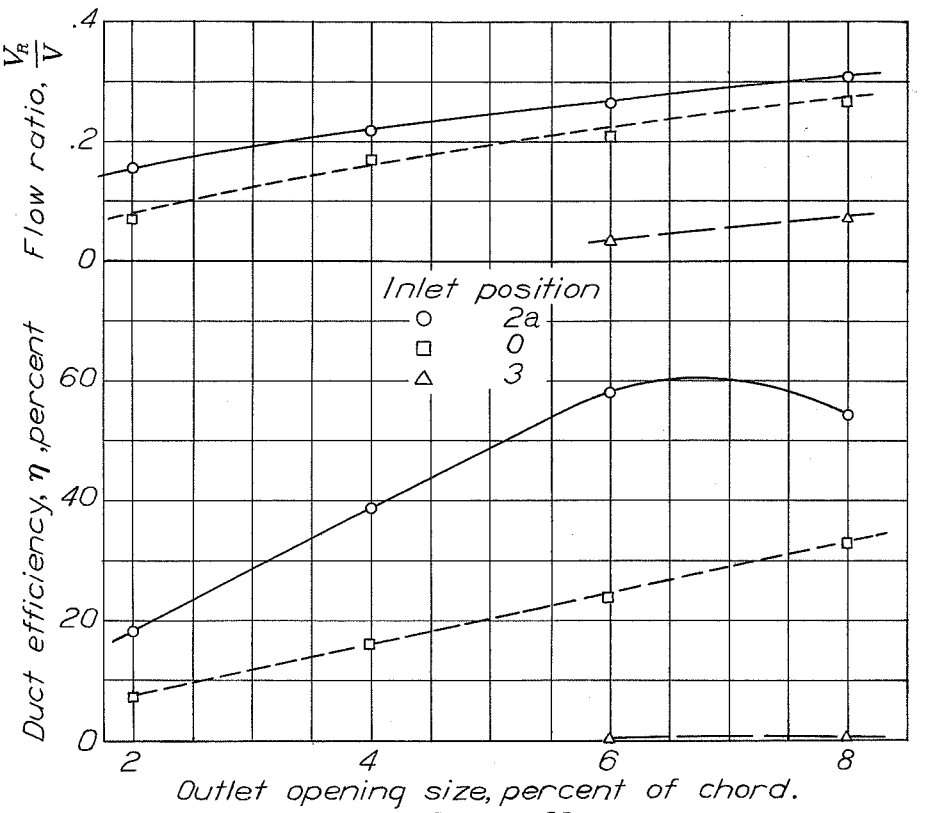

Figure 33

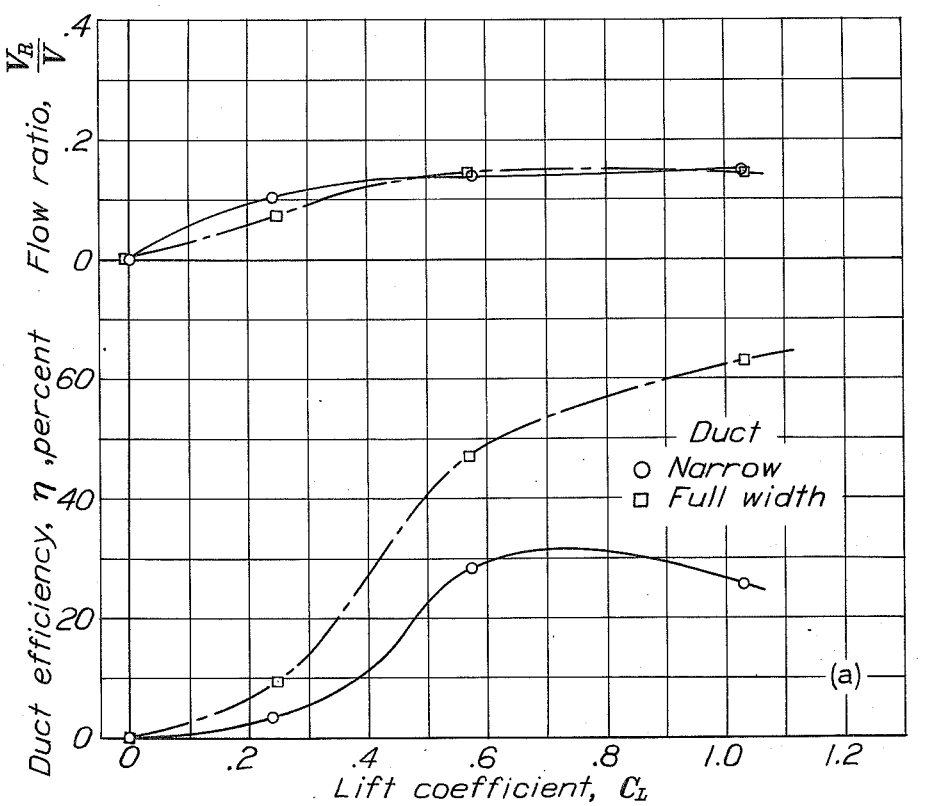

Figure 34a

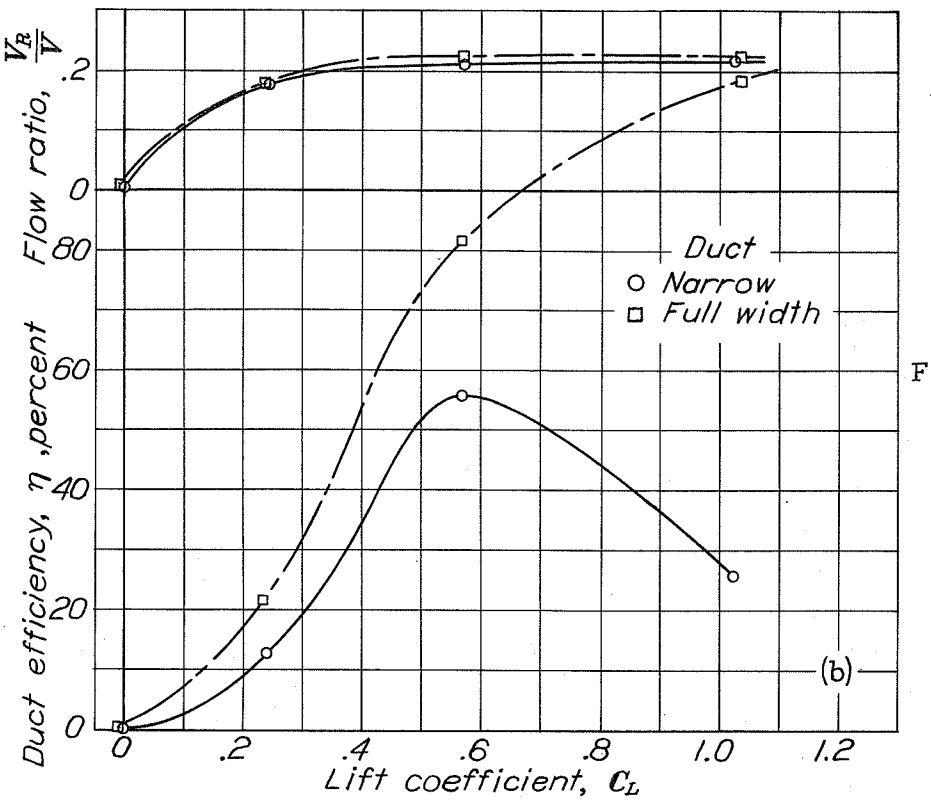

Fig. 34b

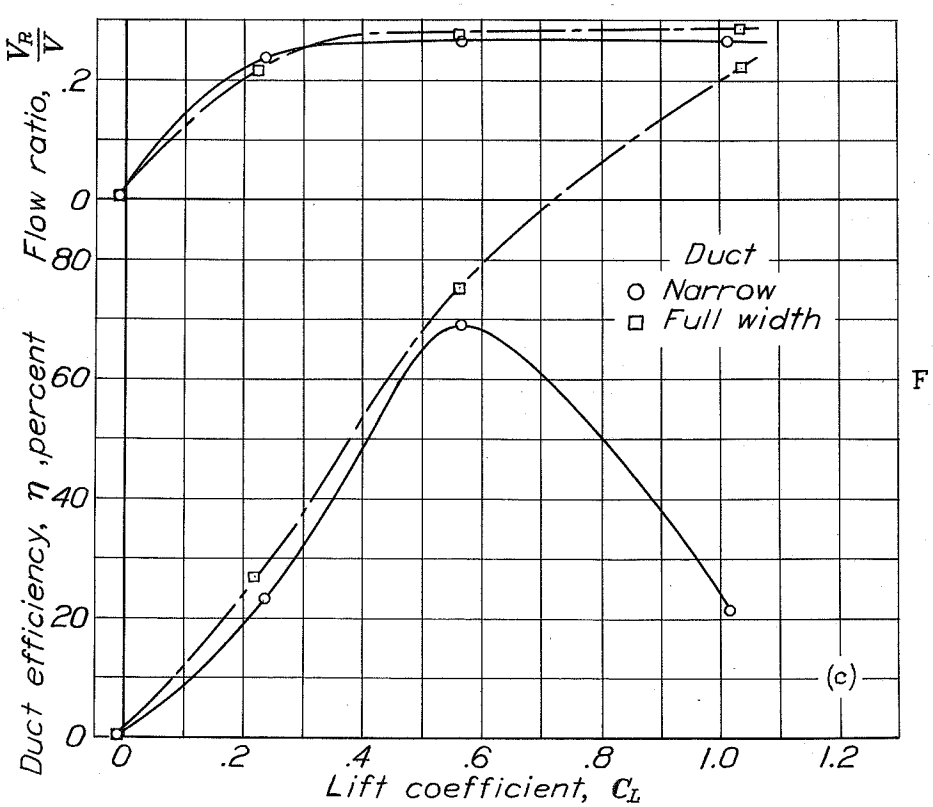

Fig. 34c

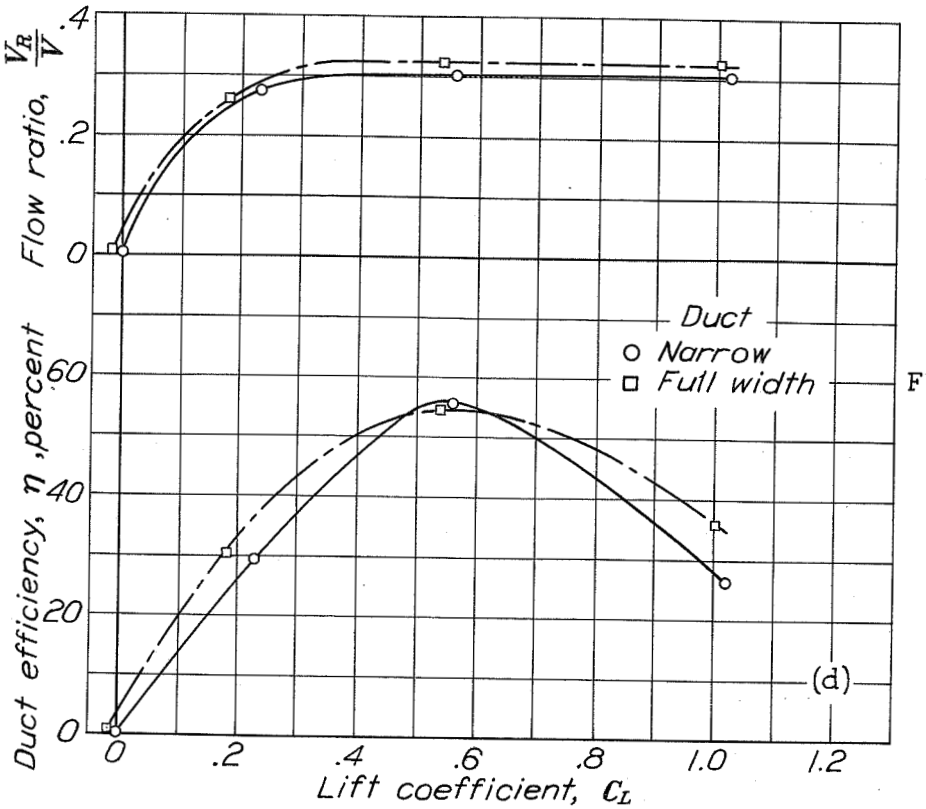

Fig. 34d

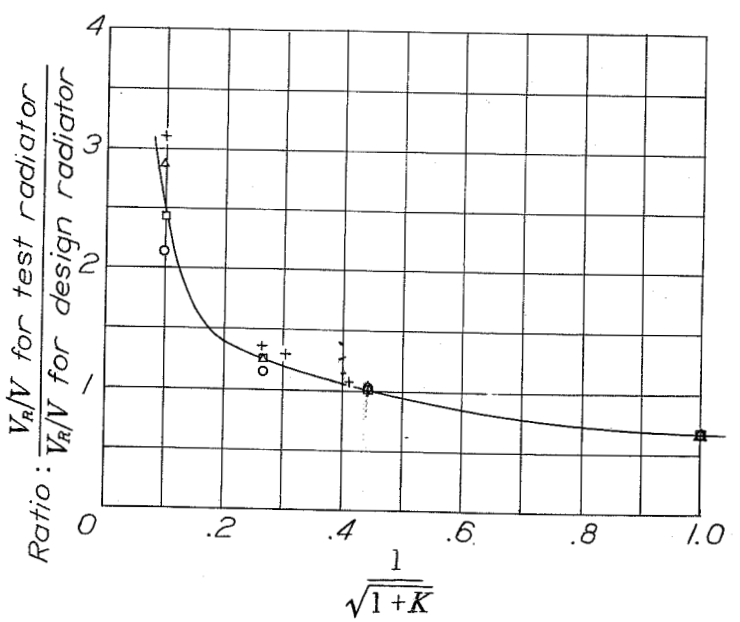

Figure 36

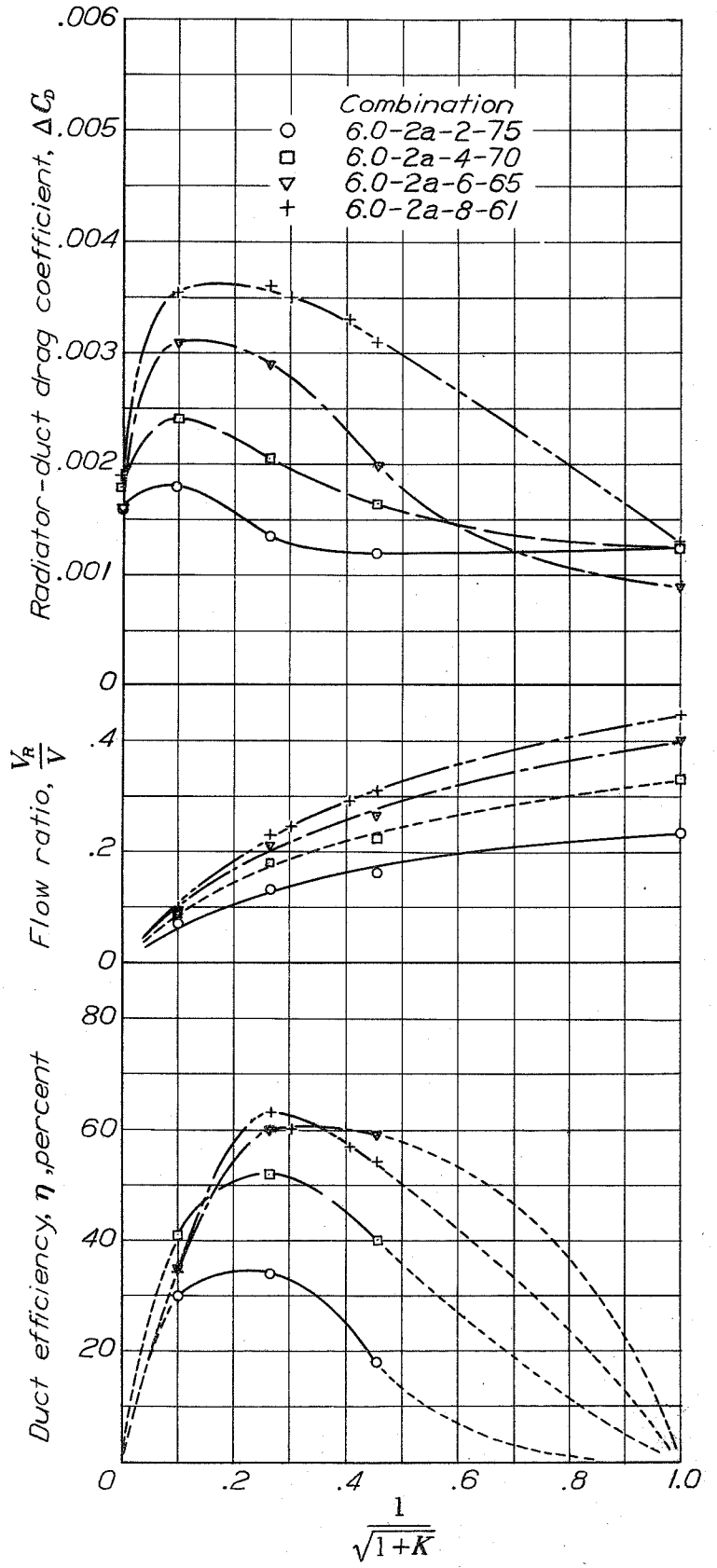
Combination
6.0-2a-2-75
6.0-2a-4-70
6.0-2a-6-65
6.0-2a-8-61
Radiator-duct drag coefficient, ΔC_D
.006
.005
.004
.003
.002
.001
0
Flow ratio, $\frac{V_R}{V}$
.4
.2
0
Duct efficiency, η, percent
80
60
40
20
0
.2
.4
.6
.8
1.0
$\frac{1}{\sqrt{1+K}}$

Figure 35.

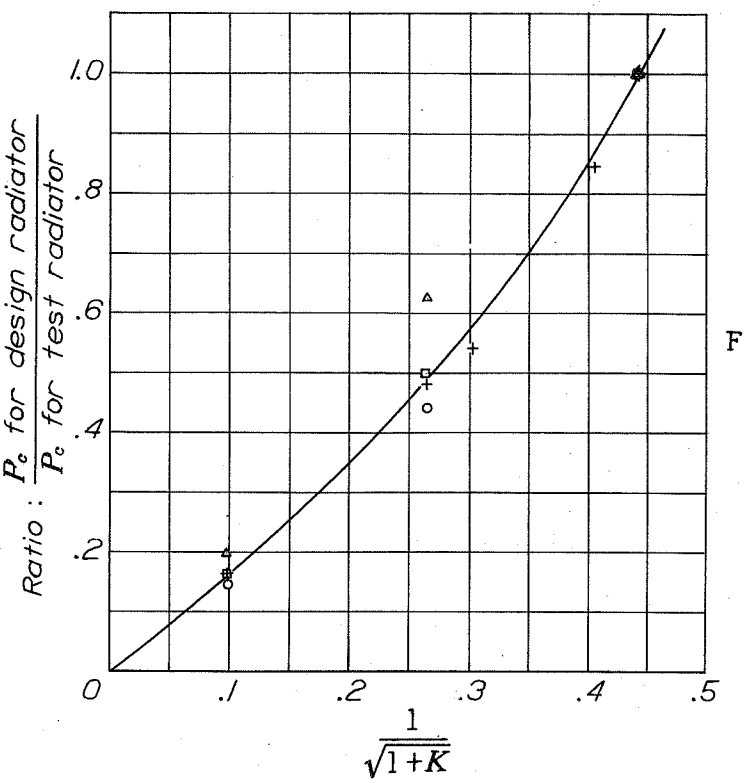

Figure 37

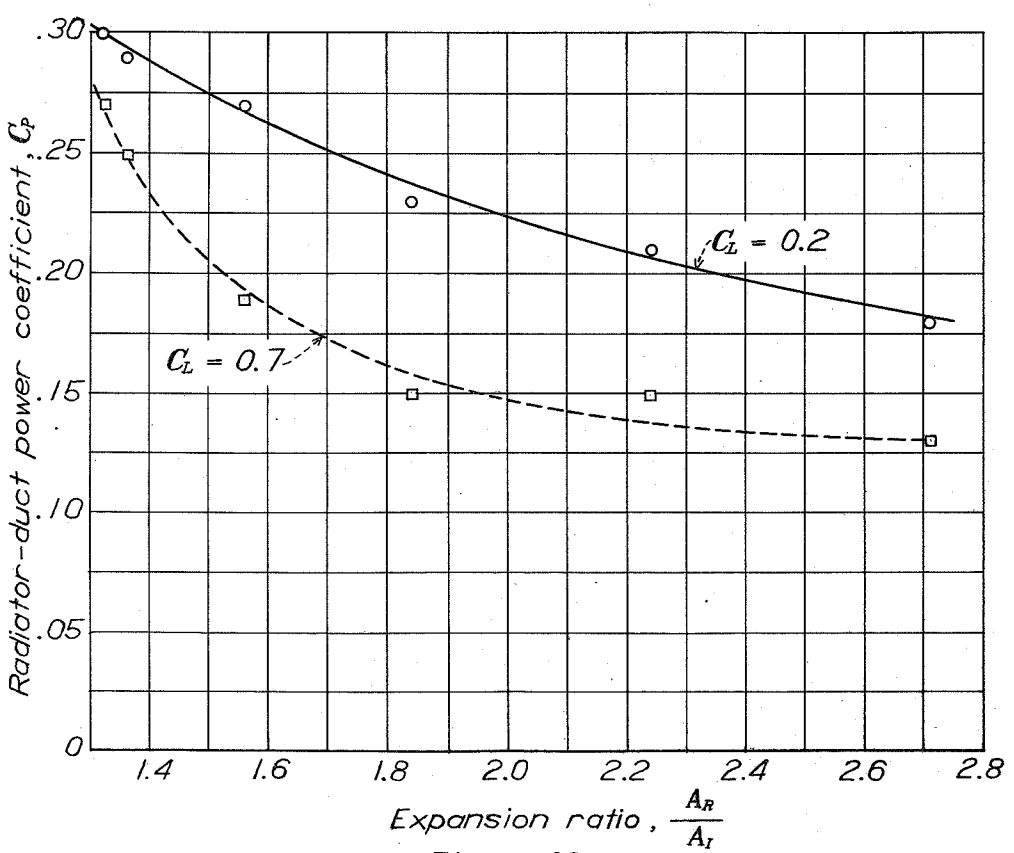

Figure 38